Identification and Functional Characterization of Novel Phosphorylation Sites in MDC1

Dissertation

zur

Erlangung der naturwissenschaftlichen Doktorwürde

(Dr. sc. nat.)

vorgelegt der

Mathematisch-naturwissenschaftlichen Fakultät

der Universität Zürich

von

Christoph Spycher

von Köniz BE und Zürich ZH

Promotionskomitee

Prof. Dr. Michael O. Hengartner (Vorsitz)

Dr. Manuel Stucki (Leitung der Dissertation)

Prof. Dr. Dr. Michael O. Hottiger

Prof. Dr. Thanos D. Halazonetis

Zürich, 2009

Table of Contents

1 Summary

It is crucial for every cell of an organism to sense and repair defects that occur in its genetic material. Cells are constantly exposed to DNA-damaging agents from exogenous and endogenous sources such as the Sun's radiation or metabolically produced free oxygen radicals. The mechanisms to deal with DNA damage consist of repair systems as well as kinase-dependent signaling pathways (so-called DNA damage checkpoints) that delay or arrest cell cycle progression. The response to DNA damage also includes alteration of transcription and regulation of apoptosis. This complex signaling network is referred to as the DNA damage response (DDR).

Of all types of DNA damage, DNA double strand breaks (DSBs) pose the greatest challenge to cells. If DSBs remain un-repaired or are repaired incorrectly, the genome can suffer translocations and deletions, which may ultimatively lead to genome instability and harmful diseases such as cancer. In response to DSBs, the MRE11/RAD50/NBS1 (MRN) complex acts as sensor and activates the proximal kinases ATM and DNA-PKcs. These kinases phosphorylate various target proteins including the histone variant H2AX. MDC1 is an essential mediator/adaptor protein that directly binds to phosphorylated H2AX (γH2AX) through its tandem BRCT domains. In addition, MDC1 is necessary for the amplification of the signal and for establishing a chromatin environment that is proficient for efficient repair of DSBs.

In this study, we describe the molecular mechanism of MDC1-mediated accumulation and retention of the MRN complex in chromatin regions flanking DSBs. MDC1 is constitutively phosphorylated at multiple conserved SDT motifs by Casein kinase 2 (CK2). The MRN accumulation is achieved through direct binding of the FHA and BRCT tandem domain of NBS1 to the phosphorylated SDT motifs of MDC1. Mutations in conserved amino

acids within the NBS1 FHA and BRCT domains, which are essential for the binding to the phospho-epitope, revealed that the accumulation of MRN in IRIF is not required for the activation of the G2/M checkpoint response. Interestingly, while cells containing a mutation in the BRCT domain of NBS1 had only a minor G2/M checkpoint defect, cells harboring a NBS1 mutated in its FHA domain showed a clear G2/M checkpoint defect at low doses of irradiation. These results suggest an additional function of the FHA domain of NBS1 in checkpoint signaling.

During the search for ATM-dependent phosphorylation sites in MDC1 we identified the Thr4 residue to be targeted in a DNA damage specific manner. Interestingly, this residue bound to the FHA domain of MDC1 itself leading to dimerization of the protein. This interaction was confirmed by isothermal titration calorimetry (ITC) and X-ray crystallography, revealing that the FHA domains of two MDC1 molecules associate in a head-to-tail orientation in a DNA damage-dependent manner. These findings add MDC1 to the growing list of mediator/adaptor proteins that show dimerization and/or oligomerization.

In summary, this work thus contributes substantially to our understanding of the mechanisms by which the mediator/adaptor protein MDC1 functions in the mammalian DDR.

2 Zusammenfassung

Es ist von entscheidender Bedeutung für jede Zelle eines Organismus, Defekte im Genom zu erkennen und zu reparieren. Zellen sind andauernd Substanzen ausgesetzt, welche die DNS beschädigen. Diese können von der Umwelt (z.B. Sonnenstrahlung) oder durch den Organismus selbst (z.B. freie Sauerstoffradikale) produziert werden. Die Mechanismen, um auf solche DNS Schäden zu reagieren, bestehen aus Reparatur-systemen sowie Kinase abhängigen Signalwegen (so genannte Kontrollpunkte), welche den Zellzyklus verzögern oder anhalten. Die zelluläre Antwort auf Schäden in der DNS beinhaltet ausserdem die Regulierung der Transkription und des programmierten Zelltodes (Apoptose).

Von allen Arten von Schäden der DNS stellt der Doppelstrangbruch die grösste Gefahr für eine Zelle dar. Wenn Doppelstrangbrüche nicht erkannt oder falsch repariert werden, kann das Genom durch Translokationen und Deletionen verändert werden. Diese Veränderungen können zu Instabilität des Genoms und zu gefährlichen Krankheiten (z.B. Krebs) führen. Der MRE11/RAD50/NBS1 (MRN) Komplex dient als Sensor für die Erkennung von Doppelstrangbrüchen. Er aktiviert die Kinasen ATM und DNA-PKcs, welche verschiedene Proteine phosphorylieren, darunter auch die Histon Variante H2AX. MDC1 ist ein essenzielles Adapterprotein, welches via seine BRCT Domänen direkt an phosphoryliertes H2AX bindet. Im Weiteren ermöglicht MDC1 die Rekrutierung von verschiedenen Proteinen, welche für die Reparatur und die Signalübertragung wichtig sind. Dadurch hilft MDC1 bei der Bildung einer Chromatinumgebung, welche die effiziente Reparatur von Doppelstrangbrüchen ermöglicht.

In dieser Arbeit beschreiben wir den molekularen Mechanismus, wie MDC1 den MRN Komplex bindet und zu Doppelstrangbrüchen rekrutiert. MDC1 wird in mehreren SDT

Motiven durch die Casein Kinase 2 konstitutiv phosphoryliert. Die Akkumulierung von MRN erfolgt durch die direkte Bindung der FHA und BRCT Domänen von NBS1 an die phosphorylierten SDT Motive von MDC1. Mutationen in konservierten Aminosäuren innerhalb der FHA und BRCT Domänen von NBS1 zeigten, dass die Bindung von MRN nicht für die Aktivierung des G2/M Kontrollpunktes verantwortlich ist. Interessanterweise hatten nur die Zellen mit einer Mutation in der FHA Domäne von NBS1 einen Defekt im G2/M Kontrollpunkt, nicht aber die Zellen mit einer Mutation in der BRCT Domäne von NBS1. Diese Resultate deuten auf eine zusätzliche Funktion der FHA Domäne von NBS1 im Signalweg nach DNS Schäden hin.

Die Suche nach ATM abhängigen Phosphorylierungs-Stellen in MDC1 zeigte, dass die Aminosäure Thr4 als Folge von DNS-Schäden phosphoryliert wird. Diese Aminosäure bindet an die FHA Domäne von MDC1, was zu einer Dimerisierung des Proteins führt. Diese Bindung konnte mit Hilfe von Isothermaler Titrations Kalorimetrie sowie Röntgenstrahl-Kristallographie bestätigt werden. Dabei stellten wir fest, dass die FHA Domänen von zwei MDC1 Molekülen in umgekehrter Orientierung aneinander binden. Diese Resultate fügen MDC1 zur wachsenden Liste von Adapterproteinen hinzu, welche Dimere oder Oligomere bilden können.

Insgesamt trägt diese Arbeit substanziell zu unserem Verständnis der Mechanismen bei, wie das Adapterprotein MDC1 in der zellulären Antwort auf Schäden in der DNS wirkt.

3 Abbreviations

ATM	Ataxia telangiectasia mutated
ATR	Ataxia telangiectasia and Rad3 related
BRCA1	Breast cancer 1
BRCT	BRCA1 C-terminal
CHK1/2	Checkpoint protein 1/2
CK2	Casein kinase 2
DDR	DNA damage response
DNA-PKcs	DNA-dependent protein kinase catalytic subunit
DSB	DNA double strand break
FHA	Forkhead-associated
GFP	Green fluorescent protein
HR	Homologous recombination
IR	Ionizing radiation
IRIF	Ionizing radiation induced foci
ITC	Isothermal titration calorimetry
MDC1	Mediator of DNA damage checkpoint 1
MEF	Mouse embryonic fibroblast
MRN	MRE11-RAD50-NBS1
NBS	Nijmegen breakage syndrome
NHEJ	Non homologous end joining
NMR	Nuclear magnetic resonance
PIKK	Phosphoinositide-3-kinase-related protein kinase
PNK	Polynucleotide kinase
PST	Pro-Ser-Thr
RNF8	Ring finger protein 8
SCD	SQ-TQ cluster domain
SDT	Ser-Asp-Thr
TBB	Tetrabromo-2-azabenzimidazole

4 Introduction

4.1 General introduction

4.1.1 Importance of maintenance of genome stability for the cell in the context of cancer development

It is very crucial for the survival of each organism that the DNA, which carries the genetic information, is accurately duplicated and transferred from each cell to its daughter cells. Moreover, the DNA has to be protected from mutations, which can cause a variety of diseases including cancer. As the genome is under constant attack from DNA damaging agents, either generated within the cell or originating externally as chemicals or radiation, the surveillance and repair mechanisms that ensure genomic stability are of great importance for all organisms (Figure 1).

Many different types of DNA damages can occur, such as base damage, single-strand breaks, or bulky adduct formation on the DNA. Among the most dangerous lesions for a cell are DNA double-strand breaks (DSBs). Un-repaired DSBs can cause cell death and

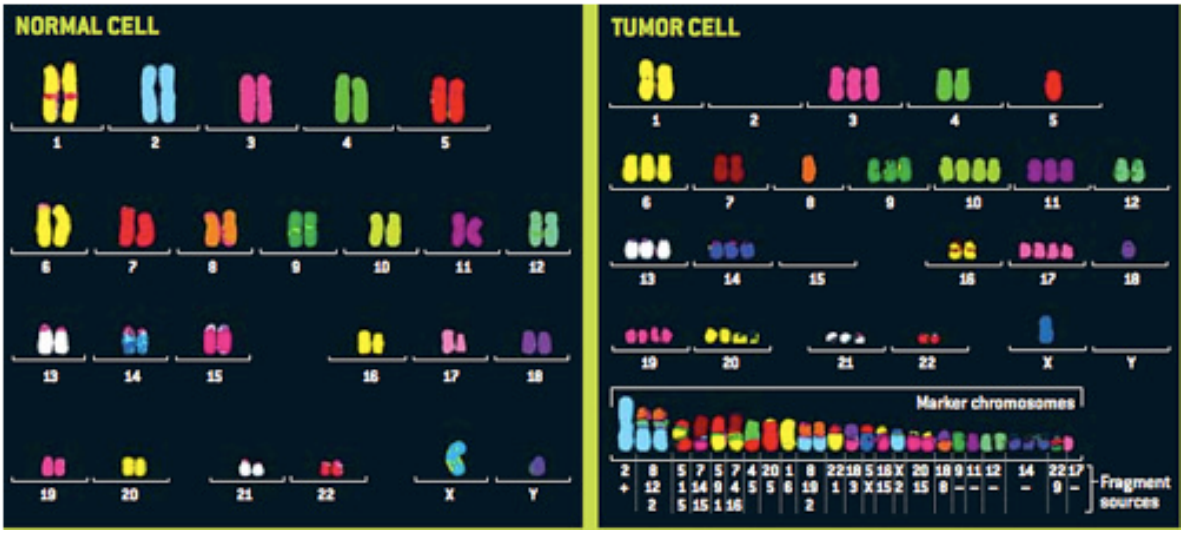

Figure 1 Karyotypes of a normal human cell compared with that of a tumor cell. A normal human's set of chromosomes contains pairs of 23 standard chromosomes (left), whereas a tumor cell exhibits the irregular karyotype (right) described as aneuploid: some whole chromosomes are missing, extra copies of others are present, and many have exchanged fragments. (from: www.physorg.com/news102179512.html; Peter Duesberg, UC Berkeley)

potential outcomes of incorrect repair are chromosomal rearrangements or unfaithful chromosome distribution to daughter cells, with both results being hallmarks of cancer (Khanna and Jackson, 2001). Intrinsic DNA damaging agents such as the metabolically produced reactive oxygen species primarily lead to the damage of single bases or to the formation of single-strand breaks. However, it is generally believed that all of these lesions can lead to the formation of DSBs, for example when two single-strand breaks occur face to face in close proximity on both strands of the DNA double helix, or during unsuccessful repair of other lesions. In addition, DSBs can also arise when the replication fork encounters damaged DNA and collapses (Paulsen and Cimprich, 2007), or as programmed cellular mechanisms such as the generation of antibody diversity (during V(D)J recombination and class switch recombination) and meiotic recombination in the germ cells (Bassing and Alt, 2004).

The importance of efficient detection and accurate repair of DSBs is emphasized by the existence of several human diseases with defects in these processes that often exhibit a predisposition towards cancer (O'Driscoll et al., 2004). Treatment of tumor tissue using irradiation or radiomimetic drugs to kill cancer cells is widely used in the clinics. Although the treatment is more and more optimized to hit only the cancerous tissue, side effects arising from irradiated healthy cells can still not be excluded. Therefore, it is very important to understand the mechanisms that are activated in the surrounding healthy tissue. This would help to predict and assess a patient’s response to radiotherapy, and to optimize the treatment. One major drawback for the use of radiotherapy to treat cancer is the fact that cancerous lesions can acquire radio-resistance (e.g. glioblastomas). Understanding these mechanisms may help to develop efficient methods to sensitize tumor tissues to radiation.

There is another direct link between DSB formation and cancer. The analysis of precancerous and cancerous lesions from human patients showed formation of DSBs in the

absence of any exogenous damaging agent. These observations suggested that a deregulated cell cycle (e.g. through the expression of oncogenes such as ras and myc) might be sufficient to induce high numbers of DSBs, even without inactivation of genes involved in DNA repair and cell cycle checkpoints (so-called caretaker genes). In particular, precancerous lesions showed several indications of DSB formation, such as phosphorylation of H2AX, ATM, CHK2, and p53. In cancer tissue indications for DSB formation was visible as well, but the DNA damage checkpoint pathway was compromised, most often by p53 mutations (Bartkova et al., 2005; DiTullio et al., 2002; Gorgoulis et al., 2005). By reviewing these findings, Halazonetis et al. proposed an oncogene-induced DNA damage model for cancer development (Halazonetis et al., 2008). According to this model, p53 activation in precancerous lesions leads to apoptosis or senescence, thereby raising a barrier to tumor progression. The development into cancer is achieved by impairment of the DNA damage response, most often by p53 mutations. This implies that DSB-formation can serve as an early marker for the onset of cancer. It remains to be shown if this model holds true for all cancers and if (or to what extent) chromosomal instability drives malignant transformation.

4.1.2 The DNA damage response

During the past decade, our understanding of the different signaling pathways that are activated after DNA damage has greatly improved. The whole reaction network to deal with such DNA lesions is generally referred to as the DNA damage response (DDR) (recently reviewed in (Harper and Elledge, 2007)). It has become clear that the central role of the DDR is to ensure accurate repair of DNA lesions, faithful completion of DNA replication and activation of programmed cell death (apoptosis) in the presence of high numbers of DNA

lesions. The first descriptions of the DDR included three main groups of proteins that together formed a complex signaling network (Rouse and Jackson, 2002; Zhou and Elledge, 2000). The sensor proteins are characterized by their ability to bind to aberrant DNA structures and to activate a global DNA damage response. Recognition of aberrant DNA structures then activates transducer proteins (usually kinases) that transmit the signal to a variety of effector proteins. These effectors define the various outcomes of the DDR. Among the most important effector pathways are the regulation and coordination of the different repair mechanisms dealing with different types of DNA lesions. In addition, aberrant DNA structures such as DSBs or long stretches of single-stranded DNA activate cell cycle checkpoints that delay cell cycle progression to allow sufficient time for the completion of the repair. Even failing of the repair pathways does not necessarily result in potentially deleterious consequences for the organism, as cells with too much DNA damage usually undergo apoptosis. For all mechanisms, a specific subset of genes can be activated or repressed at the transcriptional level by the DDR (Figure 2).

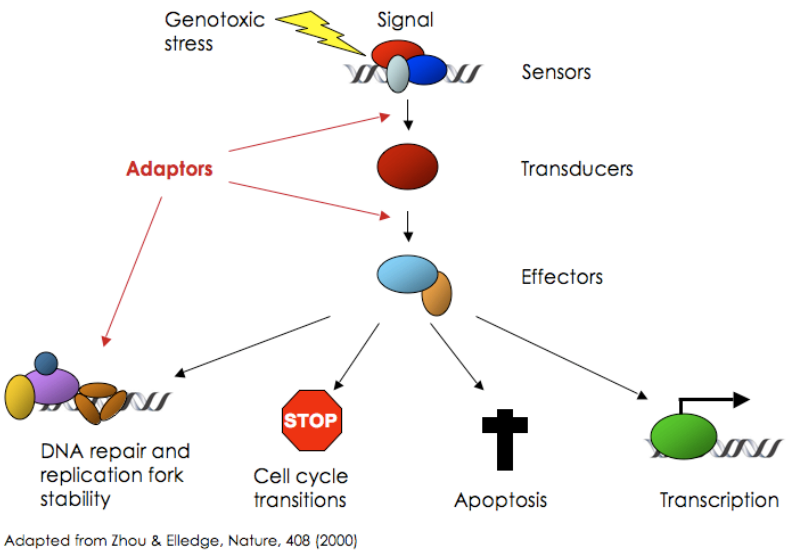

Figure 2 Schematic representation of the DNA damage response. See text for details.

Among the many factors participating in the DDR, two types of kinases play a prominent role. First, there are three kinases related to phosphoinositide 3-kinases (PIKKs) namely ATM, ATR, and DNA-PKcs. These are the first kinases activated after DNA damage and therefore, they are usually referred to as proximal kinases. Second, two classical

transducer kinases exist: CHK1 and CHK2. The various effector proteins are either targeted directly by the proximal kinases or by one or both of the transducer kinases. Moreover, a new group of proteins has recently emerged. These proteins do not have enzymatic activity but instead are composed of protein-protein interaction domains, which serve as recruiting platforms for many proteins involved in DNA damage signaling and repair. Therefore, this group of proteins acts as molecular “matchmakers”, and they are generally referred to as mediators or adaptors.

4.1.3 Ionizing radiation induced nuclear foci formation

A hallmark feature of DSB induction in mammalian cells is the formation of so-called ionizing radiation-induced nuclear foci (IRIF). These nuclear foci can be observed by microscopy and are detectable within minutes after exposure of the cells to ionizing radiation (Fernandez-Capetillo et al., 2003). Maximal brightness and size of IRIF is reached after about 30 minutes. As DSBs are repaired, the IRIF disappear. The major regulator of IRIF formation is the histone H2A variant H2AX, which becomes phosphorylated on Ser139 (termed γH2AX) (Rogakou et al., 1998). While ATR is the primary kinase that phosphorylates H2AX in response to replication stress and UV irradiation (Ward and Chen, 2001; Ward et al., 2004), it has been shown that ATM phosphorylates H2AX in response to DSBs (Burma et al., 2001; Fernandez-Capetillo et al., 2002). In addition, γH2AX is not only present directly at the DNA lesion but spreads over large chromatin regions on both sides of the break. In cells that cannot form γH2AX because of mutations in the phospho-acceptor site, the recruitment of DDR factors to IRIF formation was severely compromised (Celeste et al., 2003a). In addition, mice lacking H2AX are radiosensitive, show male-specific infertility, growth retardation, and defects in immunoglobulin class-switch recombination

(Celeste et al., 2002). This indicates that γH2AX defines an epigenetic signal at sites of DSBs that is recognized by one or several factors, which then promote IRIF formation.

Many proteins that are recruited to IRIF contain protein interaction domains that can specifically recognize phospho-epitopes on other proteins. The best-studied example is the forkhead-associated (FHA) domain, which interacts with proteins containing phosphorylated threonine residues (reviewed in (Durocher et al., 2000a)). Another phospho-interaction domain often observed in proteins that accumulate in IRIF is the tandem BRCT (BRCA1 carboxyl-terminal) domain, which preferentially binds phorsphorylated serine residues (Clapperton et al., 2004; Manke et al., 2003; Williams et al., 2004; Yu et al., 2003).

4.1.4 MDC1 – a key factor for chromatin retention of DDR factors

A few years ago, it was shown that the mediator protein MDC1 (mediator of DNA damage checkpoint 1) directly binds to γH2AX via its tandem BRCT domains (Stucki et al., 2005). In cells where this interaction is disrupted, recruitment of other DDR factors such as NBS1, 53BP1 and the phosphorylated form of ATM to sites of DNA damage is compromised (Lukas et al., 2004; Rodriguez et al., 2003; Stewart et al., 2003; Stucki et al., 2005). The importance of the MDC1-γH2AX interaction was also revealed in MDC1 deficient mice. They recapitulate many phenotypes of the H2AX deficient mice including growth retardation, male infertility, immune defects, chromosome instability, DNA repair defects and radiation hypersensitivity (Lou et al., 2006). It is important to mention that initial recruitment of NBS1, BRCA1, and 53BP1 is independent of H2AX (Celeste et al., 2003b) and MDC1 (Bekker-Jensen et al., 2005; Lou et al., 2006; Lukas et al., 2004), but efficient accumulation and sustained retention of these factors require H2AX and MDC1 (Celeste et al., 2002; Lou et al., 2006; Stewart et al., 2003; Stucki et al., 2005; Ward et al., 2003). The

adaptor protein MDC1 contains several functional domains (Figure 3). Besides the C-terminal tandem BRCT domain responsible for γH2AX binding, MDC1 contains an FHA domain at its N-terminus and a prolin-serine-threonine (PST) rich cluster domain, which seems to be important for DNA repair by homologous recombination (Xie et al., 2007). In addition, the SQ-TQ cluster domain (SCD) of MDC1 is important for DNA damage signaling by recruiting the RNF8 ubiquitin ligase into IRIF (Huen et al., 2007; Kolas et al., 2007; Mailand et al., 2007).

Figure 3 Schematic representation of MDC1 and its functional domains. See text for details.

Recent advances in life cell microscopy of green fluorescent protein (GFP)-tagged protein dynamics together with a new technology to induce DSBs in a defined sub-nuclear volume made it possible to dissect the events that occur in the establishment of IRIF in a spatio-temporal manner. This technique uses cells pre-sensitized with halogenated thymidine analogues in combination with a focused UV laser beam to generate DNA damage in a defined sub-nuclear volume (Lukas et al., 2003). GFP-tagged versions of the DDR proteins MDC1, NBS1, 53BP1, and BRCA1 revealed a fast accumulation of MDC1 and NBS1 at sites of microlaser-induced DNA damage, followed by a second wave of protein recruitment including factors such as 53BP1 and BRCA1 (Bekker-Jensen et al., 2006). It has also become clear that the accumulation and retention of a subset of these factors require the activity of the RNF8 ubiquitin ligase. RNF8 is recruited to chromatin regions flanking DSBs by MDC1 in a mechanism that requires prior phosphorylation of MDC1 by ATM. Recruitment of RNF8 then leads to the ubiquitinylation of the histones H2A

and H2AX and to the subsequent recruitment of another ubiquitin ligase, RNF168. RNF168 amplifies the chromatin ubiquitinylation, which ultimately leads to the efficient IRIF formation by 53BP1 and BRCA1 (Huen et al., 2007; Kolas et al., 2007; Mailand et al., 2007; Wang and Elledge, 2007).

Based on the findings on IRIF formation and the crucial role of γH2AX and MDC1 in this process, the following model for the recognition of DNA DSBs was proposed (Stucki and Jackson, 2006). The initial sensor of a DSB is the MRN complex, which helps to recruit and activate ATM kinase. ATM phosphorylates various target proteins including H2AX molecules that are located in close proximity to the break. In a second step, γH2AX is recognized and bound by MDC1. MDC1 acts as an adaptor protein by binding more molecules of the MRN complex and thereby recruiting more ATM. This leads to a positive feedback loop and to the amplification of the phosphorylation signal over large chromatin regions. A recent publication refined this model by showing that the positive feedback loop does not regulate the spreading of γH2AX, but the density of γH2AX in chromatin flanking

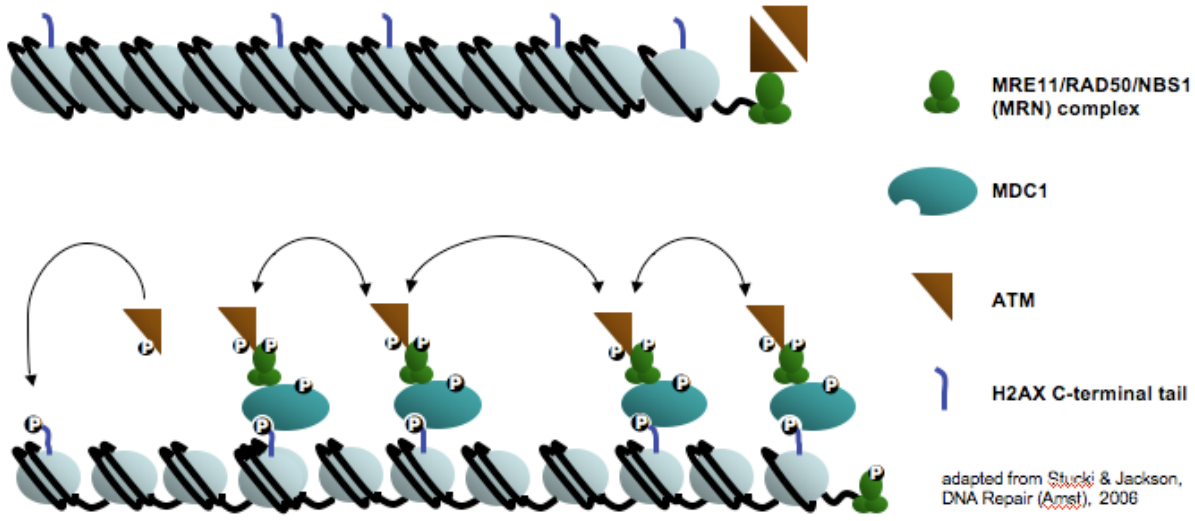

Figure 4 Model for the regulation of H2AX phosphorylation by MDC1. See text for details.

sites of DSBs. In addition, it was shown that although both ATM and DNA-PKcs generate γH2AX, only ATM promotes spreading of the signal to maximal distance and maintains γH2AX densities. MDC1 was not required for spreading of the signal over distal sequences but only for establishment and maintenance of high γH2AX densities near the DSB (Savic et al., 2009) (Figure 4).

4.2 The interaction between MDC1 and the MRN complex

4.2.1 The MRE11-RAD50-NBS1 complex

The MRE11-RAD50-NBS1 (MRN) complex is a highly conserved and essential protein complex involved in DSB repair, checkpoint signaling, DNA replication, meiotic recombination, telomere maintenance, and induction of apoptosis (Difilippantonio et al., 2007; Stracker et al., 2007; Stracker et al., 2004). Each of the three components of the complex is vital for cell survival, as null mutations in any of the three genes (*MRE11*, *RAD50*, and *NBS1*) lead to embryonic lethality in mice (Luo et al., 1999; Xiao and Weaver, 1997; Zhu et al., 2001). MRE11 is a structure specific nuclease and is involved in the 5' to 3' resection of DNA ends, an essential step required for both DSB repair by homologous recombination and activation of the ATR-CHK1 branch of the DNA damage checkpoint response (Jazayeri et al., 2006). The second component of the complex is the ATPase and adenylate kinase subunit RAD50, which is thought to facilitate, together with MRE11, the tethering of DNA molecules to promote repair (Bhaskara et al., 2007; Costanzo et al., 2004). NBS1 has no catalytic activities and could be classified as an adaptor/mediator protein from its domain structure. It contains a FHA and a tandem BRCT domain at its N-terminus and it was shown that the C-terminus of NBS1 interacts directly with ATM (Falck et al., 2005). NBS1 is mutated in a human disease called Nijmegen breakage syndrome

(NBS), and cells from NBS patients show DNA repair and DNA damage signaling deficiencies, including radiosensitivity, chromosomal instability, and checkpoint defects (D'Amours and Jackson, 2002). In addition, a mouse model where the *NBS1* gene was exchanged with hypomorphic mutant alleles recapitulated many features of NBS in the mouse. Although these mice were viable, they displayed defects in development and checkpoint initiation, showed increased chromosomal aberrations, and attenuated ATM activity after a low dose of ionizing radiation (Difilippantonio et al., 2005; Difilippantonio et al., 2007). The MRN complex is thought to be the major sensor for DSBs in mammalian cells. It has intrinsic DSB binding activity (de Jager et al., 2001), is rapidly recruited to DSBs, and is essential for efficient activation of the ATM kinase. Microscopic studies revealed that the MRN complex is distributed to different subcompartments at sites of DSBs (Bekker-Jensen et al., 2006; Lukas et al., 2004). Although a fraction of MRN interacts with single-stranded DNA formed after enzymatic DSB resection, most of the MRN accumulates in IRIF marked by γH2AX.

4.2.2 The interaction between MRN and MDC1

Intensive investigation has been done on the function of the MRN complex at sites of DSBs. It has become clear, that the N-terminal region of NBS1, which contains the FHA and BRCT domain, is necessary for the retention of MRN on chromatin. The disruption of the FHA domain impairs IRIF formation of the entire MRN complex (Cerosaletti and Concannon, 2003; Zhao et al., 2002). In addition, reconstitution experiments of NBS cells revealed that the N-terminus of NBS1 is important for survival, optimal ATM activity, and the intra-S-phase checkpoint after ionizing radiation (Cerosaletti and Concannon, 2004;

Cerosaletti et al., 2006; Cerosaletti and Concannon, 2003; Horejsi et al., 2004; Lee et al., 2003a; Tauchi et al., 2001; Zhao et al., 2002).

Although it was known that the FHA domain of NBS1 is required for MRN IRIF formation, it remained unclear as to how the interaction with the DSB-flanking chromatin is established in detail. An earlier publication suggested that the NBS1-FHA domain interacts directly with γH2AX (Kobayashi et al., 2002). However, recent evidence suggests that the interaction between NBS1 and γH2AX is not direct but mediated by MDC1. Most significantly, several independent studies revealed that siRNA-mediated knockdown of MDC1 in human cells (Goldberg et al., 2003; Lukas et al., 2004; Stewart et al., 2003) or knock out of the MDC1 gene in mouse cells (Lou et al., 2006) prevented the accumulation of the MRN complex at sites of DSBs. Consistent with this, kinetic measurements in living cells showed that NBS1 could not accumulate at DSB-flanking chromatin from the earliest time points after DNA damage in the absence of MDC1, despite the fact that H2AX was efficiently phosphorylated in these regions (Lukas et al., 2004). Moreover, most of the MDC1 could be immunodepleted form cell lysates with antibodies against the MRN core components, indicating that MDC1 interacts with the MRN complex in cell extracts from undamaged cells (Goldberg et al., 2003). This holocomplex dissociates upon modification of the NBS1-FHA domain, suggesting that the N-terminus of NBS1 is important for the interaction between these two factors (Lukas et al., 2004). The observation that MDC1 and NBS1 were recruited with almost identical kinetics to laser-microirradiated stripes in the nucleus supported the model of constitutive MDC1-MRN complex formation. Another indication that the chromatin retention of MRN is mediated by MDC1 came from phospho-peptide pull-down experiments with phosphopeptides derived from the H2AX C-terminus. The MRN complex interacted with these phospho-peptides only in the presence of MDC1 (Lukas et al., 2004). In addition, MDC1 was shown to bind to the phosphorylated C-

terminus of H2AX with high specificity and the crystal structure of the MDC1 BRCT domains together with a γH2AX peptide was solved. This structure suggested that the BRCT domains of MDC1 are uniquely tailored to bind γH2AX (Stucki et al., 2005). Moreover, experimental disruption of the MDC1-γH2AX interaction abrogated the retention of the MRN complex at sites of DNA damage (Stucki et al., 2005). Collectively, these data support the model where MDC1 functions as a molecular matchmaker to induce sustained accumulation of the MRN complex within the DSB-flanking chromosomal region marked by γH2AX. However, the mechanism of MDC1-MRN complex formation remained elusive. In chapter 5.1 and 5.2 of this thesis, the mechanism by which MDC1 mediates MRN accumulation at sites of DSBs is revealed. Moreover, potential functional implication of MRN accumulation is discussed.

4.3 The FHA domain of MDC1 mediates MDC1 dimerization

4.3.1 Structure and binding characteristics of the FHA domains

The forkhead-associated (FHA) domain was discovered originally in forkhead family transcription factors (Hofmann and Bucher, 1995). So far it has been identified in more than 2000 proteins (Pfam database) in prokaryotes and eukaryotes and it is present in many regulatory proteins, kinases, phosphatases, and transcription factors (recently reviewed in (Mahajan et al., 2008)). Among all the different classes of phosphoprotein binding domains, the FHA domain is the only one that specifically recognizes phosphothreonine (pThr) residues. Other domains such as WW and 14-3-3 proteins recognize both pThr and phosphoserine (pSer) residues. FHA domains play important roles in many biological processes such as cell growth, signal transduction, and cell cycle regulation. In particular,

many proteins of the DDR contain FHA domains, as for example the human proteins MDC1, NBS1, RNF8, CHK2 and its yeast orthologue RAD53p.

To date, 16 structures of either free FHA domains, or FHA domains bound to their ligand peptides have been solved by nuclear magnetic resonance (NMR) or X-ray crystallography. Despite low sequence homology between the different FHA domains, they all have a similar fold. The FHA domain consists of approximately 95 to 121 amino acids and contains 11 mandatory β-strands. They form two large β-sheets, which are folded into a β-sandwich structure. The major structural differences occur in the loops and turns that connect the β-strands, and these regions are responsible for the ligand-specificity of the different FHA domains (Figure 5).

Combinatorial peptide library approaches were previously used to identify the ligand specificity of different peptide interaction domains (Songyang et al., 1993; Yaffe and Smerdon, 2004). This method was also applied to identify FHA domain interaction motifs

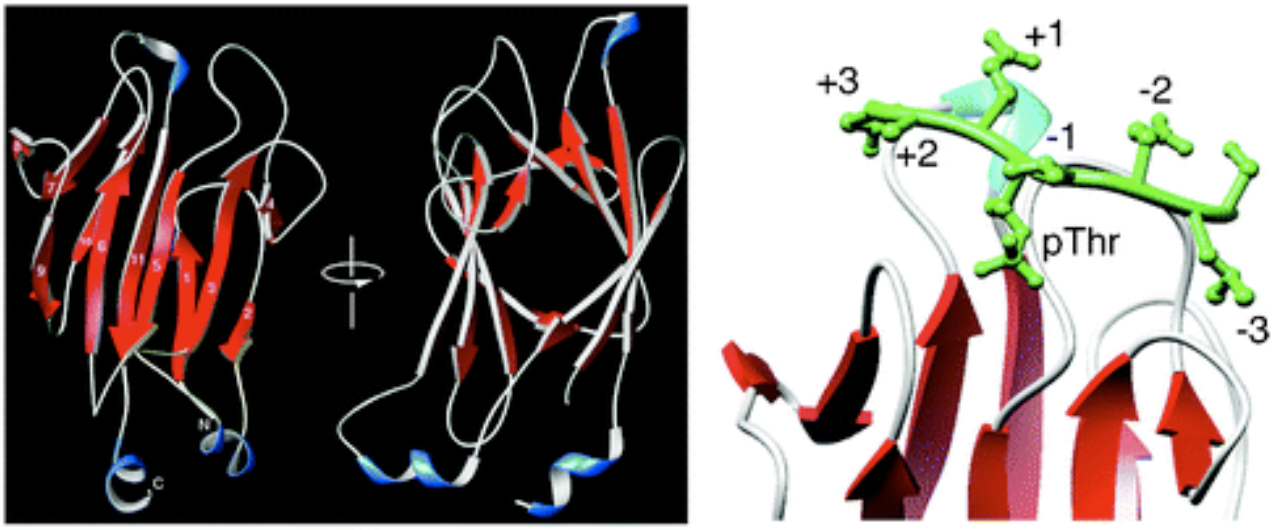

Figure 5 Structure of the RAD53p FHA1 domain. Left: Ribbons representation of the RAD53p FHA1 domain. Right: In vitro-selected pThr-containing peptides bind at one end of the FHA domain, interacting with loops and turns between the β-strands (from: Yaffe and Smerdon, 2004).

using pThr, pSer, or pTyr peptide libraries with two or three randomized residues on each side. The first library screenings were done with the RAD53p-FHA1 domain, and two independent groups showed specificity towards peptides that contain an Asp at the +3 position after the phosphoacceptor Thr residue (pTXXD) (Durocher et al., 2000b; Liao et al., 2000). For the RAD53p-FHA2 domain, the results were less clear suggesting both pYXL (Wang et al., 2000) and pTXXL (Durocher et al., 2000b; Liao et al., 2000) as preferred recognition motifs. Overall, the results of different screenings led to the suggestion of the so called “pThr+3 rule” for FHA domains with the pThr and the residue at the pThr+3 position being the primary and secondary recognition sites, respectively. The preferred +3 residues usually came from two major categories: either Asp or Ile/Leu (Durocher et al., 2000b; Li et al., 2000). There are some exceptions to this rule, as the FHA domain of KAPP (kinase-associated protein phosphatase) prefers Ser or Ala (Ding et al., 2007; Durocher et al., 2000b), whereas the FHA domain of RNF8 (RING-finger protein 8) binds with a strong preference to peptides with Tyr or Phe at the +3 position (Huen et al., 2007).

In addition to this “pThr+3 rule” suggested by the library screenings, other biochemical approaches to identify binding partners of FHA domains revealed different binding specificities. Some FHA domains showed multiple pThr+3 specificities, as for example the FHA1 domain of RAD53 can bind to pTXXD as well as pTXXI sequences (Mahajan et al., 2005). In addition, there are FHA domains that recognize residues both N-terminal and C-terminal to the pThr. This was shown for the interaction of the murine PNK-FHA domain complexed with a peptide derived from its biological target XRCC4, where only the residues N-terminal to pThr were essential for binding (Bernstein et al., 2005). Another example is the DUN1p-FHA domain that interacts with the phosphorylated SQ-TQ cluster domain (SCD) of RAD53p. This interaction leads to the activation of DUN1p (Lee et al., 2003b).

Finally, the FHA domain of KI67 recognizes an extended binding surface rather than a short phosphopeptide sequence (Byeon et al., 2005; Li et al., 2004).

4.3.2 FHA domains that mediate protein dimerization

The human checkpoint kinase 2 (CHK2) is a tumor suppressor, and mutations in *Chk2* were identified in a subset of malignancy-prone Li-Fraumeni syndromes and in sporadic human cancer. CHK2 contains an N-terminal SQ-TQ cluster domain (SCD), an FHA domain, and the kinase domain. Together with CHK1, CHK2 plays a critical role in cell cycle regulation, DNA repair, and DNA damage induced apoptosis (Bartek et al., 2001). Upon DNA damage, CHK2 is phosphorylated by ATM and ATR at Thr68 in the SCD domain (Ahn et al., 2000). This phospho-Thr residue is bound by the FHA domain of other CHK2 molecules, which leads to dimerization or oligomerization of the protein. In a second activation step CHK2 undergoes autophosphorylation at the kinase activation loop, and this is necessary for the full activation of CHK2 (Ahn et al., 2002; Xu et al., 2002). In a more recent approach using expressed protein ligation to generate the N-terminal regulatory region of CHK2, Li et al. were able to show that the phosphorylation of Thr68 stabilized the weak FHA-FHA interactions that occur in the absence of phosphorylation. This study proposed that the dimerization modulates potential phosphodependent interactions with effector proteins and substrates. Furthermore, a mechanism allowing the dissociation of the CHK2 dimer following kinase domain activation was proposed, since the phosphorylation of the FHA domain at Ser140 led to a release of the Thr68 binding (Li et al., 2008). Activated CHK2 phosphorylates various downstream targets, which leads to the activation of cell cycle checkpoints or apoptosis (Bartek et al., 2001).

Similar two-step activation and dimerization mechanisms were also reported for the CHK2 orthologues in yeast: CDS1 in *S.pombe* and RAD53p in *S.cerevisiae*. Upon replication stress, CDS1-FHA domain binds to phosphorylated MRC1, which leads to the recruitment of CDS1 to the upstream kinase RAD3 and the phosphorylation of Thr11 of the CDS1-SCD (Tanaka et al., 2001; Tanaka and Russell, 2004). The CDS1-FHA domain then binds to pThr11, which leads to dimerization and autophosphorylation of CDS1 (Xu et al., 2006). In the case of RAD53p, the mechanism of transactivation is less clear. RAD53p contains two FHA domains, FHA1 and FHA2, which may play diverse and overlapping roles in regulating RAD53p activation and binding to phosphorylated substrates (Pike et al., 2003; Schwartz et al., 2003). In response to DNA damage and replication stress, RAD53p is recruited by two adaptor proteins, RAD9 and MRC1, and phosphorylated by MEC1 (Alcasabas et al., 2001; Osborn and Elledge, 2003; Sun et al., 1998; Sweeney et al., 2005). Following this initial phosphorylation, RAD53 forms dimers or oligomers, which undergo autophosphorylation (Ma et al., 2006)

4.3.3 The FHA domain of MDC1

As mentioned above, MDC1 contains an FHA domain in its N-terminal region. The functional implication of this domain is still not clear, although several interaction partners for the MDC1-FHA domain have been proposed. First, *in vitro* binding assays suggested that the MDC1-FHA domain binds to CHK2 phosphorylated at Thr68. In addition, MDC1 colocalized with pThr68-CHK2 in immunofluorescence experiments (Lou et al., 2003). However, in another study, neither phosphorylated nor unphosphorylated CHK2 could be detected in microlaser-induced DSBs using fixed cells or in cells expressing a GFP-tagged version of the protein. When the recruitment of CHK2 to chromatin was forced by fusing

CHK2 to histone H2B, the DDR was severely compromised. This suggested that upon phosphorylation of CHK2 by ATM and subsequent activation, CHK2 is rapidly distributed throughout the nucleus to reach its physiological targets (Lukas et al., 2003). Second, pull down experiments using the MDC1-FHA domain efficiently retrieved MRE11 out of HeLa nuclear extract, indicating that the MDC1-FHA domain interacts with the MRN complex (Goldberg et al., 2003). Third, the phosphorylated form of the ATM kinase was suggested to bind to the MDC1-FHA domain as well (Lou et al., 2006). In addition to these attempts to identify binding partners for the MDC1-FHA domain, several functional studies were carried out using transient over-expression of the MDC1 FHA domain in cells or using cell lines that express an FHA deletion mutant of MDC1 (MDC1-ΔFHA). These studies revealed that over-expression of the FHA domain alone caused an attenuation of MDC1 recruitment and consequently also abrogated MRN foci formation after IR (Goldberg et al., 2003). Moreover, it was shown that cells expressing the MDC1-ΔFHA deletion mutant had defects in activation of checkpoints and apoptosis pathways, ATM recruitment, and repair of DSBs by homologous recombination (Goldberg et al., 2003; Lou et al., 2006; Lou et al., 2003; Xie et al., 2007).

In chapter 5.3 of this thesis, we provide biochemical, structural and cell biological evidence that the FHA domain of MDC1 regulates DNA damage-induced MDC1 dimerization in a mechanism that is reminiscent of the CHK2 dimerization.

5 Results

5.1 Constitutive phosphorylation of MDC1 physically links the MRE11-RAD50-NBS1 complex to damaged chromatin

J Cell Biol, 2008, Vol **181**, Pages 227-240

My contribution to this work was:

- Discovery of the mechanism of the interaction between MDC1 and MRN
- Design of the experiments (together with M. Stucki)
- Generation of most of the reagents
- Gathering most of the data (except Fig. 4A and 5)
- Proofreading of the manuscript

THE JOURNAL OF CELL BIOLOGY

Published April 14, 2008

JCB: ARTICLE

Constitutive phosphorylation of MDC1 physically links the MRE11–RAD50–NBS1 complex to damaged chromatin

Christoph Spycher,[1] Edward S. Miller,[3] Kelly Townsend,[3] Lucijana Pavic,[1] Nicholas A. Morrice,[4] Pavel Janscak,[2] Grant S. Stewart,[3] and Manuel Stucki[1]

[1]Institute of Veterinary Biochemistry and Molecular Biology and [2]Institute of Molecular Cancer Research, University of Zürich, 8057 Zürich, Switzerland
[3]Cancer Research UK Institute for Cancer Studies, Birmingham University, Birmingham B15 2TT, England, UK
[4]Medical Research Council Protein Phosphorylation Unit, School of Life Sciences, University of Dundee, Dundee DD1 5EH, Scotland, UK

The MRE11–RAD50–Nijmegen breakage syndrome 1 (NBS1 [MRN]) complex accumulates at sites of DNA double-strand breaks (DSBs) in microscopically discernible nuclear foci. Focus formation by the MRN complex is dependent on MDC1, a large nuclear protein that directly interacts with phosphorylated H2AX. In this study, we identified a region in MDC1 that is essential for the focal accumulation of the MRN complex at sites of DNA damage. This region contains multiple conserved acidic sequence motifs that are constitutively phosphorylated in vivo. We show that these motifs are efficiently phosphorylated by caseine kinase 2 (CK2) in vitro and directly interact with the N-terminal forkhead-associated domain of NBS1 in a phosphorylation-dependent manner. Mutation of these conserved motifs in MDC1 or depletion of CK2 by small interfering RNA disrupts the interaction between MDC1 and NBS1 and abrogates accumulation of the MRN complex at sites of DNA DSBs in vivo. Thus, our data reveal the mechanism by which MDC1 physically couples the MRN complex to damaged chromatin.

Introduction

Eukaryotic cells are equipped with sophisticated mechanisms to detect, signal the presence of, and repair DNA damage. Of particular importance are the pathways that deal with DNA double-strand breaks (DSBs): highly toxic lesions that, if unrepaired or repaired incorrectly, can cause cell death, mutations, and chromosomal translocations and can lead to diseases such as cancer. Cells react to DSBs by rapidly deploying a host of proteins to the damaged chromatin regions. Some of these factors engage in DNA repair, whereas others trigger a signaling pathway (called the DNA damage checkpoint) that provokes delays in cell cycle progression and coordinates the repair process; together, these events comprise the so-called DNA damage response (DDR; Zhou and Elledge, 2000).

Among the first proteins that accumulate at sites of DSBs in eukaryotic cells is the MRE11–RAD50–Nijmegen breakage syndrome 1 (NBS1 [MRN]) complex, a conserved and essential DDR factor that functions in a multitude of cellular processes involving DSBs, including DSB repair, checkpoint signaling, DNA replication, meiotic recombination, and induction of apoptosis (Stracker et al., 2004, 2007; Difilippantonio et al., 2007). The MRN complex consists of three subunits. The first is the structure-specific nuclease MRE11, which is most likely involved in nucleolytic processing of DNA ends to allow homologous recombination repair (Jazayeri et al., 2006), and the second is the ATPase and adenylate kinase subunit RAD50, which, together with MRE11, appears to facilitate tethering of DNA molecules to promote DSB repair (Costanzo et al., 2004; Bhaskara et al., 2007). The third subunit of the MRN complex, NBS1, does not exhibit any catalytic activities. Instead, its domain composition suggests that it belongs to the family of adaptor/mediator proteins of the DDR, a group of recently emerging factors that integrate, coordinate, and enhance the various cellular responses to DNA damage by promoting protein–protein interactions (D'Amours and Jackson, 2002). Consistent with this notion, NBS1 features both forkhead-associated (FHA) and BRCA1 C-terminal (BRCT) domains at its N terminus, which are protein interaction modules that specifically mediate the interaction with

Correspondence to Manuel Stucki: m.stucki@vetbio.uzh.ch

Abbreviations used in this paper: ATM, ataxia telangiectasia mutated; BRCT, BRCA1 C terminal; CK, caseine kinase; DDR, DNA damage response; DSB, double-strand break; FHA, forkhead associated; IR, ionizing radiation; MEF, mouse embryonic fibroblast; MR, MRE11 and RAD50; MRN, MRE11–RAD50–NBS1; NBS, Nijmegen breakage syndrome; PIKK, phosphoinositide-3-kinase–related protein kinase; PNK, polynucleotide kinase; pSDpT, phosphorylated SDT peptide; PST, Pro-Ser-Thr; SDT, Ser-Asp-Thr; TBB, tetrabromo-2-azabenzimidazole.

The online version of this article contains supplemental material.

The Journal of Cell Biology, Vol. 181, No. 2, April 21, 2008 227–240
http://www.jcb.org/cgi/doi/10.1083/jcb.200709008

Supplemental Material can be found at:
http://jcb.rupress.org/cgi/content/full/jcb.200709008/DC1

Published April 14, 2008

phosphorylated proteins (Durocher and Jackson, 2002; Glover et al., 2004). Moreover, several NBS1 interaction partners have been described; most prominent among these is the ataxia telangiectasia mutated (ATM) kinase, the key upstream component of DSB signaling (Falck et al., 2005). Mutations in the *NBS1* gene leads to NBS in humans, and cells derived from NBS patients display a DSB repair and signaling deficiency, including radiosensitivity, chromosomal instability, and checkpoint defects (D'Amours and Jackson, 2002). Mouse models in which the native mouse *NBS1* allele was exchanged with hypomorphic mutant alleles recapitulate many features of NBS in the mouse, including developmental defects, chromosomal instability, and checkpoint deficiency (Difilippantonio et al., 2005, 2007).

Accumulation of the MRN complex at sites of DSBs is manifested by the formation of microscopically discernible subnuclear structures, so-called nuclear foci that represent large chromatin regions containing one or several unrepaired DSBs (Maser et al., 1997). The key regulator of nuclear foci formation in higher eukaryotes is the histone variant H2AX, an integral component of the nucleosome core structure that comprises 10–15% of total cellular H2A in higher organisms (Fernandez-Capetillo et al., 2004). H2AX is phosphorylated extensively on a conserved Ser residue at its C terminus in chromatin regions bearing DSBs, and this is mediated mainly by the ATM kinase, a member of the phosphoinositide-3-kinase–related protein kinase (PIKK) family (Burma et al., 2001).

Although it has been previously suggested that MRN accumulation at sites of DSBs occurs through interaction between the FHA/BRCT region of NBS1 and phosphorylated H2AX (γ-H2AX; Kobayashi et al., 2002), recent evidence suggests that the interaction between NBS1 and γ-H2AX is not direct but is mediated by MDC1, a large nuclear factor that interacts with the MRN complex and also features the criteria of a DDR mediator/adaptor protein, including the presence of FHA and BRCT domains (for review see Stucki and Jackson, 2004). First, it was shown that MDC1 exists in a complex with MRN in extracts of undamaged cells (Goldberg et al., 2003). This complex dissociates upon modification of the N-terminal FHA domain of NBS1, suggesting that the NBS1 FHA domain may be participating in the interaction between the two factors (Lukas et al., 2004). Second, MDC1 directly and specifically interacts with the phosphorylated H2AX C terminus through its tandem BRCT domains (Stucki et al., 2005). The x-ray structure of the MDC1–γ-H2AX complex suggests that the MDC1 BRCT domains are uniquely tailored to interact with the γ-H2AX chromatin mark (Stucki et al., 2005). Third, a phosphopeptide derived from the H2AX C terminus interacted with the MRN complex only in the presence of MDC1 (Lukas et al., 2004). Fourth, experimental disruption of the interaction between MDC1 and γ-H2AX (Stucki et al., 2005) or loss of MDC1 expression by genetic manipulation and/or siRNA-mediated depletion leads to a complete abrogation of MRN foci formation (Goldberg et al., 2003; Stewart et al., 2003; Lukas et al., 2004; Lou et al., 2006). Finally, mutations in the N-terminal FHA/BRCT region of NBS1 also interfere with MRN accumulation at sites of DSBs (Kobayashi et al., 2002; Zhao et al., 2002; Cerosaletti and Concannon, 2003; Lee et al., 2003; Horejsi et al., 2004).

MDC1 is composed of several distinct sequence domains. Besides an FHA domain at its N terminus and the γ-H2AX–interacting BRCT tandem domain at the C terminus, MDC1 also features a unique repeat region in the middle of the protein (Pro-Ser-Thr [PST] repeat) and contains several highly conserved putative PIKK target sites, some of which are phosphorylated in response to DNA damage in vivo (Matsuoka et al., 2007). In addition, MDC1 is also phosphorylated in the absence of DNA damage: several recent large-scale phosphorylation site screens of the human and mouse proteome revealed that MDC1 is constitutively phosphorylated on a significant number of Ser and Thr residues in vivo (Beausoleil et al., 2004; Olsen et al., 2006; Villen et al., 2007).

Although it is well established that MDC1 mediates the accumulation of many DDR factors in damaged chromatin regions (including the MRN complex, 53BP1, BRCA1, and ATM; Stucki and Jackson, 2006), it is still unclear how MDC1 mediates MRN recruitment. The observation that MDC1 exists in a complex with MRN in extracts from undamaged cells suggests that MDC1 may recruit MRN to γ-H2AX–containing chromatin in a simple "piggyback ride" mechanism whereby the physical interface between the two factors is made up by the NBS1 N-terminal FHA/BRCT region and by one or several phosphoepitopes on MDC1.

To put such a mechanism to the test, we set up an in vivo complementation system for MDC1 to search for a region in MDC1 that is responsible to mediate MRN foci formation. Through this approach, we identified a new region in MDC1 that is composed of several acidic repeats featuring a unique sequence motif, the Ser-Asp-Thr (SDT) motif. Furthermore, we provide evidence that these SDT repeats are constitutively phosphorylated by caseine kinase 2 (CK2) and that the phosphorylated form of these motifs constitute the phosphoepitope that the NBS1 FHA domain is binding to. These findings allow us to draw a model of the mechanism by which MDC1 physically links the MRN complex to damaged chromatin.

Results

An acidic region near the N terminus of MDC1 is essential for NBS1 foci formation

Efficient accumulation of the MRN complex in foci at sites of DSBs is critically dependent on MDC1 (Goldberg et al., 2003; Lukas et al., 2004). To determine the region of MDC1 that mediates MRN foci formation, we transfected MDC1$^{-/-}$ mouse embryonic fibroblasts (MEFs; Lou et al., 2006) with a series of N-terminal deletion mutants of mouse MDC1 and assessed MRN accumulation by indirect immunofluorescence using an antibody specific for mouse NBS1 (Celeste et al., 2003). Consistent with published data (Lou et al., 2006), MDC1$^{-/-}$ MEFs were completely defective for NBS1 accumulation (unpublished data), but transient transfection of these cells with HA-tagged full-length mouse MDC1 readily restored NBS1 foci formation in response to 5 Gy of ionizing radiation (IR; Fig. 1 B, WT). Deletion of 153 and 295 N-terminal amino acids of MDC1 did not result in any detectable reduction of NBS1 foci (Fig. 1 B, ΔN1 and ΔN2), but deletion of 452 and 645 amino acids led to a complete loss of NBS1 accumulation (Fig. 1 B, ΔN3 and ΔN4). This indicated that the region in MDC1 essential for mediating NBS1 accumulation is located somewhere between amino acids 295 and 452. Indeed, internal deletion of this 157–amino acid region completely abolished

Published April 14, 2008

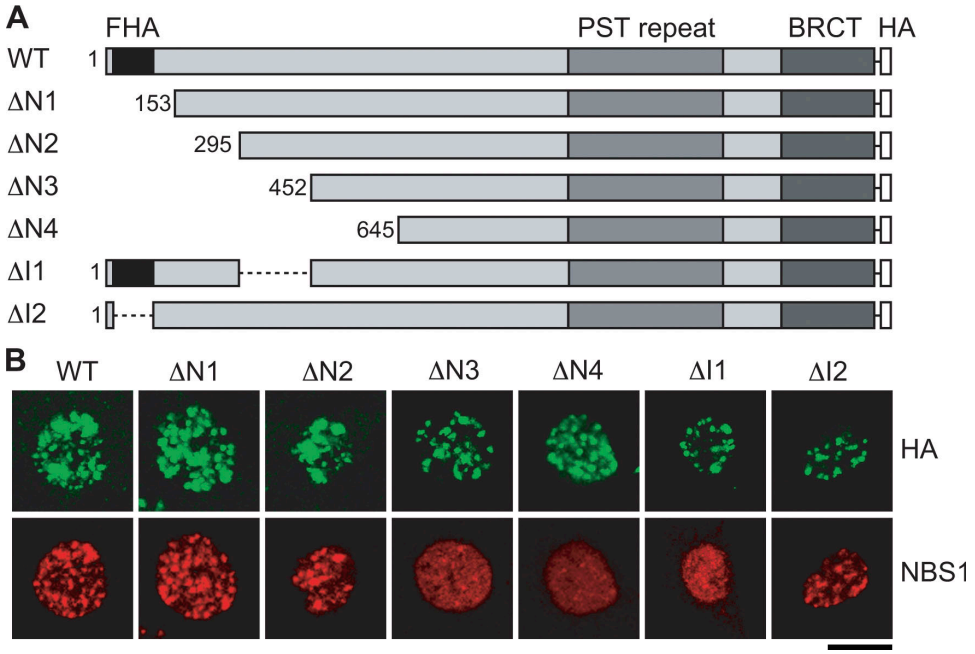

Figure 1. **An acidic domain near the N terminus of MDC1 is essential for NBS1 foci formation.** (A) Schematic representation of HA-tagged full-length mouse MDC1 and various deletion mutants. (B) MDC1$^{-/-}$ MEFs were transiently transfected with wild-type (WT) MDC1 and the individual deletion constructs. 48 h later, cells were irradiated, fixed with methanol, and stained with antibodies specific for HA and mouse NBS1. Nuclear foci were assessed by confocal microscopy. Bar, 10 µm.

the ability of MDC1 to mediate NBS1 foci formation (Fig. 1 B, ΔI1). Preliminary sequence analysis of this region revealed a significant abundance of acidic amino acids as compared with other regions of MDC1 (Fig. 2 A).

Interestingly, deletion of a region between amino acids 51 and 107 of mouse MDC1 (containing the FHA domain) did not have any effect on NBS1 accumulation (Fig. 1, ΔI2) even though overexpression of the FHA domain was reported to trigger a dominant-negative effect on NBS1 foci formation (Goldberg et al., 2003). In summary, these results suggest that an acidic region near the N terminus of MDC1 mediates MRN accumulation at sites of DSBs.

Phosphorylation-dependent interaction between the MDC1 N terminus and the MRN complex

To understand how the region identified by the systematic deletion analysis mediates MRN foci formation, we carefully analyzed the sequence between amino acids 295 and 452 of mouse MDC1. As mentioned in the previous section, this region of MDC1 is highly acidic with a calculated isoelectric point of 4.04. To detect conserved sequence motifs within this region, we compared the mouse sequence to MDC1 sequences from other vertebrate species (including human, dog, swine, and zebrafish). This analysis revealed several conserved patches of 8–10 amino acids interspersed with less conserved regions of variable length (Fig. 2 A; patches are highlighted by horizontal bars). The conserved patches feature a repeated sequence motif: Ser and Thr residues are embedded in an acidic sequence environment. A single amino acid (typically Asp) sits in between the highly conserved Ser and Thr residues. Thus, we hereafter refer to this motif as the SDT motif. The motif also contains two to three consecutive acidic amino acids (usually Glu) that are five residues C terminal to the initial Ser. Mammalian MDC1 contains a total of six SDT motifs (Fig. S1, available at http://www.jcb.org/cgi/content/full/jcb.200709008/DC1): five are located within the region of MDC1, whose deletion abrogates MRN foci (Fig. 2 A), and one is located ∼80 amino acids N terminal to this region (not depicted). Zebrafish MDC1 features a total of eight SDT motifs, and even honey bee MDC1 (the only clear nonvertebrate MDC1 orthologue identified to date) comprises a very similar motif (Fig. S1), indicating that the SDT motif is conserved in all known MDC1 orthologues.

In untreated mammalian cells, MDC1 is a phosphoprotein that becomes rapidly hyperphosphorylated in response to DNA damage in a PIKK-dependent manner (Goldberg et al., 2003; Stewart et al., 2003). A large number of constitutive and DNA damage–induced phosphorylation sites have recently been identified in MDC1 by means of several large-scale mass spectrometry screens of the human and mouse proteome (Beausoleil et al., 2004; Olsen et al., 2006; Matsuoka et al., 2007; Villen et al., 2007). Interestingly, many of the constitutive phosphorylation sites of MDC1 are located within the SDT motifs (Fig. 2 A). In summary, it appears that in human cells, a population of MDC1 molecules is phosphorylated on any Ser and Thr residue in at least four of the six SDT motifs in vivo (Beausoleil et al., 2004; Olsen et al., 2006). In addition, mouse MDC1 appears to be phosphorylated in at least one SDT motif (Villen et al., 2007).

Published April 14, 2008

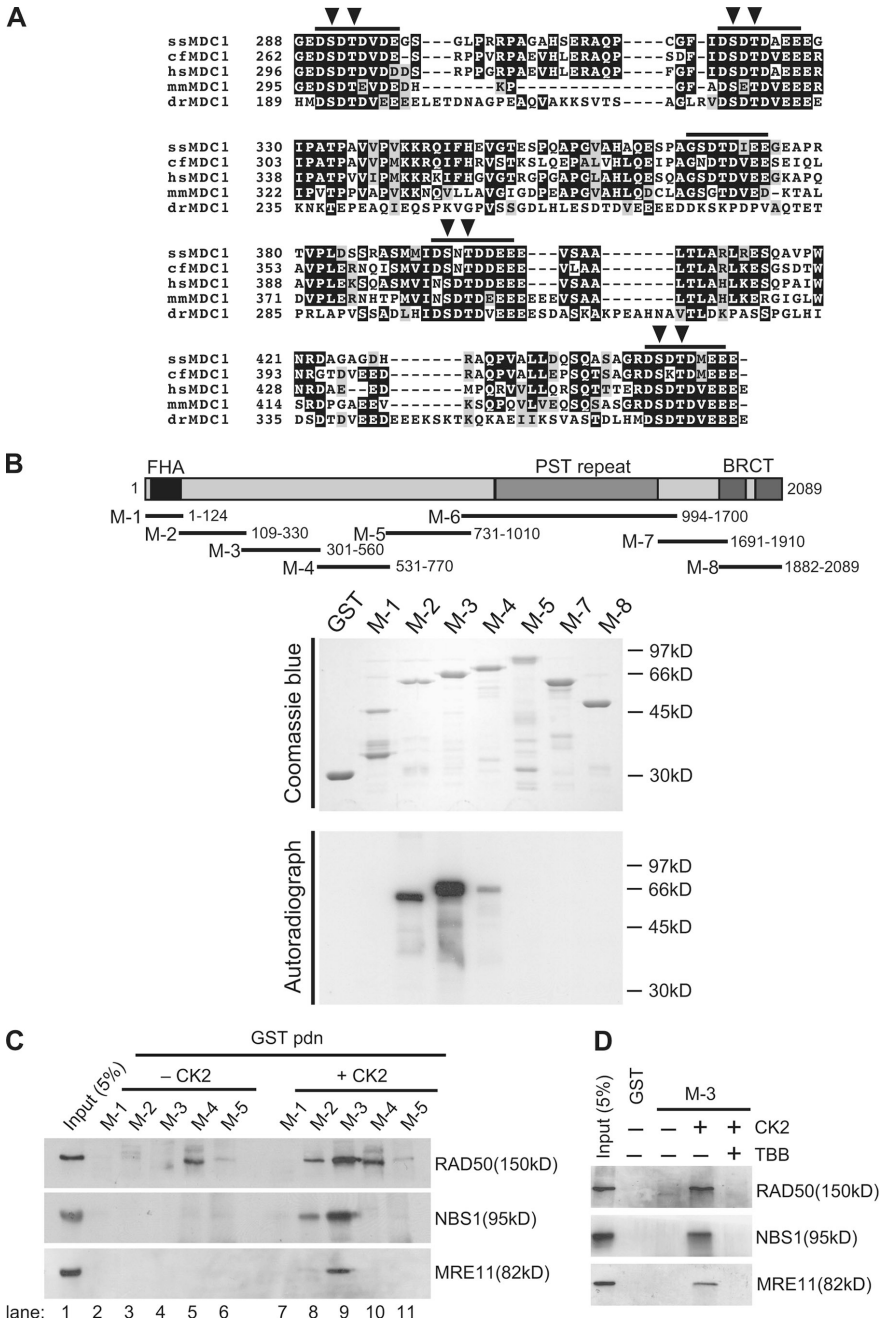

Figure 2. **Phosphorylation-dependent interaction between the MDC1 N terminus and the MRN complex.** (A) Sequence alignment of the region in MDC1 that is essential for MRN foci. The conserved acidic motifs are highlighted by horizontal bars. Phosphorylated residues identified by in vivo phosphorylation site mapping are highlighted by arrowheads (Beausoleil et al., 2004; Olsen et al., 2006; Villen et al., 2007). (B, top) Representation of human MDC1 and the overlapping GST fragments. (bottom) Two fragments at the N terminus of MDC1 are phosphorylated by CK2 in vitro. Purified GST-MDC1 fragments were incubated with purified recombinant CK2 in the presence of radioactive ATP. Proteins were separated by SDS-PAGE, and dried gels were subjected to autoradiography. A Coomassie blue–stained gel of the purified GST fragments is shown on top of the autoradiograph. Note that fragment M-6 (PST repeat region) was not expressed in bacteria. (C) Purified GST-MDC1 fragments (M-1–5) were preincubated with and without recombinant CK2 in the presence of ATP. (D) Purified GST-MDC1 fragment M-3 was preincubated with CK2 either in the presence or absence of the CK2 inhibitor TBB. (C and D) The fragments were then used to pull down proteins from HeLa nuclear extract. Bound proteins were separated on SDS-polyacrylamide gels followed by immunoblotting. The blots were probed with antibodies against RAD50, NBS1, and MRE11.

Published April 14, 2008

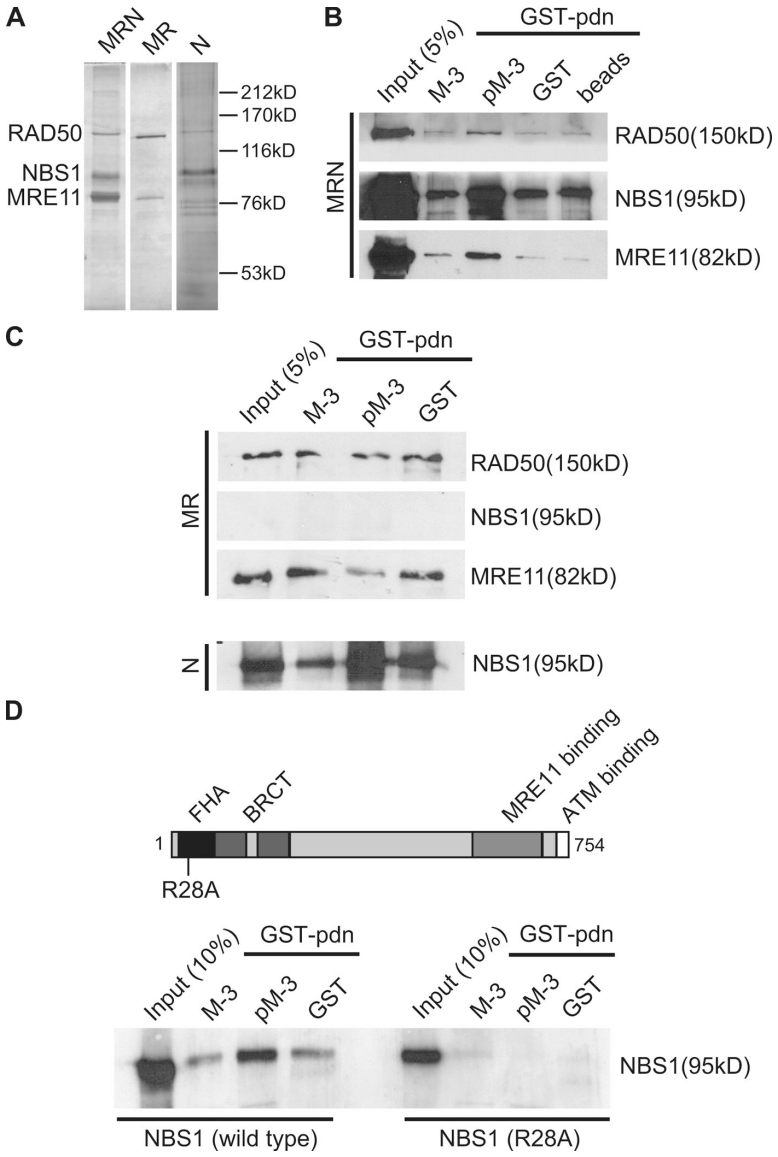

Figure 3. **Direct interaction between the phosphorylated MDC1 N terminus and the MRN complex is mediated by the NBS1 FHA domain.** (A) MRN proteins were purified as described in Materials and methods. Proteins were separated on SDS-polyacrylamide gels and stained with silver. MR, MRE11–RAD50 subcomplex; N, partially purified NBS1. (B and C) Purified GST-MDC1 fragment M-3 comprising part of the SDT region was preincubated with CK2 and ATP. The fragment was incubated with purified MRN complex (B), purified MR subcomplex (C, top), and partially purified NBS1 (C, bottom) followed by GST pull-down analysis. Bound proteins were separated on SDS-polyacrylamide gels followed by immunoblotting. The blots were probed with antibodies against RAD50, NBS1, and MRE11. (D, top) Schematic representation of NBS1 with its functional domains. (bottom) Purified GST-MDC1 fragment M-3 was preincubated with CK2 and ATP. The fragment was incubated with purified MRN complex where the NBS1 subunit was either wild type or contained a point mutation in the FHA domain (R28A). Bound proteins were separated on SDS-polyacrylamide gels followed by immunoblotting. The blots were probed with a polyclonal antibody against NBS1.

The acidic nature of the SDT motif suggests that it may be targeted by acidophilic kinases such as CK1 and 2. Indeed, analysis of the MDC1 SDT domain by Scansite (Yaffe et al., 2001) revealed that the sequence encompassing the Ser and Thr residues within the SDT motifs conform to consensus CK2 phosphorylation sites. To test whether CK2 would specifically phosphorylate MDC1 in the SDT region, we generated eight overlapping random fragments of the human MDC1 cDNA and expressed them in *Escherichia coli* as GST fusion proteins. Seven fragments were expressed well and were purified (Fig. 2 B, top), whereas one fragment (M-6) comprising the MDC1 PST repeat region was not expressed in bacteria. The purified fragments were subjected to an in vitro kinase assay using recombinant CK2. CK2 efficiently phosphorylated fragment M-2 (amino acids 109–330) and M-3 (amino acids 301–560) but none of the other five fragments. Fragment M-2 contains two SDT motifs, and fragment M-3 contains the other four SDT motifs.

MDC1 exists in a complex with MRN in extracts derived from undamaged cells, indicating that these proteins interact constitutively (Fig. S2, available at http://www.jcb.org/cgi/content/full/jcb.200709008/DC1). However, the mechanism of this interaction has not yet been elucidated. Significantly, GST pull-down analysis with our GST-MDC1 fragments revealed that fragment M-2 and M-3 only pulled down significant quantities of the MRN complex from HeLa nuclear extract when preincubated with recombinant CK2 and ATP (Fig. 2 C, compare lanes

Published April 14, 2008

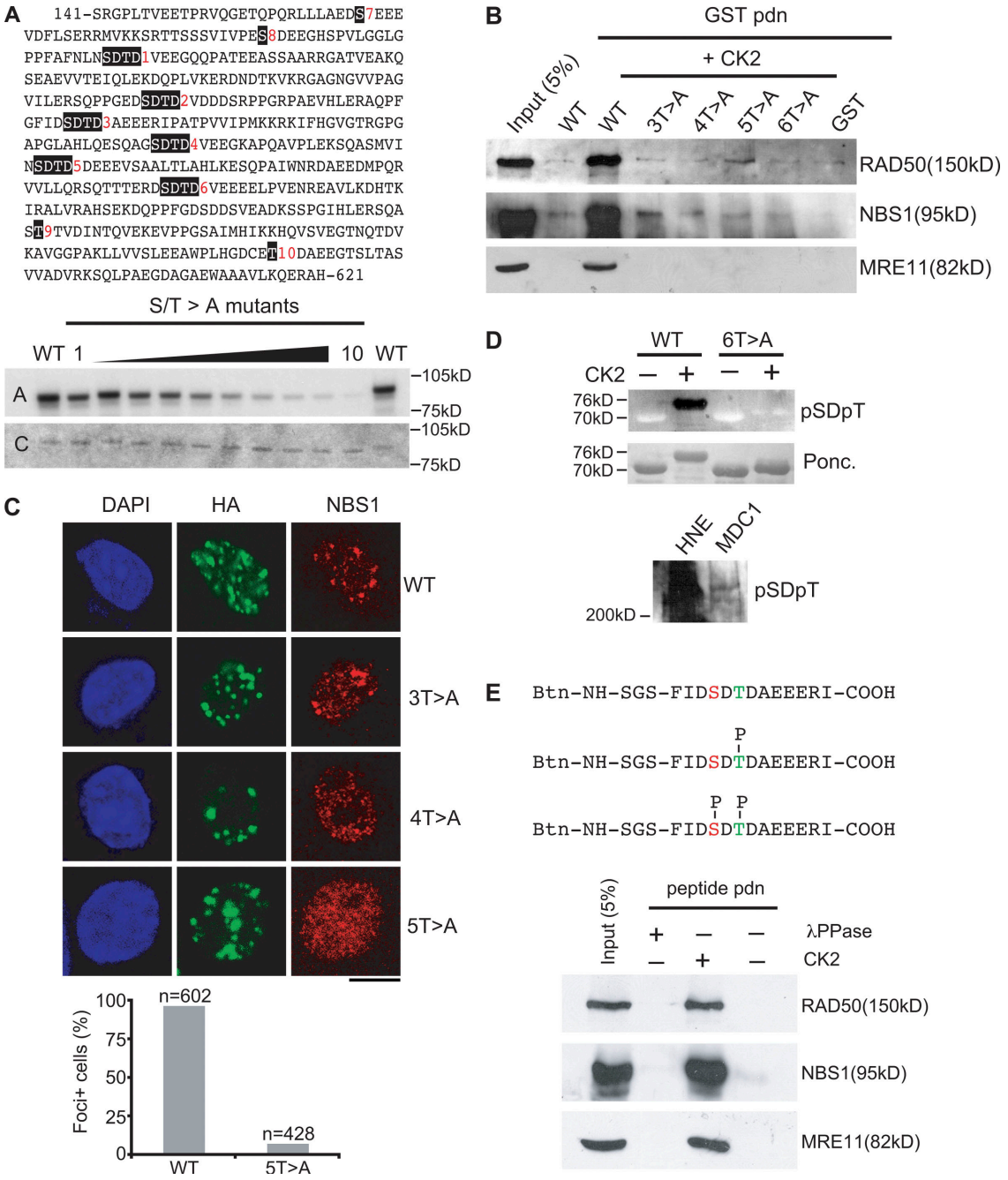

Figure 4. **A repeated phosphorylated motif in MDC1 mediates the interaction between MDC1 and NBS1.** (A) In vitro mapping of the CK2 phosphorylation sites in MDC1. (top) Sequence of the human MDC1 fragment comprising the conserved CK2 consensus sites (highlighted in black). The CK2 consensus sites are numbered from 1 to 10. (bottom) All of the putative CK2 phosphoacceptor Ser and Thr residues in the above MDC1 fragment (amino acids 141–621) were mutated to Ala, and the mutants were expressed as GST fusion proteins in *E. coli*. The GST fragments were incubated with purified recombinant CK2 in the presence of radioactive ATP. Proteins were separated by SDS-PAGE, and dried gels were subjected to autoradiography. A, autoradiograph; C, Coomassie blue–stained gel. (B) The SDT repeats are essential for the interaction between MDC1 and NBS1 in vitro. Several SDT motifs in a fragment derived from mouse MDC1 (amino acids 221–456) were mutated to SDA (3T>A: T362A, T387A, and T444A; 4T>A: T315A, T362A, T387A, and T444A; 5T>A: T300A, T315A, T362A, T387A, and T444A; 6T>A: T222A, T300A, T315A, T362A, T387A, and T444A) and were expressed as GST fusion proteins in *E. coli*. The purified fragments were preincubated with recombinant CK2 in the presence of ATP. The fragments were then used to pull down proteins from HeLa nuclear extract. Bound proteins were separated on SDS-polyacrylamide gels followed by immunoblotting. The blots were

Published April 14, 2008

Table I. **Tryptic MDC1 phosphopeptides**

MDC1 tryptic peptide	CK2 phosphorylation site
162-LLLAEDpSEEEVDFLSER-179	pS168
186-TTSSSVIVPESDEEGHSPVLGGLGPPFAFNLN(pSDpT)DVEEGQQPATEEASSAAR-238	$+2PO_4$
247-QSEAEVVTEIQLEKDQPLVK-266	NA
292-SQPPGEDpSDpTDVDDDSRPPGRPAEVHLERAQPFGFIDpSDpTDAEEERIPATPVVIPMK-348	pS299, pT301, pS329, pT331
361-PGAPGLAHLQESQAGpSDpTDVEEGKAPQAVPLEKSQASMVINpSDpTDDEEEVSAALTLAHLK-420	pS376, pT378, pS402, pT404
445-SQTTTERDpSDpTDVEEEELPVENR-467	pS453, pT455

NA, not applicable.

3 and 4 with lanes 8 and 9; note that the bands in lanes 5 and 10 in the top panel result from a cross-reactivity of the RAD50 antibody with a contaminating bacterial protein in the GST–M-4 fraction). In the absence of CK2, no interaction could be observed under these conditions (Fig. 2 C, lanes 2–6). In the presence of the specific CK2 inhibitor tetrabromo-2-azabenzimidazole (TBB), recombinant CK2 did not transform fragment M-3 into a form capable of pulling down the MRN complex from HeLa nuclear extract, indicating that CK2 activity is required for this process (Fig. 2 D). Together, these data suggest that the phosphorylated N-terminal region in MDC1 mediates the interaction with the MRN complex in vitro.

Direct interaction between the phosphorylated MDC1 N terminus and the MRN complex is mediated by the NBS1 FHA domain

To determine whether the MRN complex interacts directly with the phosphorylated MDC1 N terminus, we coexpressed all three MRN subunits and a subcomplex consisting of MRE11 and RAD50 (MR) in Sf9 cells by means of recombinant baculovirus infection followed by purification of the recombinant proteins to near homogeneity (Fig. 3 A, MRN and MR). We also isolated partially purified NBS1 alone (Fig. 3 A, N). Interaction studies with purified recombinant MRN, MR, and NBS1 were complicated by the fact that these proteins exhibited a significant unspecific binding activity toward the glutathione–Sepharose beads used in this analysis (Fig. 3 B, beads alone). Nevertheless, we consistently observed a significant enrichment of purified MRN and partially purified NBS1 when we used CK2-phosphorylated fragment M-3 in the pull-down assay (Fig. 3, B and C; bottom). Untreated M-3 or GST alone did not result in such enrichment. Similarly, neither phosphorylated nor unphosphorylated M-3 was capable of efficiently binding to MRE11/RAD50 in the absence of NBS1 (Fig. 3 C, top). In summary, these results indicate that the NBS1 subunit of the MRN complex directly associates with the phosphorylated M-3 fragment of MDC1 and mediates the interaction between MDC1 and the MRN complex.

NBS1 features two well-established phosphopeptide recognition modules at its N terminus: an FHA domain and a tandem BRCT domain (Fig. 3 D, top). It was previously shown that introduction of a point mutation in the FHA domain that changes a conserved Arg residue to Ala (R28A) disrupted the interaction between MDC1 and the MRN complex in vitro (Lukas et al., 2004) and abolished MRN accumulation at sites of DSBs in vivo (Cerosaletti and Concannon, 2003; Lee et al., 2003; Horejsi et al., 2004; Lukas et al., 2004). Thus, we isolated the MRN complex harboring the same mutation in NBS1 from baculovirus-infected Sf9 cells and compared its binding activity toward the phosphorylated M-3 fragment to the wild-type complex. Significantly, although the wild-type NBS1 readily interacted with phosphorylated M-3, no interaction was detected with the R28A mutant (Fig. 3 D). This indicates that an intact NBS1 FHA domain is essential for the interaction between the phosphorylated N-terminal region of MDC1 and the MRN complex.

A repeated phosphorylated motif in MDC1 mediates the interaction between MDC1 and NBS1

To map the phosphorylation sites within fragments M-2 and M-3 of MDC1, we isolated a new GST fragment comprising amino acids 141–621 of human MDC1 (M-SDT). The purified fragment was phosphorylated in vitro by recombinant CK2 followed by digestion with trypsin. The tryptic peptides were then analyzed by mass spectrometry. Thus, several phosphorylation sites were mapped (Table I), most notably all six of the conserved SDT motifs that were targeted by CK2 on both Ser and Thr residues. Next, all of the putative CK2 target Ser and Thr residues in the M-SDT fragment were mutated to Ala and expressed in *E. coli* (Fig. 4 A, top; the SDT motifs and other putative CK2 target sites are highlighted in black and numbered from 1–10). The purified mutants were subjected to in vitro phosphorylation by re-

probed with antibodies against RAD50, NBS1, and MRE11. (C) Mutation of a subset of the conserved SDT motifs abrogates NBS1 foci formation. (top) $MDC1^{-/-}$ MEFs were transiently transfected with various forms of HA-tagged full-length mouse MDC1, including wild-type (WT) and SDT-deficient (3T>A: T362A, T387A, and T444A; 4T>A: T315A, T362A, T387A, and T444A; 5T>A: T300A, T315A, T362A, T387A, and T444A) variants. 48 h later, cells were irradiated, fixed with methanol, and stained with antibodies against HA and mouse NBS1. (bottom) HA-positive cells were scored for NBS1 foci in wild-type and 5T>A-transfected populations (results were consistent in two independent datasets). (D) The SDT in MDC1 is phosphorylated in vivo. (top) A phosphospecific antibody raised against a doubly phosphorylated SDT peptide (pSDpT) was tested on CK2-phosphorylated GST-SDT. WT, mouse MDC1 (amino acids 221–456); 6T>A, all six SDT motifs were mutated to SDA. (bottom) Immunoblot analysis of phosphorylated MDC1 isolated from HeLa nuclear extract by a H2AX phosphopeptide using the pSDpT phosphospecific antibody. (E) A synthetic biotinylated peptide comprised of the SDT sequence motif and phosphorylated on the Thr residue was either left untreated or was preincubated with λ−PPase and CK2, respectively. (top) This leads to the three indicated products: unphosphorylated peptide, singly phosphorylated peptide (Thr), and doubly phosphorylated peptide (Ser and Thr). The peptides were then used to pull down proteins from HeLa nuclear extract. Proteins were detected as in B. Bar, 10 μm.

Published April 14, 2008

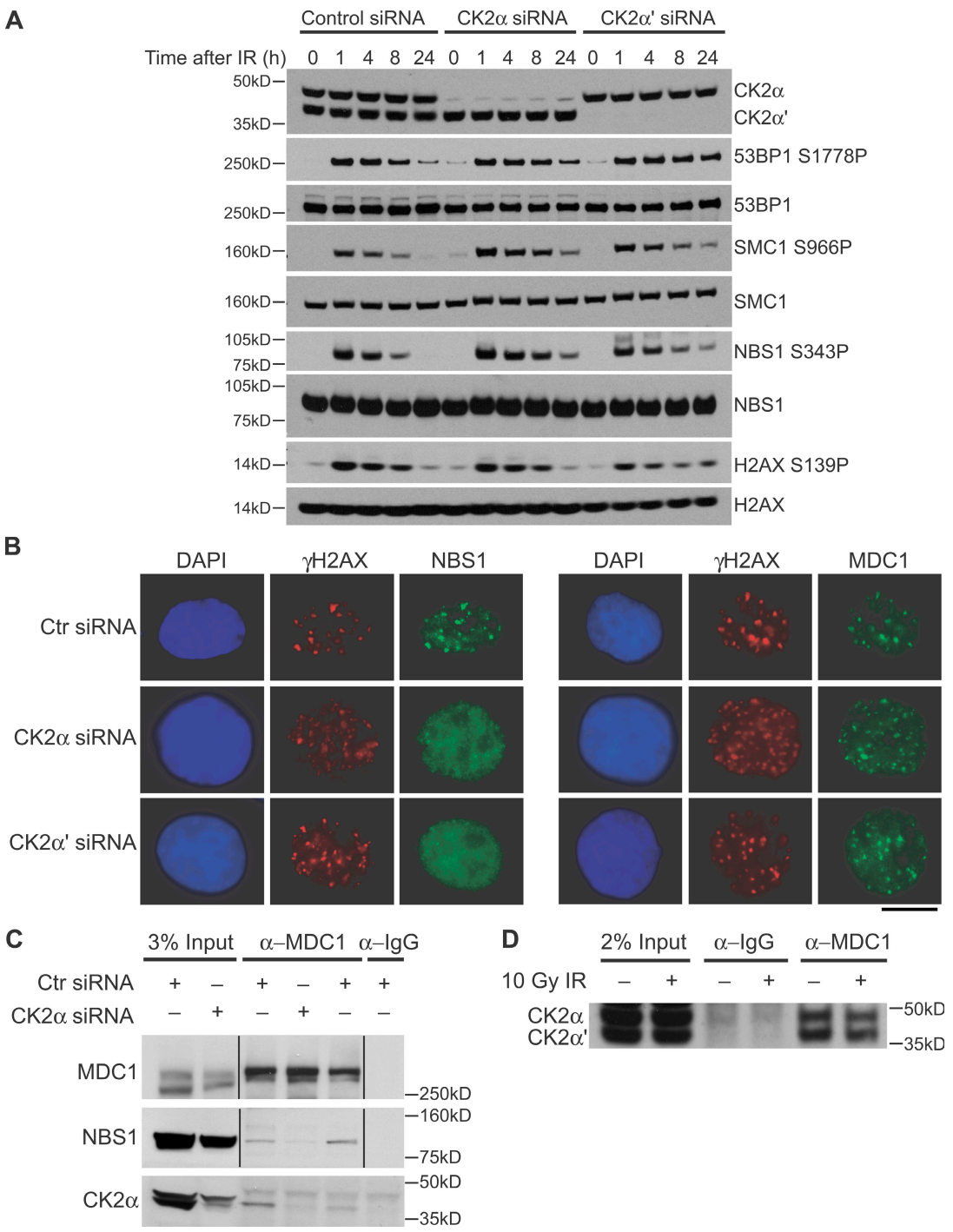

Figure 5. **CK2 is essential for the interaction between MDC1 and NBS1 and for the accumulation of NBS1 at sites of DSBs in vivo.** (A) Down-regulation of CK2α and CK2α′ by siRNA triggers a prolonged DDR. 72 h after transfection with siRNA duplexes, cells were irradiated and harvested at the indicated time points. Extracts were prepared and resolved by SDS-PAGE followed by immunoblotting. The blots were probed with the indicated antibodies. (B) Down-regulation of CK2α and CK2α′ by siRNA abrogates NBS1 accumulation at sites of DSBs. 72 h after transfection with siRNA duplexes, cells were irradiated, fixed with methanol, and stained with antibodies against γ-H2AX and NBS1. (C) Down-regulation of CK2α by siRNA disrupts the interaction between MDC1 and NBS1 in vivo. 72 h after transfection with siRNA duplexes, cells were lysed, and immunoprecipitation was performed using the

Published April 14, 2008

combinant CK2, and radioactive phosphate incorporation was measured by autoradiography (Fig. 4 A). This analysis revealed that all of the SDT motifs and other putative CK2 target sites were efficiently phosphorylated in vitro.

To test whether the highly conserved SDT repeats were necessary for the interaction with the MRN complex, we changed the conserved Thr residues to Ala within several SDT motifs and phosphorylated the isolated GST fusion proteins by CK2 in vitro. Significantly, GST pull-down analysis with the mutant fragments revealed that only the phosphorylated wild type was capable of pulling down significant quantities of the MRN complex from HeLa nuclear extract, whereas alteration of the three C-terminal SDT motifs (Fig. 4 A, 4–6) already reduced the interaction to almost background level (Fig. 4 B).

To test whether the SDT repeats of MDC1 mediate NBS1 accumulation at sites of DSBs in vivo, we introduced the same SDT mutations as before (Fig. 4 B) in the tagged full-length mouse MDC1 cDNA followed by transient transfection of MDC1$^{-/-}$ MEFs with those mutants and assessment of MDC1 and NBS1 foci formation by indirect immunofluorescence. Surprisingly, alteration of the last three C-terminal SDT motifs (Fig. 4 A, 4–6) did not trigger any significant reduction in NBS1 foci formation (Fig. 4 C, 3T>A) even though the corresponding GST fusion protein only weakly interacted with the MRN complex in vitro (Fig. 4 B, 3T>A). However, mutation of four SDT motifs (Fig. 4 A, 3–6) led to a detectable reduction in NBS1 accumulation even though small NBS1 foci were still detectable in a subset of the transfected cells (Fig. 4 C, 4T>A). Altering five of the six SDT motifs (Fig. 4 A, 2–6) completely abrogated NBS1 foci formation in all MDC1-positive cells (Fig. 4 C, 5T>A). Significantly, although the 5T>A mutant was unable to mediate NBS1 focal accumulation in response to IR, it still localizes to foci itself, indicating that an intact SDT region is not required for MDC1–γ-H2AX interaction.

Collectively, these results show that the SDT motifs are essential for the interaction between MDC1 and the MRN complex in vitro and for NBS1 accumulation at sites of DSBs in vivo, suggesting that the SDT motif may define a novel phospho-specific MRN-interacting element within MDC1. To test this directly, we first sought to ascertain that the SDT motifs of MDC1 are constitutively phosphorylated in vivo. To this end, we generated two phosphospecific antibodies against doubly phosphorylated SDT peptides (pSDpTs) derived from the human SDT repeat region (see Materials and methods for details). These antibodies were affinity purified and tested against the purified CK2-phosphorylated GST-SDT fragment and its 6T>A mutated derivative. Although one of the two antibodies did not recognize the CK2-phosphorylated GST-SDT fragment (not depicted), the other antibody specifically recognized GST-SDT only when it was preincubated with CK2 and ATP (Fig. 4 D, top). Significantly, the 6T>A mutant was not recognized at all by this antibody, indicating that it is specific for doubly phosphorylated SDT repeats. We next used this antibody to detect MDC1 in extracts from undamaged and irradiated mammalian cells. Unfortunately, the pSDpT antibody unspecifically cross-reacted with many proteins in whole cell and nuclear extracts, and, thus, we were unable to assess the MDC1 phosphorylation status in crude cell extracts (Fig. 4 D, bottom; first lane). However, MDC1 can be isolated along with the MRN complex from HeLa nuclear extract to near homogeneity by a phosphopeptide pull-down strategy using a phosphopeptide derived from the H2AX C terminus (Fig. S2; Stucki et al., 2005). When we probed the isolated MDC1–MRN complex with the pSDpT antibody, we observed two bands at the position where MDC1 runs on SDS gels, indicating that it is indeed phosphorylated on at least a subset of the SDT motifs in vivo (Fig. 4 D, bottom; second lane).

To clarify whether the MRN complex interacts with a single doubly phosphorylated SDT motif, we designed a biotinylated synthetic phosphopeptide comprising the sequence of one of the SDT motifs (Fig. 4 A, 3), which was phosphorylated on the Thr residue. This peptide was either left untreated or was treated with λ phosphatase and CK2. Mass spectrometry and in vitro CK2 assays revealed that such treatment resulted in singly phosphorylated SDpT peptide, unphosphorylated SDT peptide, and doubly phosphorylated pSDpT peptide (Fig. 4 E, top; and not depicted). Significantly, only the doubly phosphorylated peptide, in which both Ser and Thr residues are being phosphorylated, retrieved the MRN complex from HeLa nuclear extract (Fig. 4 E). Collectively, these results suggest that doubly phosphorylated SDT motifs interact with MRN and determine MRN accumulation in vivo.

CK2 is essential for the interaction between MDC1 and NBS1 and for the accumulation of NBS1 at sites of DSBs in vivo

Because the SDT repeats are efficiently targeted by CK2 in vitro (Fig. 4), we next sought to investigate whether CK2 activity was required for NBS1 accumulation at sites of DSBs in vivo. Several commercial small-molecule CK2 inhibitors are available, and two of them were tested on human and mouse cells (TBB and DMAT). Surprisingly, neither of the two inhibitors triggered a detectable reduction in NBS1 foci formation in cultured human and mouse cells (unpublished data). Thus, we speculated that there may either exist additional acidophilic kinases that are capable of efficiently phosphorylating the SDT repeats in MDC1 or that the inhibitors are not potent enough to completely eliminate SDT phosphorylation in our experimental settings.

To test the latter possibility, we took an siRNA approach to down-regulate the two catalytic subunits of CK2 (CK2α and CK2α′) in U2OS cells. 72 h after siRNA transfection, CK2α and CK2α′ expression reached background levels (Fig. 5 A). At the same time, we observed massive cell death and severe mitotic defects, corroborating the essential role of CK2 in the cellular metabolism and life cycle. Interestingly, we also

indicated antibodies. Proteins were separated by SDS-PAGE followed by immunoblotting. The blots were probed with antibodies against MDC1, NBS1, and CK2α. Black lines indicate that intervening lanes have been spliced out. (D) MDC1 is associated with CK2 in vivo. HeLa cell extracts were used to immunoprecipitate proteins with the indicated antibodies. The immunocomplexes were separated by SDS-PAGE followed by immunoblotting. The blot was probed with antibodies against CK2α and CK2α′. Bar, 10 μm.

Published April 14, 2008

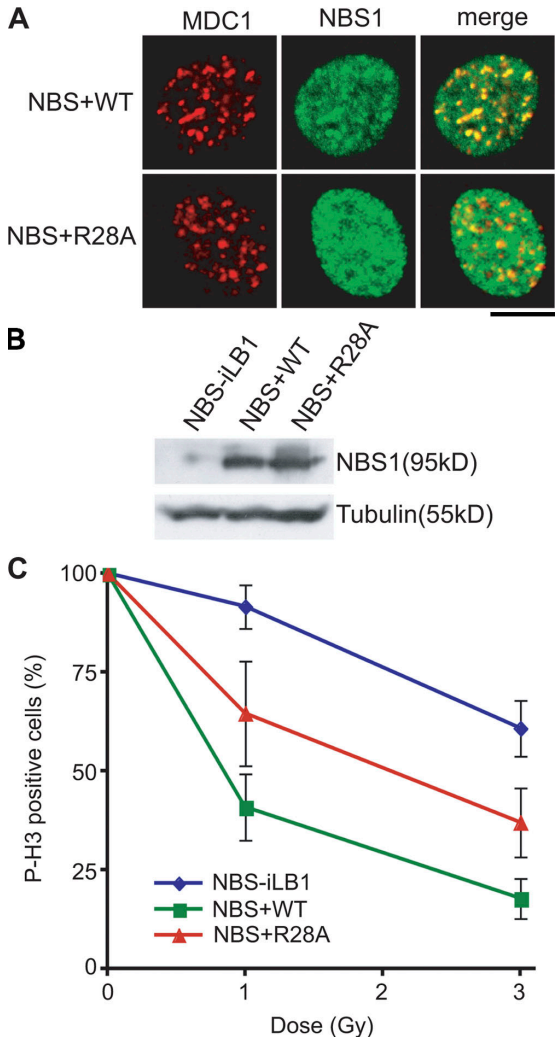

Figure 6. **Disruption of the MDC1–NBS1 interaction triggers a partial G2/M checkpoint defect.** (A) NBS-iLB1 fibroblasts and NBS-iLB1 fibroblasts stably transduced with wild-type NBS1 and R28A mutant NBS1 were irradiated, fixed with methanol, and stained with antibodies against MDC1 and NBS1. (B) Whole cell extracts of NBS-iLB1 fibroblasts and NBS-iLB1 fibroblasts stably transduced with wild-type (WT) NBS1 and R28A mutant NBS1 were resolved by SDS-PAGE followed by immunoblotting. The blot was probed with antibodies against NBS1 and tubulin. (C) NBS-iLB1 fibroblasts and NBS-iLB1 fibroblasts stably transduced with wild-type NBS1 and R28A mutant NBS1 were left untreated or irradiated with 1 Gy and 3 Gy, respectively. Cells were harvested 1 h after irradiation, fixed with methanol, and stained with an antibody against phosphorylated H3 (P-H3) and propidium iodine. The percentage of phosphorylated H3–positive cells was determined by FACS analysis. Error bars represent SD. Bar, 10 μm.

observed a prolonged phosphorylation of ATM substrates in response to IR (Fig. 5 A), suggesting that down-regulation of CK2 by siRNA may cause a repair defect.

Significantly, down-regulation of either CK2α or CK2α′ led to a marked defect in NBS1 foci formation in response to IR (Fig. 5 B, left). At the same time, MDC1 accumulation at sites of DSBs was not significantly reduced (Fig. 5 B, right) even though the foci appeared smaller as compared with the foci in control siRNA-treated cells. This indicates that CK2 is essential for the accumulation of NBS1 at sites of DSBs, whereas it is dispensable for the interaction between MDC1 and γ-H2AX.

Next, we tested whether CK2 was required for the constitutive interaction between MDC1 and NBS1. To this end, MDC1 antibodies were used to coimmunoprecipitate NBS1 from extracts derived from siRNA-treated human cells. No NBS1 coimmunoprecipitated with MDC1 from cells that were transfected with CK2α siRNA, whereas a small but significant amount of NBS1 coimmunoprecipitated with MDC1 from cell extracts that were prepared from control siRNA-transfected cells (Fig. 5 C). The membrane was also probed with an antibody against CK2α to monitor the efficiency of CK2α depletion (Fig. 5 C, bottom; note that CK2α corresponds to the faster migrating band). Interestingly, we noticed that CK2α also coimmunoprecipitated with MDC1 (Fig. 5 C, bottom; third and fifth lanes), indicating that CK2 may exist in a complex with MDC1 in vivo. Indeed, antibodies raised against MDC1 efficiently coimmunoprecipitated both CK2α and CK2α′ from HeLa cell extracts (Fig. 5 D). Notably, the interaction does not change upon the introduction of DNA damage by IR (Fig. 5 D, compare the last two lanes), indicating that it is constitutive and not induced by DNA damage.

Collectively, these data reveal that CK2 is essential for NBS1 foci formation and for the interaction between MDC1 and NBS1. In addition, CK2 exists in a complex with MDC1 and, thus, may be the primary kinase to target the SDT repeats in vivo.

Disruption of the MDC1–NBS1 interaction triggers a partial G2/M checkpoint defect

As shown in Fig. 3 D, the R28A mutation in the NBS1 FHA domain triggers a severe defect in the association of NBS1 with the CK2-phosphorylated MDC1 SDT region in vitro (Fig. 3 D). Consistent with previous studies (Cerosaletti and Concannon, 2003; Lee et al., 2003; Horejsi et al., 2004), we also observed that this mutant is unable to accumulate in foci in stably transduced NBS fibroblasts, whereas MDC1 accumulation is not affected (Fig. 6 A). It was previously shown that the R28A mutant was not capable of rescuing the radiation sensitivity phenotype of NBS cells, whereas it did fully rescue the intra–S-phase checkpoint defect, at least at higher doses of irradiation (Lee et al., 2003). In contrast, primary B cells derived from a humanized mouse model in which another key amino acid at the phosphopeptide recognition interface of the NBS1 FHA domain had been mutated to Ala (H45A) showed partial G2/M and intra–S-phase checkpoint defects specifically at lower doses of irradiation (Difilippantonio et al., 2007). To test whether the R28A mutation causes a similar checkpoint defect, we measured alterations in the mitotic index in response to low (sublethal) doses of irradiation (1–3 Gy) in NBS fibroblasts stably transduced with full-length wild-type and R28A NBS1. Consistent with previous findings (Falck et al., 2005), NBS-iLB1 fibroblasts displayed a clear G2/M checkpoint defect in this dose range (Fig. 6 C). Stable transduction with wild-type NBS1 fully rescued the G2/M checkpoint arrest in response to 1–3 Gy of IR. However, stable

Published April 14, 2008

transduction with R28A mutant NBS1 only partially restored the G2/M checkpoint, which is similar to the situation in the mouse B cells expressing the H45A mutant (Fig. 6 C; Difilippantonio et al., 2007). Notably, this checkpoint defect was not caused by lower expression levels of the mutant transgene as compared with the wild type (Fig. 6 B). Collectively, these results suggest that the constitutive CK2-dependent association of the MRN complex with MDC1 plays an important role in eliciting a full cell cycle checkpoint arrest.

Discussion

Previously, we and others have shown that MDC1 mediates accumulation of the MRN complex at sites of DSBs (Goldberg et al., 2003; Stewart et al., 2003; Lukas et al., 2004; Stucki et al., 2005). We also presented evidence that MDC1 exists in a complex with MRN in extracts from undamaged cells and that an intact NBS1 FHA domain is essential for the stability of this interaction and for efficient retention of the MRN complex in γ-H2AX–containing damaged chromatin regions (Goldberg et al., 2003; Lukas et al., 2004; Stucki et al., 2005). However, the precise mechanism by which MDC1 regulates the MRN complex remained unknown.

In this study, we identify a region in MDC1 that is essential for efficient accumulation of the MRN complex at sites of DSBs. This region of MDC1 features a repeated acidic sequence motif (the SDT motif), and our data, in combination with the accompanying study by Melander et al. (see p. 213 of this issue) and several recently published large-scale phosphorylation site screens of the human and mouse proteome (Beausoleil et al., 2004; Olsen et al., 2006; Villen et al., 2007), suggest that at least a subset of the SDT motifs in MDC1 are constitutively phosphorylated by the acidophilic kinase CK2 on highly conserved Ser and Thr residues. Furthermore, we present unexpected evidence that the doubly phosphorylated SDT motifs regulate accumulation and retention of the MRN complex in the DSB-flanking chromatin compartment via a mechanism that involves direct interaction with the NBS1 N-terminal FHA domain. Finally, we show that CK2 is essential for NBS1 accumulation in damaged chromatin and that depletion of CK2 disrupts the MDC1–MRN complex in vivo. Thus, our data successfully integrate and explain two observations whose interrelation has previously not been appreciated: first, we provide a mechanistic explanation as to why MDC1 and the MRN complex exist in a complex even before DNA damage; and second, our findings also put into perspective the previous observation that an intact FHA domain of NBS1 is critical for efficient accumulation of the MRN complex at sites of DSBs (Kobayashi et al., 2002; Zhao et al., 2002; Cerosaletti and Concannon, 2003; Lee et al., 2003; Horejsi et al., 2004; Lukas et al., 2004) and for an intact DDR in living organisms (Difilippantonio et al., 2005, 2007).

However, it is essential to appreciate that not all MRN functions seem to require MDC1. For instance, DNA end processing activities of MRN do not appear to be dependent on MDC1 (Jazayeri et al., 2006). Furthermore, there are no indications that MRN's role in mediating ATM activation would require MDC1 (Lee and Paull, 2005). Finally, MRN seems to occupy two distinct compartments at sites of DSBs: it accumulates on single-stranded DNA regions generated by enzymatic resection of DSBs (Jazayeri et al., 2006) as well as in large chromatin domains flanking DSBs that often span several thousand base pairs (Bekker-Jensen et al., 2006). Although the accumulation of MRN on single-stranded DNA does not require MDC1 (Bekker-Jensen et al., 2006), accumulation and retention of MRN in γ-H2AX–containing chromatin are critically dependent on MDC1 (Goldberg et al., 2003; Stewart et al., 2003; Lukas et al., 2004; Stucki et al., 2005) and on CK2-dependent phosphorylation of its SDT repeats (Melander et al., 2008; this study).

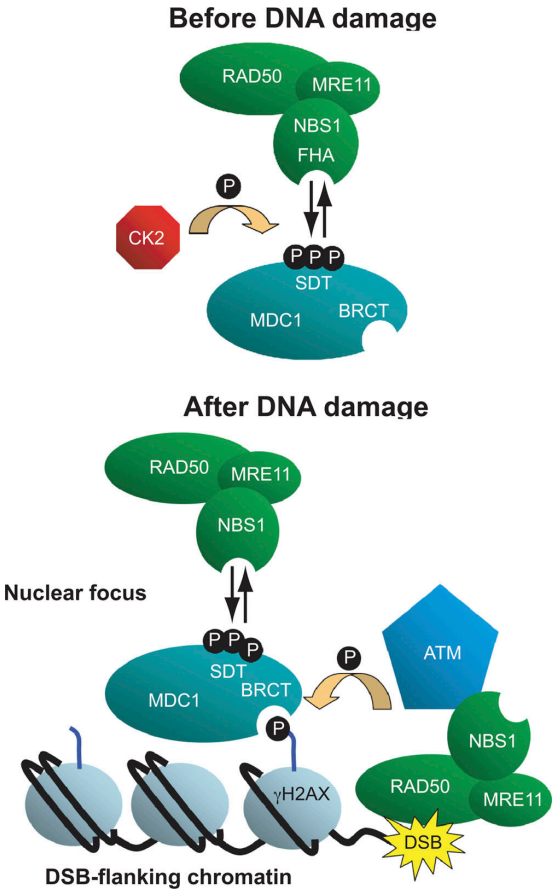

Figure 7. **Model of the mechanism of the MDC1–MRN interaction before and after DNA damage.** See Discussion for details.

Based on these novel findings and on previously published observations, we propose the following model of the events that occur before and after a cell has suffered genotoxic stress that generates DSBs (Fig. 7): in the absence of DNA damage, MDC1 is phosphorylated on multiple sites by CK2 and perhaps other constitutively active kinases. The MRN complex associates with MDC1 through direct interaction between the N-terminal FHA domain of the NBS1 subunit and the CK2-phosphorylated SDT repeat region of MDC1. Upon induction of DSBs in the genome, a fraction of MRN (that is probably not associated with MDC1) is rapidly deployed to the free DNA ends. Once bound to the

Published April 14, 2008

DNA, MRN participates in a multitude of events that include DNA end processing and tethering of DNA molecules that may facilitate accurate repair as well as activation of the ATM signaling cascade (for review see Williams et al., 2007). Although the precise mechanisms of these processes are still not understood in detail, there is no experimental indication that the MRN complex would require MDC1 for these functions. However, in a second step, after the ATM signaling cascade has been initiated, the MDC1-bound fraction of MRN enters the stage; once activated, ATM phosphorylates a vast variety of targets. Among these targets are H2AX molecules in nucleosomes that are located close to the break site. Phosphorylated H2AX is recognized by MDC1 through its C-terminal BRCT domains (Stucki et al., 2005). MDC1, along with the MDC1-bound fraction of MRN, forms a tight complex with phosphorylated H2AX, thus recruiting more MRN to the chromatin compartments flanking DSBs (Stucki et al., 2005; Lou et al., 2006). This process is manifested by the formation of microscopically discernible nuclear foci containing both MDC1 and the MRN complex.

Although such a model of MDC1–MRN interplay is intriguing, there are several outstanding issues that need to be discussed. It is clear that the interaction between MDC1 and the MRN complex is constitutive, but it is still dependent on the phosphorylation of MDC1 by CK2. A very similar mechanism has recently been described in two different aspects of the mammalian DDR, namely single-strand DNA break repair and DSB repair by nonhomologous end joining (Koch et al., 2004; Loizou et al., 2004). CK2 phosphorylates XRCC1, an adaptor protein that recruits several repair factors to single-stranded break sites (Loizou et al., 2004). In this case, the CK2 phosphorylation mark creates a binding site for the FHA domain–containing proteins polynucleotide kinase (PNK), aparataxin, and Xip1 (Loizou et al., 2004; Luo et al., 2004; Bekker-Jensen et al., 2007). In addition, PNK recruitment to sites of DSBs by XRCC4 is also mediated by the CK2-dependent phosphorylation of XRCC4 (Koch et al., 2004). Thus, the mechanisms of PNK, aparataxin, and Xip1 recruitment by XRCC1 and PNK recruitment by XRCC4 closely resemble MRN chromatin retention by MDC1. However, although the recruitment of PNK by XRCC1 was abolished by the CK2 inhibitor TBB (Loizou et al., 2004), we were unable to abolish NBS1 recruitment to damaged chromatin by using the same inhibitor and other (even more potent) small-molecule CK2 inhibitors. One possible explanation for this discrepancy may lie in the existence of one or more CK2-related acidophilic kinases that are capable of targeting the MDC1 SDT repeats. However, the fact that down-regulation of CK2 by siRNA completely abolishes NBS1 recruitment to damaged chromatin argues against this possibility but rather suggests that the CK2 inhibitors were not potent enough to reduce CK2 activity sufficiently to produce an effectual reduction in MDC1 phosphorylation. Indeed, in vivo phosphorylation analysis of MDC1 by Melander et al. (2008) reveals that treatment of cells with CK2 inhibitors maximally reduced SDT phosphorylation levels to 50%. This may not be enough for a visually discernible defect in NBS1 foci formation.

With the discovery of the mechanism by which MDC1 mediates accumulation and retention of the MRN complex in γ-H2AX–containing damaged chromatin regions, an important step in the hierarchy of events that lead to the formation of nuclear foci at sites of DSBs has been resolved. Although we do not yet understand the function of MRN in the DSB-flanking chromatin compartment, one intriguing possibility is that MDC1-bound MRN may act as a mediator of downstream phosphorylation events of the DDR. In this case, the MDC1–MRN complex may enhance the DSB-induced signal by means of a positive feedback loop: MDC1–MRN accumulates as the γ-H2AX mark spreads into more distal chromatin regions, thus helping to trigger a global DDR even in the presence of very low numbers of DSBs. Consistent with such a scenario is the observation that cells expressing NBS1 with a mutated FHA domain display a partial G2/M checkpoint defect at low doses of irradiation (Difilippantonio et al., 2007; this study), whereas the checkpoint seems to be normal at higher doses (Difilippantonio et al., 2007). This suggests that the prevalent role of the MDC1–MRN complex in checkpoint activation may not constitute the initiation of the signal but rather its amplification. The discovery of the SDT region of MDC1 and its specific role in MRN localization in response to DNA damage will greatly facilitate the investigation of functional aspects of MRN in the DSB-flanking chromatin compartment.

Materials and methods

Cell culture and gene transfer

MDC1$^{-/-}$ and MDC1$^{+/+}$ MEFs were gifts from J. Chen (Yale University, New Haven, CT). NBS-iLB1 cells stably transduced with wild-type NBS1 and R28A mutant NBS1 were gifts from S. Jackson (University of Cambridge, Cambridge, UK) and K. Cerosaletti (University of Washington, Seattle, WA), respectively. MEFs, HeLa, U2OS, and NBS-iLB1 cells were cultured in DME (Invitrogen) supplemented with 10% FCS. Transfection of plasmids was performed using either Lipofectamine 2000 (Invitrogen) or calcium phosphate. Sf9 cells were cultured in Grace's insect medium (Invitrogen) supplemented with 10% FCS. Recombinant MRE11, RAD50, and NBS1 baculoviruses were gifts from V. Bohr (National Institute on Aging, Baltimore, MD). The Bac-To-Bac Baculovirus Expression System (Invitrogen) was used to generate and amplify recombinant baculoviruses. All steps were performed according to the manufacturer's protocols. CK2 inhibitors TBB and DMAT were purchased from EMD. Irradiation of MEFs was performed in an x-ray cabinet (Faxitron) at 5–10 Gy/min.

Plasmids

The full-length mouse MDC1 cDNA was a gift from A. Nussenzweig (National Institutes of Health, Bethesda, MD) and was HA tagged at the C terminus by PCR and cloned into pcDNA3.1(+) mammalian expression vector (Invitrogen). Human MDC1-GST constructs were generated by PCR amplification of the human MDC1 cDNA followed by cloning into pGEX4T3 bacterial expression vector (GE Healthcare). Myc-NBS1 (Falck et al., 2005) was subcloned into pFastBac transfer vector (Invitrogen) to generate recombinant NBS1 baculoviruses. Deletion mutants were generated by a standard PCR-based method, and point mutations were introduced using the QuikChange Site-Directed Mutagenesis kit (Stratagene).

siRNA and transfections

The siRNA duplexes were 21 bp with a two-base deoxynucleotide overhang (Dharmacon Research). The sequences of the CK2α and CK2α′ siRNA oligonucleotides used were GAUGACUACCAGCUGGUUCdTdT and CAGUCUGAGGAGCCGCGAGdTdT, respectively. The control siRNA used was CGUACGCGGAAUACUUCGAdTdT. Cells were transfected with siRNA duplexes by using Oligofectamine (Invitrogen) according to the manufacturer's instructions. Cells were routinely harvested 72 h after siRNA transfection.

Cell extraction and protein purification

HeLa nuclear extract was purchased from Cilbiotech. Cell extraction for immunoblot analysis was described previously (Stewart et al., 2003).

Published April 14, 2008

MDC1-GST fragments were affinity purified on glutathione–Sepharose beads (GE Healthcare). Sf9 cells expressing recombinant MRN, MR, and N were lysed by sonication in buffer A (50 mM sodium phosphate, pH 7.0, 0.3 M NaCl, 10% glycerol, and 0.5 mM PMSF) containing 20 mM imidazol followed by centrifugation. The supernatants were loaded on HiTrap chelating (Ni^{2+}) columns (GE Healthcare) equilibrated with buffer A. The columns were washed with 50 ml buffer A/20 mM imidazol and with 50 ml buffer A/50 mM imidazol. Proteins were eluted with a 50-ml linear concentration gradient of 50–350 mM imidazole in buffer A. MRN-containing fractions were pooled and either used directly for analysis after dialysis against buffer B (20 mM Tris-HCl, pH 8.0, 150 mM NaCl, 10% glycerol, and 1 mM DTT) or loaded on 1-ml HiTrapQ columns (GE Healthcare) for further purification. The HiTrapQ columns were eluted with a 10-ml linear concentration gradient of 50–500 mM NaCl.

Antibodies and immunological techniques

Mouse monoclonal HA antibodies were purchased from Covance Research Products. The anti–mouse NBS1 antibody was a gift from A. Nussenzweig. The antibodies used against human Nbs1 were obtained from Genetex, Novus, and Millipore. Antibodies against phospho-Nbs1 Ser-343 and anti-phospho-H2AX were obtained from Genetex and Millipore, respectively. Anti-SMC1, phospho-SMC1 Ser-966, and H2AX antibodies were purchased from Bethyl, and the antiphospho-53BP1 and anti-53BP1 antibodies were obtained from Cell Signaling Technology. Sheep polyclonal antibodies against human MDC1, MRE11, and RAD50 have been described previously (Goldberg et al., 2003). Rabbit polyclonal antibodies to MDC1 have been described previously (Stewart et al., 2003). The anti-CK2α and -CK2α′ antibodies were purchased from Santa Cruz Biotechnology, Inc. Phosphospecific MDC1 antibodies were raised in rabbits to the MDC1 phosphopeptides GFIDS(P)DT(P)DA and TERDS(P)DT(P)DV and were affinity purified using the phosphorylated and nonphosphorylated peptides (Eurogentec).

For immunoprecipitation, HeLa cells were lysed for 30 min in NETN lysis buffer (50 mM Tris-HCl, pH 7.5, 150 mM NaCl, 1 mM EDTA, 2 mM $MgCl_2$, 1% NP-40 supplemented with protease inhibitors [Roche], and benzonase [EMD]). The clarified extract was precleared with the appropriate IgG (Dako) and protein A or G beads (GE Healthcare) for 1 h at 4°C. 5 µg of immunoprecipitating antibody was added with protein A or G beads to the precleared supernatant and incubated for 3 h at 4°C. The immunocomplexes were washed four times in NETN lysis buffer (containing 0.5% NP-40), boiled in SDS sample buffer, and loaded on an SDS-polyacrylamide gel. Proteins were analyzed by immunoblotting using standard methods.

For immunofluorescence staining, cells were grown on glass coverslips, fixed in ice-cold methanol, and stained with the indicated antibodies for 1 h at room temperature. Secondary antibodies were purchased from Jackson ImmunoResearch Laboratories (FITC and rhodamine) and Invitrogen (AlexaFluor488 and -596). Images were captured at room temperature on a confocal microscope (SP2; Leica) with a 40× NA 1.25 oil immersion objective (Leica; Figs. 1, 4, and 6) and on a microscope (Eclipse E600; Nikon) with a 60× oil immersion objective (Nikon; Fig. 5).

Biochemical analysis

For GST pull-down assays, purified 5 µg GST fusion proteins were mixed with 200 µg HeLa nuclear extract or with 5 µg of purified MRN. Where indicated, GST fusion proteins were pretreated with 100 U CK2 (New England BioLabs, Inc.). The mixture was incubated at 4°C for 30 min to allow binding. Glutathione–Sepharose beads were then added, and the suspension was incubated at 4°C for a further 60 min. The beads were washed three times with wash buffer (50 mM Tris, pH 7.5, 120 mM NaCl, 1 mM DTT, and 0.2% NP-40), resuspended in SDS loading buffer, and analyzed by SDS-PAGE and immunoblotting. For peptide pull-down analysis, the biotinylated synthetic peptide Btn-NH-SGSFIDSD[pT]DAEEERI-COOH (Eurogentec) was used. Where indicated, 25 nmol of the peptide was incubated with 500 U of recombinant CK2 (New England Biolabs, Inc.) at 30°C for 45 min and with 100 U λ phosphatase (New England Biolabs, Inc.) at 30°C for 20 min. Peptide pull-down analysis was performed as described previously (Stucki et al., 2005).

CK2 in vitro kinase assays for phosphorylation site mapping was performed by adding 100 ng of recombinant CK2α (Millipore) to 1 µg GST-MDC1 (amino acids 141–621) in CK2 kinase buffer (20 mM MOPS, pH 7.2, 25 mM β-glycerophosphate, 5 mM EGTA, 1 mM sodium orthovanadate, 37.5 mM $MgCl_2$, 1 mM DTT, 100 µM ATP, and 10 µCi γ-[^{32}P]ATP) and incubating for 10 min at 30°C. Kinase reactions were inactivated by boiling in SDS sample buffer and were run on an SDS-polyacrylamide gel. Gels were stained with Coomassie blue and either dried and subjected to autoradiography, or the GST-MDC1 band was excised and processed for mass spectrometric phospho–amino acid analysis (Jowsey et al., 2007). Mutation of putative CK2 phosphorylation sites in the GST-MDC1 fragment was performed using site-directed mutagenesis (Stratagene).

Checkpoint analysis

G2/M checkpoint analysis was performed as described previously (Falck et al., 2005). In brief, cells were irradiated with the indicated doses during the exponential growth phase. 1 h later, cells were harvested, fixed with 70% ethanol/PBS, and incubated overnight at −20°C. Fixed cells were washed with PBS and permeabilized with 0.25% Triton X-100/PBS on ice for 10 min. Cells were stained with an antiphosphohistone H3 antibody (Millipore) and propidium iodide. Data were acquired with a flow cytometer (FC500; Becton Dickinson).

Phosphorylation site analysis by mass spectrometry

MDC1 samples that had been incubated with CK2 with or without ATP were subjected to electrophoresis on a 4–12% polyacrylamide gel that was stained with colloidal Coomassie blue. MDC1 bands were excised from the gel, washed with 0.1% NH_4HCO_3 and 50% acetonitrile/50 mM NH_4HCO_3, reduced with 10 mM DTT in 0.1 M NH_4HCO_3 for 45 min at 65°C, and alkylated by the addition of 50 mM iodoacetamide for 30 min at room temperature. Gel pieces were then washed in 0.1% NH_4HCO_3 and 50% acetonitrile/50 mM NH_4HCO_3, dried, and incubated with 25 mM triethylammonium bicarbonate with 5 µg/ml trypsin for 16 h at 30°C. For identification of phosphorylation sites, the extracted tryptic peptides were analyzed by liquid chromatography mass spectrometry on a spectrometer (4000 Q-TRAP; Applied Biosystems) with precursor ion scanning as described previously (Williamson et al., 2006). The tandem mass spectrometry spectra were searched against a local database containing the GST-MDC1 sequence using the Mascot search algorithm (www.matrixscience.com) run on a local server. Sites of phosphorylation were validated by manual inspection of the mass spectrometry spectra using Analyst 1.4.1 software (MDS Sciex).

Online supplemental material

Fig. S1 shows a sequence alignement of the SDT repeats in human, mouse, zebrafish, and honey bee MDC1. Fig. S2 shows the purified MDC1–MRN complex isolated from HeLa nuclear extract. Online supplemental material is available at http://www.jcb.org/cgi/content/full/jcb.200709008/DC1.

We thank Jiri Lukas for stimulating discussions and for communicating unpublished results, Steve Jackson for communicating unpublished results, and Junjie Chen, André Nussenzweig, Karen Cerosaletti, Vilhelm Bohr, Graeme Smith, and Steve Jackson for providing valuable reagents. Stéphanie Jungmichel is acknowledged for comments and critical reading of the manuscript.

This work was supported by grants from the Swiss National Foundation (grant 3100A0-111818), the UBS AG (Im Auftrag eines Kunden), and by the Kanton of Zürich. G.S. Stewart, E.S. Miller, and K. Townsend are supported by Cancer Research UK Career Development fellowships (ref: C17183/A5592).

Submitted: 4 September 2007
Accepted: 19 March 2008

References

Beausoleil, S.A., M. Jedrychowski, D. Schwartz, J.E. Elias, J. Villen, J. Li, M.A. Cohn, L.C. Cantley, and S.P. Gygi. 2004. Large-scale characterization of HeLa cell nuclear phosphoproteins. *Proc. Natl. Acad. Sci. USA.* 101:12130–12135.

Bekker-Jensen, S., C. Lukas, R. Kitagawa, F. Melander, M.B. Kastan, J. Bartek, and J. Lukas. 2006. Spatial organization of the mammalian genome surveillance machinery in response to DNA strand breaks. *J. Cell Biol.* 173:195–206.

Bekker-Jensen, S., K. Fugger, J.R. Danielsen, I. Gromova, M. Sehested, J. Celis, J. Bartek, J. Lukas, and N. Mailand. 2007. Human Xip1 (C2orf13) is a novel regulator of cellular responses to DNA strand breaks. *J. Biol. Chem.* 282:19638–19643.

Bhaskara, V., A. Dupre, B. Lengsfeld, B.B. Hopkins, A. Chan, J.H. Lee, X. Zhang, J. Gautier, V. Zakian, and T.T. Paull. 2007. Rad50 adenylate kinase activity regulates DNA tethering by Mre11/Rad50 complexes. *Mol. Cell.* 25:647–661.

Burma, S., B.P. Chen, M. Murphy, A. Kurimasa, and D.J. Chen. 2001. ATM phosphorylates histone H2AX in response to DNA double-strand breaks. *J. Biol. Chem.* 276:42462–42467.

Published April 14, 2008

Celeste, A., O. Fernandez-Capetillo, M.J. Kruhlak, D.R. Pilch, D.W. Staudt, A. Lee, R.F. Bonner, W.M. Bonner, and A. Nussenzweig. 2003. Histone H2AX phosphorylation is dispensable for the initial recognition of DNA breaks. *Nat. Cell Biol.* 5:675–679.

Cerosaletti, K.M., and P. Concannon. 2003. Nibrin forkhead-associated domain and breast cancer C-terminal domain are both required for nuclear focus formation and phosphorylation. *J. Biol. Chem.* 278:21944–21951.

Costanzo, V., T. Paull, M. Gottesman, and J. Gautier. 2004. Mre11 assembles linear DNA fragments into DNA damage signaling complexes. *PLoS Biol.* 2:E110.

D'Amours, D., and S.P. Jackson. 2002. The Mre11 complex: at the crossroads of DNA repair and checkpoint signalling. *Nat. Rev. Mol. Cell Biol.* 3:317–327.

Difilippantonio, S., A. Celeste, O. Fernandez-Capetillo, H.T. Chen, B. Reina San Martin, F. Van Laethem, Y.P. Yang, G.V. Petukhova, M. Eckhaus, L. Feigenbaum, et al. 2005. Role of Nbs1 in the activation of the Atm kinase revealed in humanized mouse models. *Nat. Cell Biol.* 7:675–685.

Difilippantonio, S., A. Celeste, M.J. Kruhlak, Y. Lee, M.J. Difilippantonio, L. Feigenbaum, S.P. Jackson, P.J. McKinnon, and A. Nussenzweig. 2007. Distinct domains in Nbs1 regulate irradiation-induced checkpoints and apoptosis. *J. Exp. Med.* 204:1003–1011.

Durocher, D., and S.P. Jackson. 2002. The FHA domain. *FEBS Lett.* 513:58–66.

Falck, J., J. Coates, and S.P. Jackson. 2005. Conserved modes of recruitment of ATM, ATR and DNA-PKcs to sites of DNA damage. *Nature.* 434:605–611.

Fernandez-Capetillo, O., A. Lee, M. Nussenzweig, and A. Nussenzweig. 2004. H2AX: the histone guardian of the genome. *DNA Repair (Amst.).* 3:959–967.

Glover, J.N., R.S. Williams, and M.S. Lee. 2004. Interactions between BRCT repeats and phosphoproteins: tangled up in two. *Trends Biochem. Sci.* 29:579–585.

Goldberg, M., M. Stucki, J. Falck, D. D'Amours, D. Rahman, D. Pappin, J. Bartek, and S.P. Jackson. 2003. MDC1 is required for the intra-S-phase DNA damage checkpoint. *Nature.* 421:952–956.

Horejsi, Z., J. Falck, C.J. Bakkenist, M.B. Kastan, J. Lukas, and J. Bartek. 2004. Distinct functional domains of Nbs1 modulate the timing and magnitude of ATM activation after low doses of ionizing radiation. *Oncogene.* 23:3122–3127.

Jazayeri, A., J. Falck, C. Lukas, J. Bartek, G.C. Smith, J. Lukas, and S.P. Jackson. 2006. ATM- and cell cycle-dependent regulation of ATR in response to DNA double-strand breaks. *Nat. Cell Biol.* 8:37–45.

Jowsey, P., N.A. Morrice, C.J. Hastie, H. McLauchlan, R. Toth, and J. Rouse. 2007. Characterisation of the sites of DNA damage-induced 53BP1 phosphorylation catalysed by ATM and ATR. *DNA Repair (Amst.).* 6:1536–1544.

Kobayashi, J., H. Tauchi, S. Sakamoto, A. Nakamura, K. Morishima, S. Matsuura, T. Kobayashi, K. Tamai, K. Tanimoto, and K. Komatsu. 2002. NBS1 localizes to gamma-H2AX foci through interaction with the FHA/BRCT domain. *Curr. Biol.* 12:1846–1851.

Koch, C.A., R. Agyei, S. Galicia, P. Metalnikov, P. O'Donnell, A. Starostine, M. Weinfeld, and D. Durocher. 2004. Xrcc4 physically links DNA end processing by polynucleotide kinase to DNA ligation by DNA ligase IV. *EMBO J.* 23:3874–3885.

Lee, J.H., and T.T. Paull. 2005. ATM activation by DNA double-strand breaks through the Mre11-Rad50-Nbs1 complex. *Science.* 308:551–554.

Lee, J.H., B. Xu, C.H. Lee, J.Y. Ahn, M.S. Song, H. Lee, C.E. Canman, J.S. Lee, M.B. Kastan, and D.S. Lim. 2003. Distinct functions of Nijmegen breakage syndrome in ataxia telangiectasia mutated-dependent responses to DNA damage. *Mol. Cancer Res.* 1:674–681.

Loizou, J.I., S.F. El-Khamisy, A. Zlatanou, D.J. Moore, D.W. Chan, J. Qin, S. Sarno, F. Meggio, L.A. Pinna, and K.W. Caldecott. 2004. The protein kinase CK2 facilitates repair of chromosomal DNA single-strand breaks. *Cell.* 117:17–28.

Lou, Z., K. Minter-Dykhouse, S. Franco, M. Gostissa, M.A. Rivera, A. Celeste, J.P. Manis, J. van Deursen, A. Nussenzweig, T.T. Paull, et al. 2006. MDC1 maintains genomic stability by participating in the amplification of ATM-dependent DNA damage signals. *Mol. Cell.* 21:187–200.

Lukas, C., F. Melander, M. Stucki, J. Falck, S. Bekker-Jensen, M. Goldberg, Y. Lerenthal, S.P. Jackson, J. Bartek, and J. Lukas. 2004. Mdc1 couples DNA double-strand break recognition by Nbs1 with its H2AX-dependent chromatin retention. *EMBO J.* 23:2674–2683.

Luo, H., D.W. Chan, T. Yang, M. Rodriguez, B.P. Chen, M. Leng, J.J. Mu, D. Chen, Z. Songyang, Y. Wang, and J. Qin. 2004. A new XRCC1-containing complex and its role in cellular survival of methyl methanesulfonate treatment. *Mol. Cell. Biol.* 24:8356–8365.

Maser, R.S., K.J. Monsen, B.E. Nelms, and J.H. Petrini. 1997. hMre11 and hRad50 nuclear foci are induced during the normal cellular response to DNA double-strand breaks. *Mol. Cell. Biol.* 17:6087–6096.

Matsuoka, S., B.A. Ballif, A. Smogorzewska, E.R. McDonald III, K.E. Hurov, J. Luo, C.E. Bakalarski, Z. Zhao, N. Solimini, Y. Lerenthal, et al. 2007. ATM and ATR substrate analysis reveals extensive protein networks responsive to DNA damage. *Science.* 316:1160–1166.

Melander, F., S. Bekker-Jensen, J. Falck, J. Bartek, N. Mailand, and J. Lukas. 2008. Phosphorylation of SDT repeats in the MDC1 N terminus triggers retention of NBS1 at the DNA damage–modified chromatin. *J. Cell Biol.* 181:213–226.

Olsen, J.V., B. Blagoev, F. Gnad, B. Macek, C. Kumar, P. Mortensen, and M. Mann. 2006. Global, in vivo, and site-specific phosphorylation dynamics in signaling networks. *Cell.* 127:635–648.

Stewart, G.S., B. Wang, C.R. Bignell, A.M.R. Taylor, and S.J. Elledge. 2003. MDC1 is a mediator of the mammalian DNA damage checkpoint. *Nature.* 421:961–966.

Stracker, T.H., J.W. Theunissen, M. Morales, and J.H. Petrini. 2004. The Mre11 complex and the metabolism of chromosome breaks: the importance of communicating and holding things together. *DNA Repair (Amst.).* 3:845–854.

Stracker, T.H., M. Morales, S.S. Couto, H. Hussein, and J.H. Petrini. 2007. The carboxy terminus of NBS1 is required for induction of apoptosis by the MRE11 complex. *Nature.* 447:218–221.

Stucki, M., and S.P. Jackson. 2004. MDC1/NFBD1: a key regulator of the DNA damage response in higher eukaryotes. *DNA Repair (Amst.).* 3:953–957.

Stucki, M., and S.P. Jackson. 2006. gammaH2AX and MDC1: anchoring the DNA-damage-response machinery to broken chromosomes. *DNA Repair (Amst.).* 5:534–543.

Stucki, M., J.A. Clapperton, D. Mohammad, M.B. Yaffe, S.J. Smerdon, and S.P. Jackson. 2005. MDC1 directly binds phosphorylated histone H2AX to regulate cellular responses to DNA double-strand breaks. *Cell.* 123:1213–1226.

Villen, J., S.A. Beausoleil, S.A. Gerber, and S.P. Gygi. 2007. Large-scale phosphorylation analysis of mouse liver. *Proc. Natl. Acad. Sci. USA.* 104:1488–1493.

Williams, R.S., J.S. Williams, and J.A. Tainer. 2007. Mre11-Rad50-Nbs1 is a keystone complex connecting DNA repair machinery, double-strand break signaling, and the chromatin template. *Biochem. Cell Biol.* 85:509–520.

Williamson, B.L., J. Marchese, and N. Morrice. 2006. Automated identification and quantification of protein phosphorylation sites by LC/MS on a hybrid triple quadrupole linear ion trap mass spectrometer. *Mol. Cell. Proteomics.* 5:337–346.

Yaffe, M.B., G.G. Leparc, J. Lai, T. Obata, S. Volinia, and L.C. Cantley. 2001. A motif-based profile scanning approach for genome-wide prediction of signaling pathways. *Nat. Biotechnol.* 19:348–353.

Zhao, S., W. Renthal, and E.Y. Lee. 2002. Functional analysis of FHA and BRCT domains of NBS1 in chromatin association and DNA damage responses. *Nucleic Acids Res.* 30:4815–4822.

Zhou, B.B., and S.J. Elledge. 2000. The DNA damage response: putting checkpoints in perspective. *Nature.* 408:433–439.

Spycher et al. Figure S1

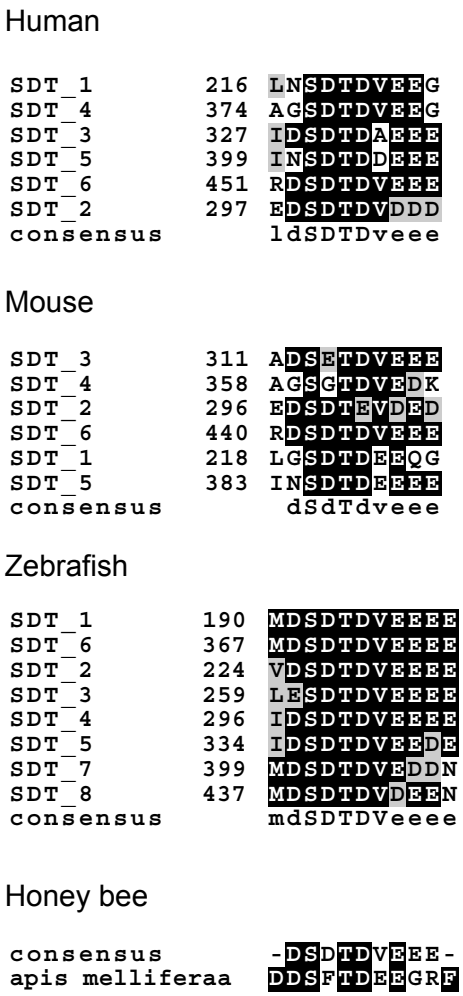

Figure S1. Sequence alignment of the SDT motifs in human, mouse, zebrafish, and bee MDC1. Alignment was performed with ClustalX for Mac OS X (Thompson, J.D., T.J. Gibson, F. Plewniak, F. Jeanmougin, and D.G. Higgins. 1997. *Nucleic Acids Res.* 25:4876–4882), and the shading was generated by using Boxshade 3.21 (www.ch.embnet.org). Bee MDC1 was identified based on structural alignment of the C-terminal BRCT domains (Stucki, M., J.A. Clapperton, D. Mohammad, M.B. Yaffe, S.J. Smerdon, and S.P. Jackson. 2005. *Cell.* 123:1213–1226). The consensus of all analyzed species is d-S-d-T-D/E-x-E, which conforms to consensus CK2 phosphorylation sites (S/T-X-X-D/E) for both Ser and Thr residues. The highlighted sequences are the conserved amino acids within the SDT motifs.

Spycher et al. Figure S2

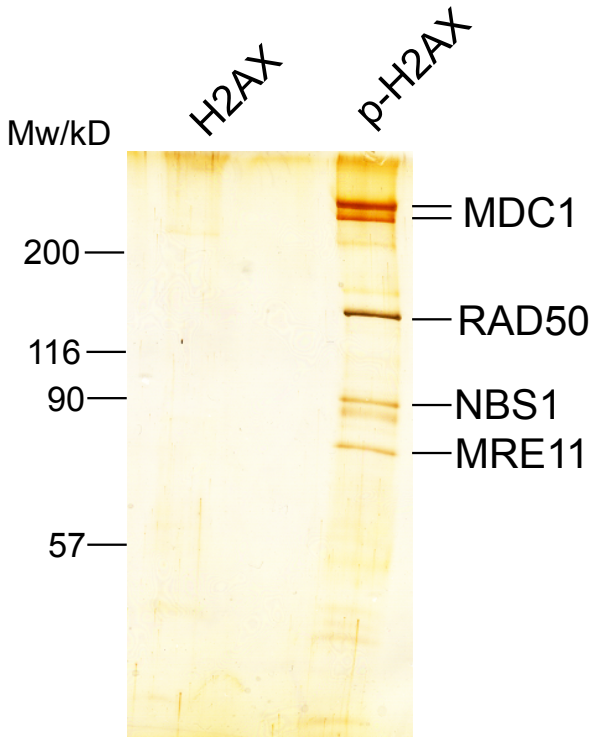

Figure S2. Purification of the MDC1–MRN complex from HeLa nuclear extract. H2AX phosphopeptide pull down was performed as described previously (Stucki, M., J.A. Clapperton, D. Mohammad, M.B. Yaffe, S.J. Smerdon, and S.P. Jackson. 2005. *Cell.* 123:1213–1226), but the beads were extensively washed with a high-stringency buffer (50 mM Tris-HCl, pH 8.0, 200 mM NaCl, and 0.5% NP-40). The bound proteins were eluted with SDS loading buffer and separated on an SDS-polyacrylamide gel followed by silver staining. The protein bands were identified by parallel immunoblot analysis using antibodies against human MDC1, RAD50, NBS1, and MRE11 (not depicted).

5.2 MDC1-dependent retention of the MRE11-RAD50-NBS1 complex in damaged chromatin is not required for activation of the G2/M DNA damage checkpoint

My contribution to this work was:

- Design of the experiments (together with M. Stucki)
- Generation of most of the reagents
- Gathering the data for Fig. 1B, 2B, and 3
- Proofreading of the manuscript

MDC1-dependent retention of the MRE11/RAD50/NBS1 complex in damaged chromatin is not required for activation of the G2/M DNA damage checkpoint

Christoph Spycher[1], Lucijana Pavic[1] and Manuel Stucki[1*]

[1]Institute of Veterinary Biochemistry and Molecular Biology, University of Zurich, Winterthurerstrasse 190, 8057 Zurich, Switzerland

* Corresponding author: Manuel Stucki, Tel. +41 44 6355421; Fax: +41 44 6356840; E-mail: m.stucki@vetbio.uzh.ch

Running head: Mechanism of MRN accumulation in damaged chromatin

Key words: DNA double-strand breaks, Chromatin, NBS1, BRCT domain, FHA domain, MDC1, G2/M Checkpoint

Abstract

The MRE11/RAD50/NBS1 (MRN) complex accumulates at sites of DNA double-strand breaks in large chromatin domains flanking the lesion site. The mechanism of MRN accumulation involves direct binding of the NBS1 subunit to phosphorylated MDC1, a large nuclear adaptor protein that directly interacts with phosphorylated H2AX (γH2AX). NBS1 contains an FHA domain and two BRCT domains at its N-terminus. Here we present evidence that both of these domains participate in the interaction between MDC1 and NBS1. Point mutations in key amino acid residues of either the FHA or the BRCT domains compromise the interaction with MDC1 and lead to defects in MRN accumulation at sites of DNA damage. Surprisingly though, only mutations in the FHA domain, but not mutations in the BRCT domains, yield a G2/M checkpoint defect. This indicates that MDC1-dependent chromatin accumulation of the MRN complex at site of DNA breaks is not required for G2/M checkpoint activation.

Introduction

Nijmegen breakage syndrome (NBS) is a rare autosomal genetic disorder. NBS patients suffer from growth retardation, microcephaly, dismorphal features, immunodeficiency and predisposition to cancer, mainly lymphomas. Cells derived from NBS patients are radio-sensitive, show chromosomal instability and cell cycle checkpoint as well as apoptotic defects (1)}(2).

The NBS gene codes for a 754 amino acid protein named NBS1 (p95; nibrin). It exclusively exists in a complex with two enzymes: MRE11, a structure-specific nuclease and RAD50, an ATPase/adenylate kinase. Together, these three proteins form the MRE11/RAD50/NBS1 (MRN) complex, a conserved and essential DDR factor that functions in a multitude of cellular processes involving DNA double-strand breaks (DSBs), including DSB repair, checkpoint signaling, DNA replication, meiotic recombination and induction of apoptosis (2,3).

The MRN complex accumulates at sites of DSBs in large microscopically discernible subnuclear structures, usually referred to as DNA damage foci. The functional implication of this massive accumulation at sites of DSBs is not yet fully understood. We and others recently showed that focus formation by the MRN complex is mediated by a direct interaction between NBS1 and phosphorylated MDC1, a large nuclear adaptor protein that specifically recognizes phosphorylated H2AX (4-7). The interaction between NBS1 and MDC1 is dependent upon the N-terminal FHA domain of NBS1 that directly interacts with a constitutively phosphorylated acidic repeat region in MDC1 (the SDT repeat; (4-6)).

No structural information of full-length NSB1 is yet available, but recent NMR structural data suggested that besides the FHA domain, NBS1 may also feature

a tandem BRCT domain at its N-terminus (8). Like FHA domains, tandem BRCT domains have been shown to act as phospho-specific protein-protein interaction modules (9). Interestingly, point mutations altering key residues in the tandem BRCT domain of NBS1 seem to disrupt foci formation by the MRN complex, similar to point mutations altering key residues in the FHA domain, thus indicating that besides the FHA domain, the BRCT domains of NBS1 may also participate in MDC1 binding (8,10).

Here we present evidence that like the FHA domain, the tandem BRCT domain of NBS1 specifically interacts with phosphorylated MDC1. We show that a single point mutation in a key residue within the tandem BRCT domain of NBS1 abrogates accumulation of the MRN complex at sites of DSBs. Surprisingly though, this mutation does not trigger a G2/M checkpoint defect, indicating that MDC1-mediated accumulation of the MRN complex at sites of DSBs is not required for G2/M checkpoint activation.

Results and discussion

The NBS1 tandem BRCT domain is not required for SDT phosphopeptide binding.

Until recently, sequence comparison and structure predication algorithms indicated that the N-terminal region of NBS1 contained an FHA domain and one single BRCT domain (reviewed in (11)). Three years ago, a second putative BRCT domain at the N-terminus of NBS was discovered by means of a refined bioinformatic analysis (12). The existence of two BRCT domains downstream of the FHA domain at the NBS1 N-terminus was partially confirmed by a recently published NMR structure of the second (more C-terminal) BRCT domain (8). Interestingly, there is no spacer between the FHA domain and the putative tandem BRCT domain, indicating that these domains may form one single compact globular structure (see Figure 1A). Moreover, the conservation of key phospho-binding amino acid residues in the BRCT tandem domain suggests that like the FHA domain, it may act as a phospho-specific protein-protein interaction module.

We and others recently showed that the FHA domain of NBS1 directly associates with a constitutively phosphorylated region in MDC1, the SDT repeat region (also termed SDTD repeat region; (4-6)). The SDT repeat region consists of several conserved patches of eight to ten amino acids, interspersed with less conserved regions of variable length. The conserved patches feature a repeated sequence motif: Ser and Thr residues are embedded in an acidic sequence environment. A single amino acid (typically Asp) sits in between the highly conserved Ser and Thr residues. Both Ser and Thr residues are constituively phosphorylated by Caseine kinase 2. Mammalian MDC1 contains a total of six SDT

motifs, and at least five of these are required for efficient MRN accumulation at sites of DSBs (4).

It was recently suggested that the tandem BRCT domain of NBS1 may contribute to the stable association of NBS1 with the phosphorylated SDT region of MDC1 (8). This hypothesis was based on the observation that mutations in conserved amino acids in the second (C-terminal) BRCT domain led to defective NBS1 accumulation at sites of DSB (8). However, this analysis was carried out with over expressed proteins in Hela cells that express normal levels of endogenous NBS1.

In order to test if the BRCT tandem domain of NBS1 would contribute to the interaction with the phosphorylated MDC1 SDT region, we first designed a biotinylated synthetic phosphopeptide comprising the sequence of one of the SDT motifs and being phosphorylated on both the Ser and Thr residues (Figure 1B; top). To confirm that this peptide was capable to efficiently interact with NBS1, it was either left untreated or it was treated with Lambda phosphatase (λ-PPase) and was then used in a peptide pull down experiment with Hela nuclear extracts. Similar to previously published data, the phosphorylated peptide pulled down significant amounts of three proteins that were identified as RAD50, NBS1 and MRE11 (Figure 1B; (6)). Next, to test if efficient association of full-length NBS1 with this phosphopeptide required the intact BRCT tandem domain, we generated a number of point mutations in the full length NBS1 cDNA, targeting conserved amino acids that mediate direct contact with phosphorylated peptides. We chose conservative mutations to preserve the structure of the tandem BRCT domain (see Figure 1A; highlighted amino acids). These mutants were expressed in rabbit reticulocyte lysates (despite many attempts, we were unable to express soluble recombinant NBS1 in other expression systems) and tested for phosphopeptide binding in a pull down assay.

Interestingly, we observed that only mutations in the FHA domain (R28A; H45A) abrogated the interaction with the pSDpT peptide, while mutations in the BRCT tandem domain (S118A, K160M, K233A) showed similar affinity to the phosphopeptide binding as the wild type NBS1 (Figure 1C). These findings suggest that stable binding of NBS1 to an immobilized SDT phosphopeptide does not require the tandem BRCT domain.

The tandem BRCT domain of NBS1 contributes to the interaction with the full-length phosphorylated SDT region of MDC1.

The MDC1 SDT region contains at least 5 phosphorylated SDT motifs that are essential for efficient NBS1 binding (4). This may indicate that more than one binding site with affinity to the phosphorylated SDT region may exist in NBS1. Thus, we decided to test whether the intact NBS1 BRCT tandem domain was required for the efficient association of NBS1 with the full-length phosphorylated SDT region. To this end, we phosphorylated (or mock treated) a GST-tagged SDT fragment and assessed its ability to interact with the in vitro-translated wild type NBS1 and its FHA and BRCT mutated derivative, respectively. Both an FHA domain mutant (R28A) and a BRCT tandem domain mutant (K160M) still interacted with the phosphorylated SDT region of MDC1 (Figure 2A). However, a double phosphopeptide-binding mutant where both FHA and tandem BRCT domain are targeted (R28A/K160M), showed no significant binding to the phosphorylated SDT region anymore. This indicates that both the FHA domain and the BRCT tandem domain are capable to interact with the phosphorylated full-length SDT region in vitro.

NBS1 does not exist on its own in the nuclei of mammalian cells, as it is always associated with MRE11 and RAD50. Thus, our assay conditions with the in

vitro-translated NBS1 does not very well reflect the in vivo situation. Therefore, we co-expressed all three subunits of the MRN complex in insect cells and tested their binding affinity to the phosphorylated SDT region of MDC1. As shown before, also in the context of the entire MRN complex, wild type NBS1 efficiently bound to the phosphorylated SDT region (Figure 2B; (4)). Surprisingly though, neither the FHA mutant (R28A) nor the BRCT tandem domain mutant (K160M) was capable to associate with the phosphorylated SDT region (Figure 2B). This indicates that when NBS1 exists in a complex with MRE11 and RAD50, both the FHA domain and the BRCT tandem domain of NBS1 are required for stable association with MDC1. It is currently not clear why the in vitro-translated NBS1 single mutants still interacted with the phosphorylated SDT region while in the context of the full MRN complex, they did not. But it is possible that when NBS1 is an integral part of the MRN complex, its N-terminal phosphopeptide binding region may be sterically less flexible so that efficient association with the SDT region is only possible when both FHA domain and BRCT tandem domain are contributing to the interaction.

The BRCT tandem domain of NBS1 is required for efficient accumulation of the MRN complex at sites of DSBs, but not for the induction of the G2/M DNA damage checkpoint.

It has previously been shown that deletion of the first (N-terminal) BRCT domain leads to a defect in MRN accumulation at sites of DSBs (13,14). Moreover, point mutations in this domain that are thought to disrupt the structure also had a negative impact upon foci formation by the MRN complex (10). This may indicate that the BRCT tandem domain of NBS1 is also required for efficient MRN accumulation. However, since the FHA domain and the BRCT tandem domain may form one single globular domain at the NBS1 N-terminus (see above), it is also

possible that structure-disrupting mutations and/or deletion of an entire BRCT domain may also compromise the structure of the FHA domain. Thus, we saught to investigate whether a conservative K160M mutation in the BRCT domain that preserves the BRCT structure would also compromise the accumulation of the MRN complex at sites of DSBs. To this end, we took the well-established approach of UV-laser microirradiation to induce DSBs in subnuclear volumes of NBS fibroblasts stably transduced with full-length wild type, R28A and K160M NBS1 (15). Under these conditions, wild type NBS1 accumulated throughout the microirradiated nuclear compartments (Figure 3A). However, mutation in either the FHA domain (R28A) or the BRCT tandem domain (K160M) prevented NBS1 binding to the γH2AX-coated areas except for a small fraction of the protein scattered along the irradiated path (Figure 3A; see enlarged areas). This indicates that phospho-specific binding of the BRCT tandem domain (presumably to the MDC1 SDT region) is essential for efficient accumulation of the protein in damaged nuclear areas.

We previously proposed that MDC1-mediated accumulation of the MRN complex in chromatin regions flanking DSBs was required for the efficient activation of the G2/M DNA damage checkpoint. This was based on the observation that point mutations in the FHA domain that disrupt its phospho-specific binding, display partial G2/M checkpoint defects (4,16,17). So we reasoned that since mutations in the BRCT domains also lead to defective MDC1 binding and thus, to reduced chromatin accumulation at sites of DSBs, they should yield a similar G2/M checkpoint defect as FHA domain mutants. Surprisingly though, we found that NBS fibroblasts stably transduced with K160M NBS1 efficiently activated the G2/M checkpoint (Figure 3B). This indicates that MDC1-binding and MDC1-mediated accumulation of the MRN complex at sites of DSBs is not required for the activation of the G2/M checkpoint.

Spycher et al. 10

Moreover, our findings also suggest that the FHA domain of NBS1 may have additional binding partners besides MDC1, and that association of NBS1 with these binding partners may regulate G2/M checkpoint activation.

Material and Methods

Cell culture and gene transfer

NBS-iLB1 cells stably transduced with wild type NBS1 and R28A mutant NBS1 were kind gifts from Steve Jackson (University of Cambridge, UK) and Karen Cerosaletti (University of Washington, USA), respectively. NBS1-iLB1 stably expressing the K160M mutant NBS1 were generated by retroviral transduction of the NBS1 cDNA cloned into the pBABE puro retroviral vector. Sf9 cells were cultured in Grace's insect medium (Gibco) supplemented with 10% fetal calf serum. Recombinant MRE11, RAD50 and NBS1 baculoviruses were a kind gift from Vilhelm Bohr (NIA, Baltimore, USA). Bac-To-Bac Baculovirus Expression System (Gibco) was used to generate and amplify recombinant baculoviruses. All steps were carried out according to the manufacturer's protocols.

Irradiation of NBS1-iLB1 cells was carried in a Faxitron X-ray cabinet at 5-10 Gy/min. or by means of single-cell laser microirradiation (see below).

Plasmids

Human MDC1-GST constructs were described (4). Myc-NBS1 (18) was subcloned into pFastBac transfer vector (Gibco) to generate recombinant NBS1 baculoviruses and into pBABE puro to generate retroviral particles, respectively. Point mutations were introduced using the QuickChange site-directed mutagenesis kit (Strategene).

Cell extraction and protein purification

Hela nuclear extract was purchased from Cilbiotech (Mons, Belgium). MDC1-GST-SDT fragment was affinity purified on Glutathione-Sepharose (GE Healthcare Biosciences). Recombinant MRN purification from Sf9 cells was described (4). For in vitro-translation of NBS1, the TNT system (Promega) was used.

Microirradiation and single-cell analysis

In order to generate DSBs in defined nuclear volumes laser microirradiation was performed with a MMI CELLCUT system containing a 355 nm UVA laser (55 Hz, Molecular Machines & Industries, Switzerland) coupled to an Olympus IX71 microscope station and focused through an LUCPLFLN 40X objective. The MMICELLTOOLS software with MMIUVCUT plug-in assisted the laser operation using an energy output of 55% (unless stated otherwise). Prior to laser irradiation, cells were grown on coverslips in cell culture dishes in the presence of 10 μM BrdU (Bromodeoxyuridine; Sigma) for 24 h. Coverslips were then transferred into LabTek chamber slides (Nunc) and mounted on the microscope stage for irradiation. After irradiation, cells were placed back in the incubator for 30-60 min before fixation.

Antibodies and immunological techniques

Antibodies against human NBS1 and γH2AX were obtained from Upstate Biotechnology.

For immunofluorescence staining, cells were grown on glass coverslips, fixed in ice-cold methanol and stained with the indicated antibodies for 1h at room temperature. Secondary antibodies were from Jackson laboratories (FITC and

Rhodamine) and Invitrogen (Alexa-488 and Alexa-596). Images were captured at room temperature on a Leica SP2 confocal microscope (Leica Microsystems) with a 40x (oil immersion, NA 1.25) objective.

Biochemical analysis

For peptide pull down analysis, the biotinylated synthetic peptide Btn-NH-SGSFID[pS]D[pT]DAEEERI-COOH (Eurogentec) was used. Where indicated, 25 nmol of the peptide were incubated with 100 U λ−PPase (New England BioLabs) at 30°C for 20 min. Peptide pull down analysis from Hela nuclear extract was done as described (19). Peptide pull down analysis with in vitro-translaged NBS1 was done by incubating 25 nmol of the peptide with 1/5 volume of a standard TNT reaction.

For GST pull down assays, purified GST-fusion proteins (5 µg) were mixed with 1/5 volume of a standard TNT reaction and 5 µg of purified MRN, respectively. Where indicated, GST fusion proteins were pre-treated with 100 U of CK2 (New England BioLabs). The mixture was incubated for at 4°C for 30 min. to allow binding. Glutathione sepharose beads were then added and the suspension was incubated at 4°C for further 60 min. The beads were washed 3 times with wash buffer (50mM Tris pH 7.5, 120 mM NaCl, 1 mM DTT, 0.2% NP-40), resuspended in SDS loading buffer and analyzed by SDS polyacrylamide gel electrophoresis and immunoblotting.

Checkpoint analysis

G2/M checkpoint analysis was done as described (Falck et al., 2005). Briefly, cells were irradiated with the indicated doses during the exponential growth phase. 1h later, cells were harvested, fixed with 70% ethanol/PBS and incubated over night at -

20°C. Fixed cells were washed with PBS and permeabilized with 0.25% Triton/PBS on ice for 10min. Cells were stained with an anti-phospho-histone H3 antibody (Upstate) and propidium iodide. Data were acquired with a Becton Dickinson flow cytometer.

Acknowledgements

We thank Karen Cerosaletti, Vilhelm Bohr and Steve Jackson for providing valuable reagents. This work was supported by grants from the Swiss National Foundation (Grant Nr. 3100A0-111818) the UBS AG (Im Auftrag eines Kunden) and by the Kanton of Zürich. Stéphanie Jungmichel is acknowledged for comments and critical reading of the manuscript.

Literature

1. van der Burgt, I., Chrzanowska, K. H., Smeets, D., and Weemaes, C. (1996) *J Med Genet* **33**, 153-156
2. Difilippantonio, S., and Nussenzweig, A. (2007) *Cell Cycle* **6**, 2366-2370
3. Stracker, T. H., Theunissen, J. W., Morales, M., and Petrini, J. H. (2004) *DNA Repair (Amst)* **3**, 845-854
4. Spycher, C., Miller, E. S., Townsend, K., Pavic, L., Morrice, N. A., Janscak, P., Stewart, G. S., and Stucki, M. (2008) *J Cell Biol* **181**, 227-240
5. Melander, F., Bekker-Jensen, S., Falck, J., Bartek, J., Mailand, N., and Lukas, J. (2008) *J Cell Biol* **181**, 213-226
6. Chapman, J., and Jackson, S. (2008) *EMBO Rep*, 7
7. Wu, L., Luo, K., Lou, Z., and Chen, J. (2008) *Proc Natl Acad Sci U S A* **105**, 11200-11205
8. Xu, C., Wu, L., Cui, G., Botuyan, M. V., Chen, J., and Mer, G. (2008) *J Mol Biol* **381**, 361-372
9. Glover, J. N., Williams, R. S., and Lee, M. S. (2004) *Trends Biochem Sci* **29**, 579-585
10. Cerosaletti, K. M., and Concannon, P. (2003) *J Biol Chem* **278**, 21944-21951
11. D'Amours, D., and Jackson, S. P. (2002) *Nat. Rev. Mol. Cell Biol.* **3**, 317-327
12. Becker, E., Meyer, V., Madaoui, H., and Guerois, R. (2006) *Bioinformatics*
13. Lee, J. H., Xu, B., Lee, C. H., Ahn, J. Y., Song, M. S., Lee, H., Canman, C. E., Lee, J. S., Kastan, M. B., and Lim, D. S. (2003) *Mol Cancer Res* **1**, 674-681
14. Zhao, S., Renthal, W., and Lee, E. Y. (2002) *Nucleic Acids Res* **30**, 4815-4822
15. Lukas, C., Melander, F., Stucki, M., Falck, J., Bekker-Jensen, S., Goldberg, M., Lerenthal, Y., Jackson, S. P., Bartek, J., and Lukas, J. (2004) *Embo J* **23**, 2674-2683
16. Difilippantonio, S., Celeste, A., Fernandez-Capetillo, O., Chen, H. T., Reina San Martin, B., Van Laethem, F., Yang, Y. P., Petukhova, G. V., Eckhaus, M., Feigenbaum, L., Manova, K., Kruhlak, M., Camerini-Otero, R. D., Sharan, S., Nussenzweig, M., and Nussenzweig, A. (2005) *Nat Cell Biol* **7**, 675-685
17. Difilippantonio, S., Celeste, A., Kruhlak, M. J., Lee, Y., Difilippantonio, M. J., Feigenbaum, L., Jackson, S. P., McKinnon, P. J., and Nussenzweig, A. (2007) *J Exp Med* **204**, 1003-1011
18. Falck, J., Coates, J., and Jackson, S. P. (2005) *Nature* **434**, 605-611
19. Stucki, M., Clapperton, J. A., Mohammad, D., Yaffe, M. B., Smerdon, S. J., and Jackson, S. P. (2005) *Cell* **123**, 1213-1226

Figure legends

Figure 1: The NBS1 tandem BRCT domain is not required for SDT phosphopeptide binding.

A Schematic representation of full-length human NBS1 and its domain composition. The enlarged area shows a sequence alignment of the FHA and BRCT domains of human, mouse and Xenopus NBS1. The putative secondary structure of the first (N-terminal) BRCT domain is indicated by pale colors. The secondary structure of the second (C-terminal) BRCT domain (full colors) was derived from (8). Phospho-interacting amino acids are highlighted in yellow and a putative +3 interacting Lys residue is highlighted in ocre.

B A synthetic biotinylated peptide comprising the SDT sequence motif and being phosphorylated on the Ser and Thr residue was left untreated and pre-incubated λ−PPase, respectively. The peptides were then used to pull down proteins from Hela nuclear extract. The sequence of the peptide is shown on top.

C The synthetic biotinylated peptide shown in B was was left untreated and pre-incubated λ−PPase, respectively. The peptides were then incubated with in vitro-translated ^{35}S-labeled NBS1 wild type or mutants for 1 h, washed, and resolved by SDS-PAGE and autoradiography.

Figure 2: The tandem BRCT domain of NBS1 contributes to the interaction with the full-length phosphorylated SDT region of MDC1.

A Purified MDC1 GST-SDT fragment was pre-incubated with CK2 and ATP. The fragment was then incubated with in vitro-translated ^{35}S-labeled NBS1 wild type or mutants for 1 h, washed and resolved by SDS-PAGE and autoradiography.

B Purified MDC1 GST-SDT fragment was pre-incubated with CK2 and ATP. The fragment was incubated with purified MRN complex where the NBS1 subunit was either wild type or contained a point mutation in the FHA domain (R28A) or in the BRCT tandem domain (K160M). Bound proteins were separated on SDS polyacrylamide gels followed by immunoblotting. The blots were probed with a polyclonal antibody against NBS1.

Figure 3: The BRCT tandem domain of NBS1 is required for efficient accumulation of the MRN complex at sites of DSBs, but not for the induction of the G2/M DNA damage checkpoint.

A NBS-iLB1 fibroblasts stably transduced with wild type NBS1 and R28A and K160M mutant NBS1, respectively, were micro-irradiated as described in Material and Methods. Irradiated cells were incubated for 1 h, fixed with methanol and probed with the indicated antibodies. Cells were then analyzed by confocal microscopy.

B NBS-iLB1 fibroblasts and NBS-iLB1 fibroblasts stably transduced with wild type NBS1 and R28A and K160; mutant NBS1, respectively were left untreated or irradiated with 1 Gy and 10 Gy, respectively. Cells were harvested 1 hour after irradiation, fixed with methanol and stained with an antibody against phosphorylated H3 (P-H3) and propidium iodine. The percentage of P-H3 positive cells was determined by FACS analysis.

Spycher et al. Figure 1

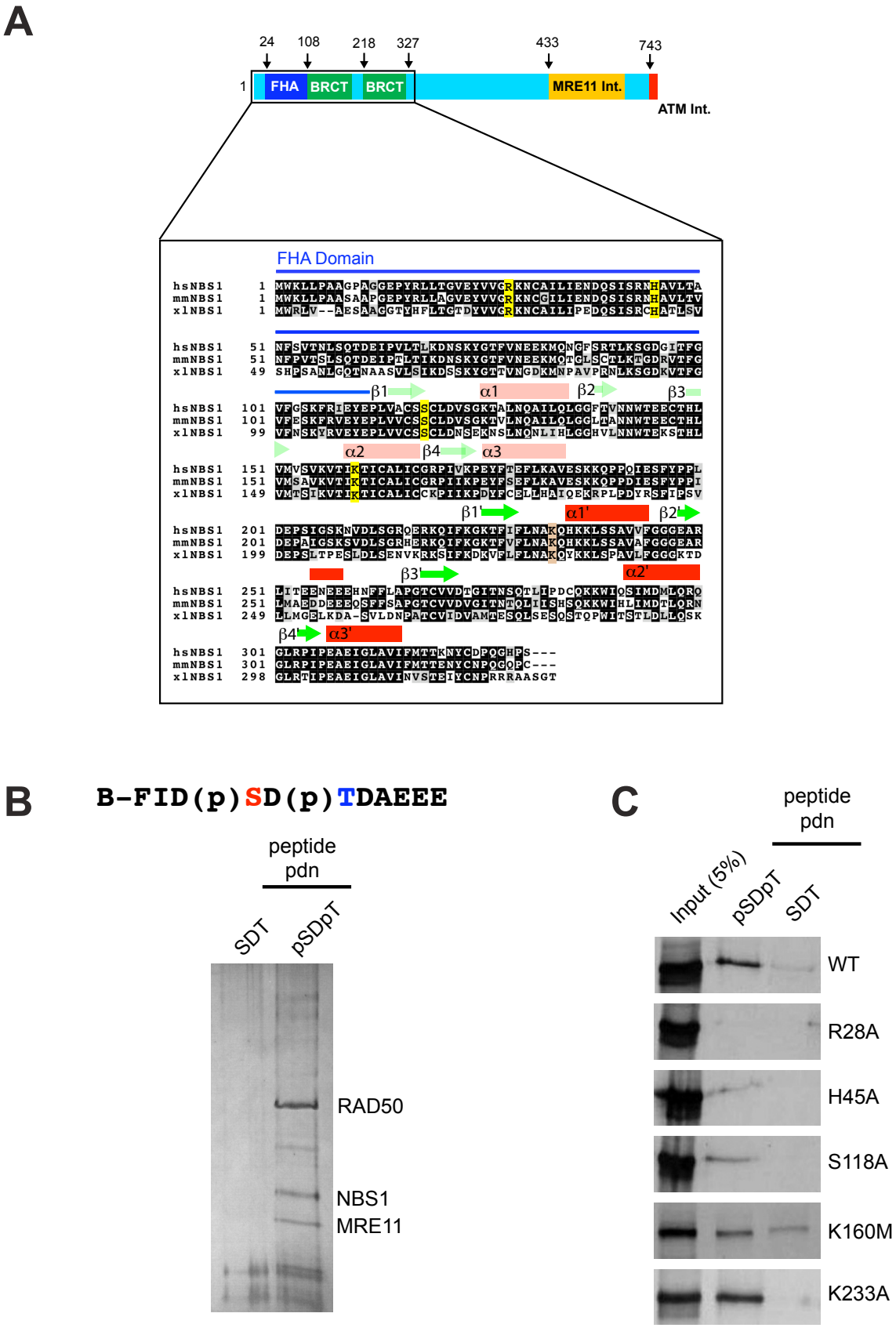

Spycher et al. Figure 2

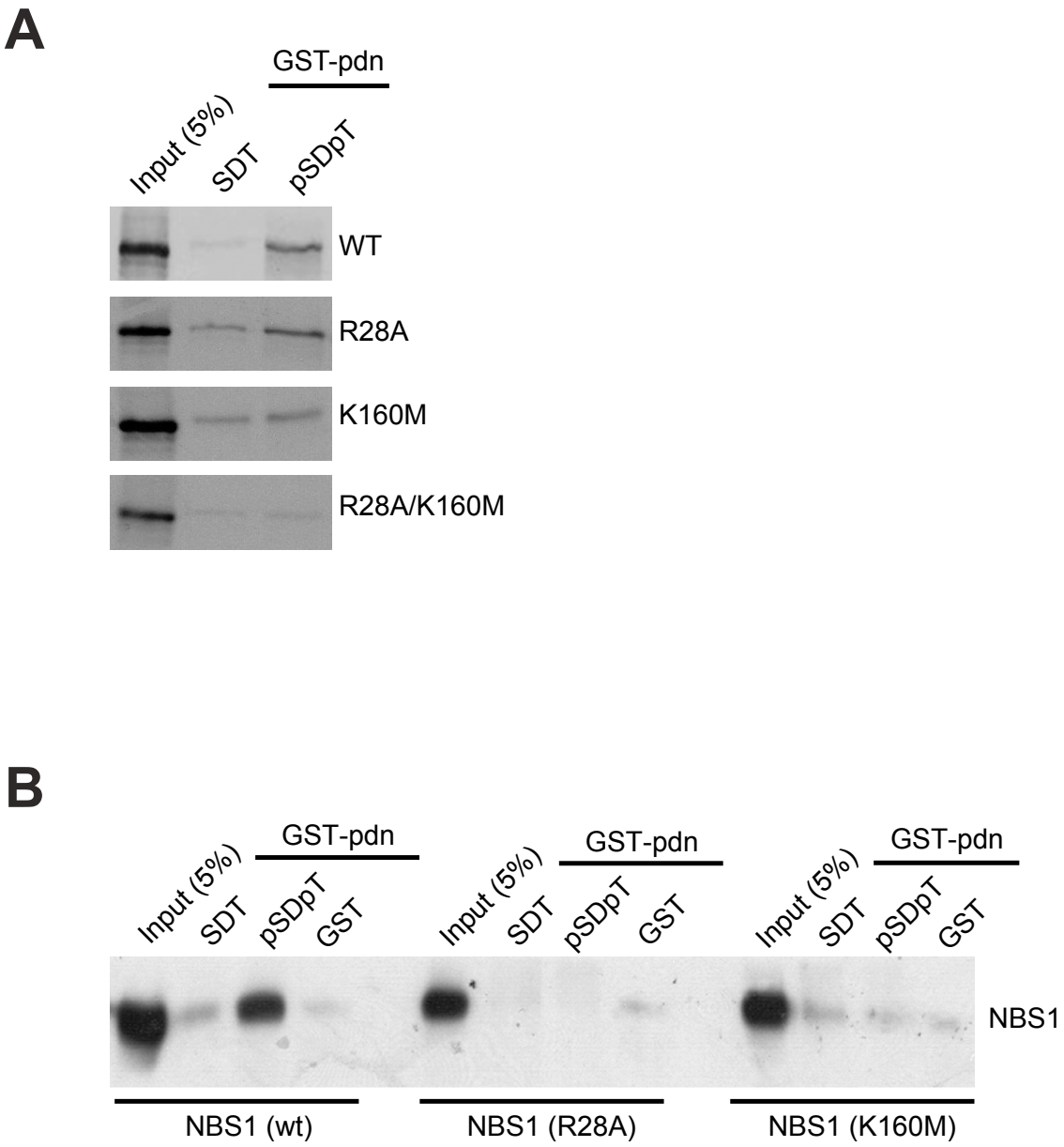

Spycher et al. Figure 3

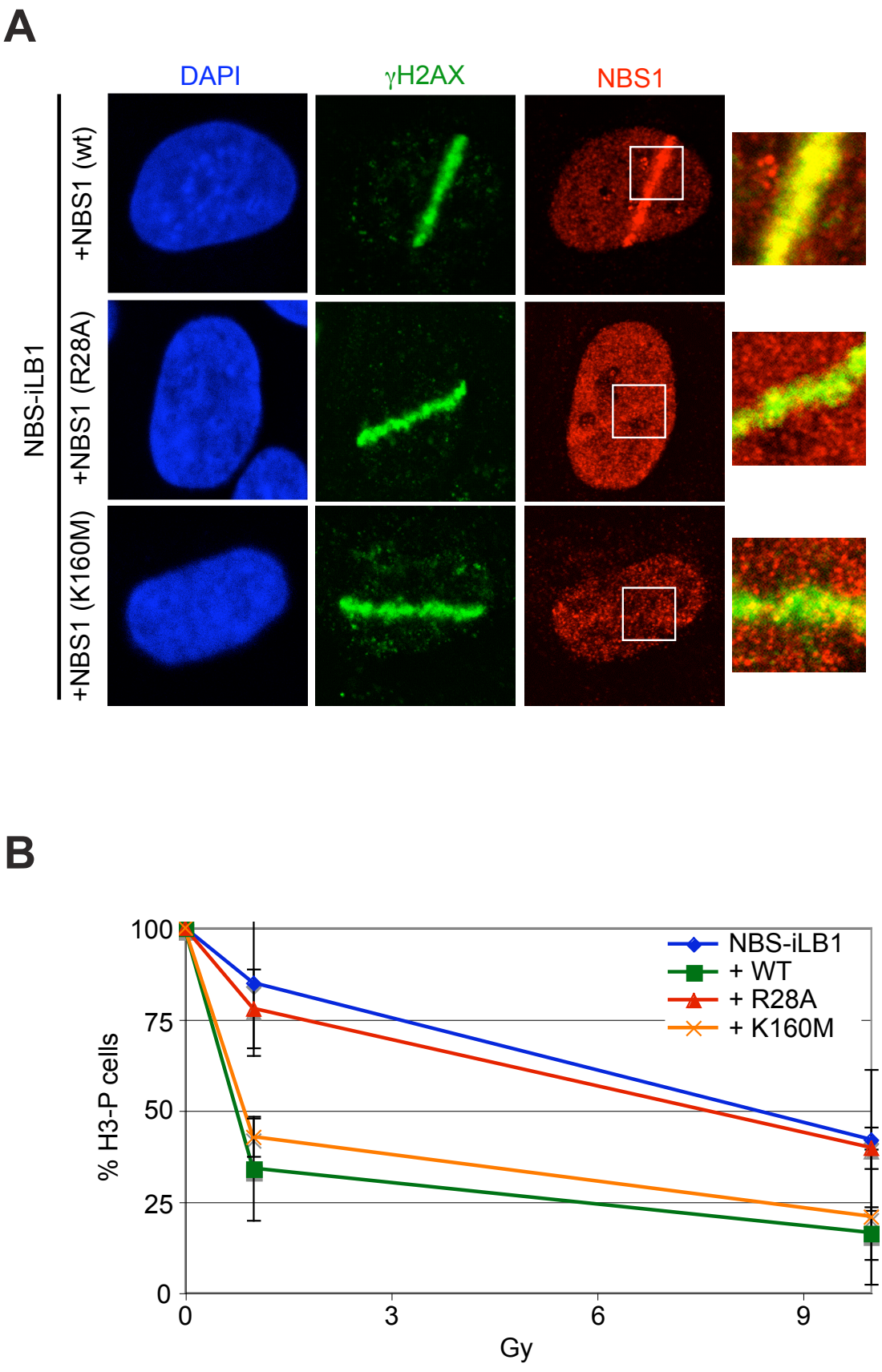

5.3 Molecular basis of ATM and FHA-dependent MDC1 dimerization in response to DNA damage

My contribution to this work was:

- Design and cloning of GST-MDC1 constructs (Figure 1A)
- Expression and purification of GST-MDC1 fragments (Figure 1A)
- In vitro ATM kinase assay with GST-MDC1 protein fragments (Figure 1A)
- Phospho-peptide pull down assay with pT4-peptide (Figure 2B)
- Phospho-peptide pull down with purified FHA and BRCT fragments (Figure 2C)
- Silver-stained SDS PAGE of phospho-peptide pull down (Figure S2)
- Proofreading of the manuscript

Molecular basis of ATM and FHA-dependent Mdc1 dimerisation in response to DNA-damage

Stephanie Jungmichel[2,*], Julie A. Clapperton[1,*], Janette Lloyd[1], Christoph Spycher[2], Lucijana Pavic[2], Jiejin Li[1], Lesley F. Haire[1], Claudia Lukas[4], Jiri Lukas[4], Derek MacMillan[3], Manuel Stucki[2] & Stephen J. Smerdon,[1]

[1]*Institute of Veterinary Biochemistry and Molecular Biology, University of Zürich, Winterthurerstrasse 190, 8057 Zürich, Switzerland.*

[2]*Division of Molecular Structure, MRC National Institute of Medical Research, The Ridgeway, London NW7 1AA, United Kingdom.*

[3]*Department of Chemistry, University College, London WC1H 0AJ, United Kingdom.*

[4]*Institute of Cancer Biology and Centre for Genotoxic Stress Research, Danish Cancer Society, Strandboulevarden 49, DK-2100, Copenhagen, Denmark.*

[*]These authors contributed equally to this work

Correspondence:
Manuel Stucki: m.stucki@vetbio.uzh.ch
Stephen J. Smerdon: ssmerdo@nimr.mrc.ac.uk

Running head: Mechanism of ATM-dependent MDC dimerisation

Subject Category: Genome Stability & Dynamics; Structural Biology

Abstract

Mediator of the DNA-damage Checkpoint-1 (Mdc1) is a large modular phosphoprotein that acts as a scaffold for assembly and maintenance of signaling and repair complexes at double-stranded DNA break sites. Mdc1 is anchored to damaged chromatin through interaction of its C-terminal BRCT-repeat domain with the phosphorylated tail of γH2AX following DNA damage, but the role of the N-terminal FHA domain remains largely obscure. Here, we show that the FHA domain binds both *in vitro* and in human cells to a novel DNA-damage and ATM-dependent phosphorylation site located at Thr-4 within the extreme Mdc1 N-terminus. We further show that while the isolated FHA domain forms phospho-independent dimers, self-association is substantially stabilised by Thr-4 phosphorylation. The X-ray structure of free and phosphopeptide-bound dimeric Mdc1 FHA domain reveals that dimerisation occurs in a 'head-to-tail' manner reminiscent of the arrangement often proposed for ATM-phosphorylated Chk2 kinase. Together, our observations highlight a novel mechanism for DNA-damage-regulated mediator dimerisation and suggest a more general significance of FHA-FHA interactions in other cellular signaling contexts.

Key words: DNA damage / ATM / chromatin / FHA domain / dimerisation

Introduction

Genomic integrity is constantly challenged by the effects of DNA-damaging agents. Double-stranded DNA breaks (DSBs) are considered to be the most genotoxic of the variety of different lesions that occur since incorrect repair can lead to chromosome breaks and other aberrations that are characteristic of and which may lead to cancer. The occurrence of DSBs initiates a program of cellular responses involving activation of cell-cycle checkpoints and deployment of the repair machinery. Central to DNA-damage response (DDR) regulation is a protein kinase cascade involving ataxia telangiectasia-mutated kinase (ATM) which acts as sensor of double-stranded breaks propogating damage signals through phosphorylation of checkpoint kinases and other diverse downstream targets. Many of these phosphorylation events are now known to sponsor protein-protein interactions mediated by phosphoserine/threonine-specific binding domains, most commonly forkhead-associated (FHA) and Brca1 C-terminal (BRCT) modules (Mohammad & Yaffe, 2009), providing for highly regulated, physical links between DDR components.

Mdc1 is a large (2089 aa), modular protein originally identified as an essential factor for establishment of the S-phase checkpoint (Goldberg et al, 2003; Lou et al, 2003a; Stewart et al, 2003). It is now known to function as an assembly platform for the localization and maintenance of signaling and repair factors at and around DSB sites (van Attikum & Gasser, 2009). As such, Mdc1 is the founding member of a class of large scaffolding/adaptor proteins known as 'mediators' that includes proteins such as human 53BP1 and yeast Rad9 and Crb2. While all of these molecules contain two or more copies of BRCT-repeat motifs, Mdc1 alone contains an additional FHA domain at its N-terminus.

Functionally, the C-terminal BRCT-repeats tether Mdc1 to regions of DNA-damage by virtue of their specific binding to ATM-phosphorylated H2AX (known as γH2AX), a

variant histone H2A which acts as the primary marker of damaged chromatin in all eukaryotic cells (Stucki et al, 2005). In contrast, the function of the FHA domain is less clear but has been suggested to include interaction with ATM itself (Lou et al, 2006), Chk2 (Lou et al, 2003a) and other repair proteins such as Rad51 (Zhang et al, 2005). In addition, although self-association has been shown to be a functional feature of 53BP1 (Zgheib et al, 2008), Rad9 (Soulier & Lowndes, 1999) and Crb2 (Kilkenny et al, 2008), the oligomeric status of Mdc1 in DNA-damaged cells has not, to our knowledge, been investigated. Using a combined biochemical, cell-biological and structural approach, we now show that the Mdc1 FHA domain mediates an inter-molecular interaction with a previously uncharacterized, ATM phosphorylation site located near the Mdc1 N-terminus, revealing a role for DNA-damage inducible Mdc1 dimerisation in the cellular response to double-stranded DNA breaks.

Results

Threonine-4 is a novel site of ATM phosphorylation *in vitro* and *in vivo*.

Mdc1 contains many potential PIKK target sites (S/TQ-motives) throughout its open reading frame and early studies have shown that upon genotoxic stress, Mdc1 is rapidly phosphorylated in a PIKK-dependent manner (Goldberg et al, 2003; Lou et al, 2003a; Stewart et al, 2003). However, only few of these potential PIKK target sites are conserved and the extent and physiological relevance of PIKK-dependent Mdc1 phosphorylation are largely unknown. In order to identify *bona fide* PIKK target sites in Mdc1, we generated eight overlapping fragments of the human Mdc1 cDNA and expressed them in *E. coli* as GST-fusion proteins (**Figure 1A**; top and (Spycher et al, 2008)). Seven fragments were expressed well and were purified (Figure 1A, upper panel) whereas one fragment (M-6) comprising the Mdc1 PST repeat region was not expressed in bacteria.

The purified GST fragments were subjected to an *in vitro* kinase assay with immunoprecipitated human ATM (Hickson et al, 2004). Surprisingly, purified ATM only phosphorylated fragment M-1 (amino acids 1-124) and fragment M-4 (amino acids 531-770), but none of the other five fragments (Figure 1A, lower panel). Fragment M-4 features a cluster of three conserved T-Q-X-F motifs that have recently been shown to form binding sites for the FHA domain of the ubiquitin ligase RNF8 following phosphorylation by ATM (Huen et al, 2007; Kolas et al, 2007; Mailand et al, 2007). Fragment M-1 contains two conserved TQ motifs: one at the very N-terminus of Mdc1 (T4/Q5) and one within the FHA domain (T98/Q99). Thr-4 appears to be the major site of ATM phosphorylation since a deletion mutant of M-1 lacking the first 18 amino acids was not phosphorylated by ATM *in vitro* (Figure S1) while a point mutation altering T4 to Ala (T4A) resulted in a protein that could no longer be phosphorylated by ATM *in vitro* (Figure 1B).

In order to investigate Thr-4 phosphorylation *in vivo*, we raised a phosphospecific antibody directed against a pT4 peptide derived from the Mdc1 N-terminus (T4p). This antibody recognized the *in vitro* phosphorylated M-1 fragment and cross-reacted only minimally with the unphosphorylated form of M-1 (Figure 1B, third panel). Moreover, the antibody did not recognize the T4A mutant M-1 fragment, even after ATM phosphorylation, indicating that this antibody is specific for the pT4 site. We then exposed U2OS cells to various doses of IR and analyzed total cell extracts by immunoblotting with the T4p antibody. The antibody cross-reacted with several proteins in total cell extracts, but one band (running at approximately 250 kDa) only emerged in extracts derived from cells that had been treated with IR. The intensity of this band increased with increasing dose of IR (Figure 1C; left panels). Stripping and re-probing the blot with an antibody against human Mdc1 revealed that the protein recognized by the T4p overlapped with at least one of the Mdc1 size variants. Time course analysis showed that 1 h post irradiation, phosphorylation levels were maximal and then slowly decreased. 21 hours post IR, the phosphorylation signal approached background levels (Figure 1C; right panels).

To exclude the possibility that the T4p antibody cross-reacted with another protein phosphorylated in response to IR, we subjected $Mdc1^{-/-}$ mouse embryonic fibroblasts and control ($Mdc1^{+/+}$) cells to various doses of IR and analyzed total cell extracts by immunoblotting using the T4p antibody. In extracts prepared from irradiated $Mdc1^{+/+}$ MEFs, a clear signal appeared on polyacrylamide gels at the position where mouse Mdc1 would be expected. No such signal was detected in extracts derived from irradiated $Mdc1^{-/-}$ cells, indicating that the protein recognized by the T4p antibody indeed corresponds to Mdc1 (Figure 1D).

Mdc1 phosphorylation in response to IR is ATM-dependent (Goldberg et al, 2003; Lou et al, 2003b; Stewart et al, 2003). Consistent with this, no Mdc1 signal was detected by

the T4p antibody in extracts from irradiated cells that had been pre-treatment with a specific ATM inhibitor or with a combination of ATM and DNA-PKcs inhibitors, while the signal was still present when the cells had been pre-treated with the DNA-PKcs inhibitor alone (Figure 1E). Together, these data suggest that Mdc1 contains a conserved PIKK target site at its very N-terminus and that in response to IR, this site is a *bona fide* ATM target *in vivo*.

The phosphorylated N-terminus of Mdc1 binds to its own FHA domain.

To understand the functional implication of Mdc1 T4 phosphorylation, we carefully analyzed the amino acid sequence surrounding the PIKK target site. Besides the TQ motif, several additional amino acids are conserved, most notably an isoleucine three residues C-terminal to the phosphoacceptor threonine. This is intriguing since pT-X-X-I was previously shown to constitute a favoured motif for certain classes of FHA domains (Durocher & Jackson, 2002). Indeed the entire N-terminal motif (M-E-D-pT-Q-A-I) closely resembles that derived for the Mdc1 FHA domain by oriented library screening in these studies. In order to test whether the phosphorylated N-terminus of Mdc1 could serve as a binding site for an FHA domain-containing proteins, we designed a phosphopeptide comprising the first 12 N-terminal residues of human Mdc1 phosphorylated on Thr-4. The phosphopeptide and its unphosphorylated derivative were coupled to magnetic beads and used to pull down proteins from Hela nuclear extracts. Both peptides retrieved several proteins that appeared as clear bands on a SDS polyacrylamide gel (Figure S2). Interestingly, at least three proteins were only pulled down by the phosphopeptide, but not by its unphosphorylated counterpart (Figure S2; highlighted by arrowheads). Most prominent were two bands of ~250kDa identified as Mdc1 itself as demonstrated by Western blot analysis with an antibody against human Mdc1 (Figure 2A). The other two bands at ~150 kDa and ~80 kDa were RAD50 and MRE11, respectively. Together with our previous finding that Mdc1 exists in a complex with MRN in

Hela nuclear extracts (Goldberg et al, 2003; Spycher et al, 2008; Stucki et al, 2005), these results indicate that Mdc1 may be the predominant interaction partner of its own phosphorylated N-terminus.

Of the two phosphospecific protein binding domains within Mdc1 (Figure 1A), phosphopeptide pull-down experiments with bacterially expressed GST fusion proteins of these regions showed that only the FHA domain bound tightly and specifically to the Mdc1 N-terminal phosphopeptide, with no significant interaction detectable for the C-terminal BRCT-repeat region (Figure 2B). Furthermore, we were able to demonstrate high affinity binding of purified Mdc1 FHA to a synthetic phosphopeptide encompassing the Thr-4 motif by isothermal titration calorimetry (ITC). Interestingly, these data could only be satisfactorily fit using a binding model incorporating two independent phosphopeptide sites (Figure 2C; see below). Thus, these results establish that Mdc1 interacts directly with its own phosphorylated N-terminus via the N-terminal FHA domain and, additionally suggest that it does so in a manner that differs somewhat from pThr-dependent FHA interactions described previously.

The Mdc1 FHA domain forms a dimer

In order to characterize the Mdc1 FHA-pThr 4 interactions further, we determined the structures of both free and phosphopeptide-bound forms at high resolution by X-ray crystallography (Table S1). The pThr 4 phosphopeptide complex was solved using the single wavelength anomalous diffraction method with crystals grown from selenomethione-substituted Mdc1 FHA domain, and a synthetic peptide in which Ala-6 was also replaced by selenomethionine, an approach we have described previously (Li et al, 2002). The refined coordinates of the complex were then used to solve the structure of the peptide-free form by molecular replacement.

As expected, the Mdc1 FHA domain adopts an 11-stranded β-sandwich fold that is characteristic of these signaling modules (Figure S3). Strikingly, we observed two FHA domains in the crystallographic asymmetric unit in both peptide-free and bound forms, each similarly arranged around a pseudo 2-fold non-crystallographic symmetry axis (Figure 3A; Figure S4). Although other FHA-FHA lattice interactions are observed in the two crystal forms, the non-crystallographic interaction surface is the most extensive burying a total of ~900Å^2/dimer in each case. Of these, ~600Å^2 are contributed by non-polar atoms from the side-chains of Phe 37, Leu 101, Leu 120, Leu 122 and Leu 127, all highly conserved in available sequences of Mdc1 orthologues (Figure 3B). Together these residues from a hydrophobic cluster on one face of each FHA β-sandwich (Figure 3B) that is tightly packed with high surface complementarity at the FHA-FHA interface (Figure 3C).

In the light of these observations, we examined the solution behaviour of the isolated FHA by size-exclusion chromatography and multi-angle laser light scattering (SEC-MALLS) that is able to conveniently measure shape-independent and highly accurate weight-averaged molecular weights of proteins and their complexes. This analysis showed significant self-association of the Mdc1 FHA domain with an apparent molecular weight of 18.3 +/- 0.06 kDa, some 40% greater than the calculated monomer mass of 12.8 kDa (Figure 3D). Moreover, a double mutation, L122E/L127E, resulted in a significant reduction in apparent molecular weight (14.3 kDa; Figure 3D) presumably due to juxtaposition of repulsive charges at the interface. Thus, we conclude that the dimeric arrangement observed in the crystal structures is likely to be representative of the dimer we observe in solution.

Thr-4 phosphorylation stabilizes a head-to-tail FHA interaction

The structure of the Mdc1 FHA/phosphopeptide complex (Figure 4A) shows a binding mode for the pThr 4 motif resembling that seen in several previously reported FHA domain

complexes. The phosphothreonine is held by a network of hydrogen-bonds with the highly conserved Arg-58 and Ser-72 side-chains along with accessory interactions with the less-well conserved Lys-73 (Figure 4B). Ile-7 occupies the pThr +3 position that has been shown to represent a major determinant of FHA specificity (Durocher et al, 2000) and interacts with the FHA domain through a shallow pocket formed by side-chains of residues 70, 96, 124 and 125. Most intriguingly, Trp-9 that is present in all available sequences of Mdc1 orthologues, is the last peptide residue visible in electron density maps and packs into a cleft formed at the edge of the FHA-FHA interface. Here, the Trp-9 indole side-chain packs against Pro-103 and the aliphatic portion of Arg-102 from the second protomer, both highly conserved**.** Due to the fact that the local 2-fold symmetry is imperfect, the interactions of the non-crystallographic symmetry-related Trp-9 are still significant but less extensive, potentially explaining the two binding sites observed in ITC measurements. Regardless, the structural data strongly suggest that pThr motif binding might contribute to the overall stability of the dimeric complex and we investigated this idea further using SEC-MALLS (Figure 4C). While the FHA domain itself shows evidence of weak dimerisation as described above, addition of the pThr-4 peptide substantially increases the apparent weight-averaged molecular weight to within 92% of that calculated for a fully dimeric, peptide-bound complex. Consistent with the structural location of Trp-9 at the FHA-FHA interface, a peptide variant containing a W9A substitution results in almost no additional dimer stabilization. Thus, accessory interactions mediated by Trp-9 of the bound phosphopeptide seem to directly stabilize dimerisation of the Mdc1 FHA domain.

These structural and hydrodynamic data reveal a novel dimeric FHA domain architecture that is stabilized through binding *in trans* to a motif representing the ATM-phosphorylated Mdc1 N-terminal region. This suggested to us that Mdc1 dimerisation might occur in a head-to-tail fashion as has been proposed for the pre-activated state of ATM-phosphorylated (pThr-68) Chk2 kinase (Li et al, 2008). Such a model is attractive since we

note that the conserved and highly acidic region (residues 10-18) C-terminal to Thr-4 could potentially interact with an equally conserved basic patch adjacent to the pThr-4 binding site but located on the adjacent protomer of the Mdc1 dimer (Figure 4D). Nonetheless, other arrangements are possible (Figure 4E). In particular the foregoing data did not eliminate the possibility of polymerization, nor did they exclude intra-molecular binding of the pThr-4 motif to its own FHA domain, potentially disrupting the weakly associated solution dimer. The latter model is particularly relevant in the light of our recent data showing just such an intra-molecular regulatory association in the Rv1827 FHA-domain protein from *M. tuberculosis* (Nott et al, 2009). In order to distinguish between these possibilities, we sought to generate an intact Mdc1 N-terminal region containing pThr-4. Given the experimental difficulty in producing quantities of active, recombinant ATM sufficient for this type of biophysical analysis, we instead chose to employ expressed protein ligation technology to generate a specifically and stoichiometrically phosphorylated sample by a semi-synthetic route (Figure 4F - top panel). In doing so we noticed that Cys-26, which could potentially act as an N-terminal nucleophile, is located immediately C-terminal to Arg-25. Thus by limited proteolytic cleavage of Mdc1 (residues 1-138), we could generate a C-terminal FHA-containing fragment with an N-terminal Cys-26. This, in turn, could be efficiently ligated to a pThr 4 phosphopeptide (residues 1-25) synthesized with a protected C-terminal thioester (Li et al, 2008). SEC-MALLS analysis of this material reported an apparent molecular weight of 31.2 kDa, essentially identical to the expected dimeric mass of the phosphorylated fragment (31.110 kDa) (Figure 4F - bottom panel). Thus, we conclude that pThr-4 phosphorylation results in Mdc1 dimerisation through a Chk2-like head-to-tail mechanism. Furthermore, the lack of any observable dissociation of this species at an on-column peak concentration of ~8 μM, also suggests that the phospho-dependent dimeric association occurs with high affinity.

Mdc1 self-association in human cells is pThr-4-dependent

Our *in vitro* data clearly demonstrate head-to-tail dimerization of the Mdc1 FHA domain via phosphorylation-dependent interactions with its N-terminal region. We next addressed the question whether this mode of interaction also occurs in cells. To do this, we first set up an experimental system that allowed the detection of interaction between different Mdc1 molecules by co-immunoprecipitation. As shown in Figure 5A, a Flag-tagged Mdc1 fragment (1-800) efficiently interacted with an identical Myc-tagged fragment. We used an N-terminal fragment lacking the BRCT domains to avoid problems with extraction due to avid association of Mdc1 with DNA damage-induced chromatin. Surprisingly, interaction between the two fragments was not dependent on IR treatment. However, when we probed the membranes with the pT4 antibody, we noticed that transiently expressed Mdc1 (1-800) fragment was constitutively phosphorylated on Thr-4 even without prior irradiation of the transfected cells (data not shown). This is probably due to the transfection procedure that has previously been shown to lead to constitutive phosphorylation of ATM targets. Nevertheless, mutation of either the FHA domain (R58A) and of the phosphoepitope (T4A) led to a significant reduction of the interaction between Flag-tagged and Myc-tagged Mdc1 (1-800). Concomitant mutation of both the FHA domain and Thr-4 resulted in a complete loss of the interaction, indicating that when expressed in human cells, the mechanism of Mdc1 dimerization is similar to the one observed in our *in vitro* binding experiments and crystal structures.

Mdc1 dimerization mediates recruitment of the FHA domain to sites of DNA damage

Next, we sought to demonstrate Mdc1 dimerization in living cells. We reasoned that if DNA damage-induced Mdc1 dimerization occurs via the FHA domain, we should detect partial recruitment of the FHA domain to sites of DSBs through association with endogenous

Mdc1. Moreover, this recruitment should be diminished by mutations in either the FHA domain or at the pThr-4 site. To circumvent limitations of the static assessment of IRIF formation in fixed cells, we used a previously described integrated imaging unit that combines microlaser-assisted generation of spatially defined DSB areas in mammalian cells with rapid, continuous and interactive image acquisition (Lukas et al, 2003; Lukas et al, 2004). Since we and others have previously observed that over expression of the Mdc1 FHA domain interferes with accumulation of DDR proteins (including Mdc1 and the Mre11/Rad50/Nbs1 complex) at sites of DSBs (Dimitrova & de Lange, 2006; Goldberg et al, 2003; Xu & Stern, 2003), we also generated a panel of cell lines derived from checkpoint-proficient U2OS cells carrying stably integrated, tetracycline-regulated expression cassettes directing the expression of the Mdc1 FHA domain fused to enhanced yellow fluorescent protein (EYFP). Significantly, when expressed at low levels, the Mdc1 FHA domain is recruited to microlaser-induced DNA damage (Figure 5B). The real-time measurements revealed a rapid accumulation of the fusion protein around the laser-generated, DSB-containing, subnuclear tracts (Figure 5C). The increase in fluorescence in the damaged nuclear compartments became detectable within 20-30 s (Figure 5C, first panel). Subsequently, the fusion protein underwent a rapid accumulation in the DSB regions, and reached a steady-state by 8-10 minutes after laser exposure. Importantly, no increase in fluorescence was observed in DSB-containing laser tracks in Mdc1-depleted cells, indicating that EYFP-FHA domain accumulation is strictly Mdc1-dependent (Figure 5D). Moreover, no accumulation was detectable in cells that express T4A or the R58A and L120/127E mutant derivatives of the FHA domain (Figure 5E). Thus, these data reveal that FHA accumulation to microlaser-induced DNA damage in living human cells mirrors the *in vitro* requirements for Mdc1 dimerization, strongly supporting the notion that Mdc1 dimerization in response to

DNA damage also occurs *in vivo* and that is does so in a manner that is consonant with our structural data.

Discussion

Mediator proteins such as Mdc1, Brca1 and 53BP1 play a variety of roles in the DDR. Phospho-dependent binding function is common to all, and all contain at least one domain capable of this function but interacting partners are not always clear. Oligomerisation now appears to be central to mediator activity and 53BP1, along with budding yeast Rad9 and fission yeast Crb2 have all been shown to self-associate albeit through different structural mechanisms. Rad9 seems to oligomerise via BRCT interactions with phosphosites generated by the ATR orthologue, Mec1, in a process that promotes activation of the Rad53 checkpoint kinase (Soulier & Lowndes, 1999; Usui et al, 2009). In contrast Crb2 and 53BP1 dimerisation appear to be independent of any post-translational modification (Kilkenny et al, 2008; Zgheib et al, 2008). To date, the oligomeric status of Mdc1 has not been examined. Here, we present a molecular description of FHA-mediated Mdc1 dimerisation in response to ATM phosphorylation of a specific and novel N-terminal motif.

A general role for dimerisation in FHA domain signaling

Our observation of phospho-independent FHA dimerisation is intriguing. Since their discovery as a conserved motif in forkhead transcription factors (Hofmann & Bucher, 1995), numerous x-ray crystallographic and NMR structures of different FHA domains have been described (Mahajan et al, 2008) but no structure of a dimeric FHA has yet been reported . Intriguingly, evolutionary trace analysis has been used to identify a novel patch of low-level sequence conservation associated with β-strands 9 and 10 and the connecting loop, leading to the suggestion that this may act as a self-interaction surface (Lee et al, 2003). Intriguingly our structure now shows that this putative surface substantially overlaps with the Mdc1 dimer-forming region (Figure S5). Moreover we also show that mutations within this region disrupt

FHA-FHA interactions *in vitro* (Figure 3D) and in living human cells (Figure 5E). These data, together with our recent observation that a similar region of a mycobacterial FHA domain mediates phospho-independent intermolecular interactions with several physiological targets (Nott et al, 2009), suggest a more expansive role for the β-sandwich architecture in FHA binding than has previously been assumed.

Dimerisation as a regulator of Mdc1 FHA interactions

While the γH2AX-binding function of the BRCT-repeat of Mdc1 is clear (Stucki et al, 2005), the *in vivo* role of the FHA domain is more enigmatic. Therefore, our observation that a major binding partner for the Mdc1 FHA domain is Mdc1 itself is intriguing and provides for means of both positively and negatively regulating FHA activity (Figure 6). As an example, Chk2 binding has been suggested to involve interaction of pThr-68, a major site of ATM-phosphorylation in the Chk2 SQ/TQ region, with the Mdc1 FHA domain (Lou et al, 2003b). We have recently shown that a tight pThr-68-dependent head-to-tail dimerisation of Chk2 results in effective occlusion of the canonical phospho-interacting FHA surfaces and prevents interactions of the pThr-68 motif with the Mdc1 FHA (Li et al, 2008). Clearly, our new data show that a similar effect would be expected for the pThr-4 Mdc1 FHA dimer. However, we and others have also shown that autophosphorylation of the Chk2 FHA releases monomeric Chk2 (Ahn & Prives, 2002; Li et al, 2008). This, in turn, would expose the pThr-68 motif and, potentially, allow binding to Mdc1 FHA domain prior to Thr-4 phosphorylation. ATM phosphorylation of Thr-4 and ensuing Mdc1 FHA dimerisation would then release Chk2, potentially explaining the observation of ejection of activated forms of Chk2 from chromatin fractions soon after DNA-damage (Li et al, 2008). Such a 'bind-and-release' mechanism could, in principle, operate for any interaction partner containing a suitable pThr-containing motif (Figure 6A). Similarly, formation of the tight, ATM-dependent

Mdc1 dimer would also occlude the FHA-FHA interaction surface that could function as a phospho-independent binding region (Figure 6B). Indeed, and as mentioned above, we have recently shown that part of this FHA domain surface can function in just such a fashion in other signaling contexts (Nott et al, 2009). Alternatively, we surmise that Mdc1 dimerisation might create new phospho-independent surfaces spanning both FHA domains (Figure 6C) and note that such an extensive, negatively charged surface is evident in our crystal structures (Figure S6).

An architectural role for Mdc1 dimers?

From an architectural viewpoint, a major effect of Thr-4 phosphorylation would be to stabilize formation of a large (~4000 aa) dimeric Mdc1 scaffold. Such a molecule would have the potential to bridge large distances in chromatin distal to DNA-break sites through γH2AX interactions with the BRCT-repeat domains at either end. Although the major means by which broken DNA ends are maintained in proximity for efficient repair is through the bridging function of the MRN complex (Williams et al, 2008), it may be that Mdc1 dimers play a contributing role in stabilizing more global structure within chromatin loops containing damage sites (Bassing & Alt, 2004). Indeed, the dependence on Mdc1 for rapid repair of dysfunctional telemores (Dimitrova & de Lange, 2006) suggests that such a tethering function may contribute to telomere maintenance and other NHEJ-mediated processes. Lastly, the existence of two BRCT-repeat domains within the Mdc1 dimer, and the significant effects of Mdc1 loss on fertility and spermatogenesis may be indicative of a bridging role in meiotic crossover events where Spo11-mediated dsDNA breaks sponsor accumulation of γH2AX binding sites for Mdc1 within each recombining homologue. In this context, it is interesting to note that Mdc1 mutants lacking the FHA domain were unable to complement the homologous

recombination defect observed in mouse embryonic fibroblasts derived from Mdc1 knockout animals (Xie et al, 2007).

Concluding remarks

Our data present compelling evidence for DNA-damage dependent Mdc1 dimerisation both *in vitro* and *in vivo* and suggest a number of ways in which this phenomenon might contribute to its activities in the DDR. Ultimately, unraveling the functional and mechanistic roles of the Mdc1-Mdc1 interactions reported here will require further investigation. However, our data now provide a firm structural and mechanistic framework for future analysis of this important and complex molecule.

Materials & Methods

Plasmids

Human MDC1-GST constructs were previously described (Spycher et al, 2008) Human MDC1 (aa 1-800) was generated by PCR and C-terminally tagged with HA/FLAG and Myc, respectively, and cloned into pcDNA3.1 (+) mammalian expression vector (Invitrogen). The MDC1 FHA domain (aa 1-154) was amplified by PCR and cloned into a modified pEYFP-nuc vector (Clontech), in which two tetracycline-repressor binding elements were inserted between promotor and coding sequences to generate an inducible expression cassette (Stucki et al, 2005). Point mutations were introduced by PCR-based methods or using the QuikChange Site-Directed Mutagenesis kit (Stratagene).

Protein expression and purification

DNA fragments encoding human Mdc1 residues 1-138 or 27-138 were amplified from a Mdc1 cDNA clone and ligated into BamH1/Xho1 digested pGEX-6P1. GST fusion proteins were affinity purified on glutathione-4B resin (Amersham) and cleaved from the affinity resin with rhinovirus 3C protease overnight at 4°C. Cleaved Mdc1 fragments were concentrated to ~ 5mg/ml and purified by gel-filtration chromatography on Superdex 75 in 20mM Tris-HCl pH 8.3, 150 mM NaCl, 5 mM DTT.

Crystallisation and X-ray data collection

Crystals of peptide-free Mdc1 (27-138) were grown by microbatch methods under Al's oil at 18°C at a protein concentration of 10 mg/ml mixed with an equal volume of 1.32 M ammonium sulphate, 50 mM sodium acetate pH 4.6 and 5% v/v methyl-pentanediol. Complex

crystals were grown from 1:1 complexes of selenomethionine substituted Mdc1 (27-138) with pThr-4 peptide containing a selenomethionine substituent at the pT+2 position, at a concentration of 15 mg/ml, mixed with an equal volume of 25% v/v ethanol, 0.1 M sodium acetate pH 5.5. Crystals were cryo-protected in mother liquor supplemented with 25% v/v glycerol (peptide-free) or 17.5% v/v ethylene glycol/10% v/v ethanol prior to data collection.

Structure solution and refinement

The structure of the selenomethionine peptide complex was solved by the single-wavelength anomalous diffraction (SAD) method using data collected on beamline 10.1 at the SRS Daresbury, UK. Four selenium sites were located and phases refined by SOLVE/RESOLVE (Terwilliger & Berendzen, 1999). The resulting map was readily interpretable allowing an essentially complete model for the two complexes in the asymmetric unit. The resulting FHA domain structure was then used to solve the non-complexed crystal form by molecular replacement using PHASER (McCoy et al, 2007). Model-building was carried out with 'Coot' (Emsley & Cowtan, 2004) and both structures were refined using REFMAC5 (Murshudov et al, 1997).

Cell culture and gene transfer

MDC1$^{-/-}$ and MDC1$^{+/+}$ MEFs were gifts from J. Chen (Yale University, New Haven, CT). U2OS, HEK 293T and MEFs were grown in D-MEM (Invitrogen) supplemented with 10% FCS (Gibco) and streptomycin/penicillin (100 U/ml, Gibco). Transfection of plasmids was done using either FuGene 6 (Roche) or Calcium phosphate. U2OS-TetOn cells stably expressing the tetracycline repressor were generated by transfection of EYFP-tagged MDC1-FHA domain following selection in G418-containing medium (Calbiochem). The siRNA oligonucleotides against endogenous human MDC1 were purchased from Ambion (siRNA

ID: 21738) containing the following sequence: sense 5'-GGAUCACACAAAGAUUAGAtt and antisense 5'-UCUAAUCUUUGUGUGAUCCtt. SiRNA transfections were performed using Lipofectamine RNAiMAX (Invitrogen) according the manufacturer's protocol. DNA damage was induced in a Faxitron X-ray cabinet at 5-10 Gy/min. or by means of single-cell laser microirradiation (see below).

Antibodies

The mouse monoclonal γH2AX antibody was obtained from Millipore and the rabbit polyclonal c-Myc antibody (sc-789) from Santa Cruz Biotechnology. The rabbit polyclonal FLAG antibody and the ANTI-FLAG M2 affinity gel, used for co-immunoprecipitation, were purchased from Sigma. Rabbit Polyclonal MDC1(889) and sheep polyclonal MDC1(3835) antibodies were raised against MDC1-FHA–GST as described previously (Goldberg et al., 2003). The phosphospecific antibody MDC1 pT4 was raised in rabbit against the phosphopeptide MEDT(P)QAIDWDVC and affinity purified using the phosphorylated and non-phosphorylated peptide (Eurogentec). Rabbit polyclonal ATM antiserum for ATM immunoprecipitation was a kind gift from Graeme Smith (KuDOS Pharmaceuticals, Cambridge, UK).

Biochemical analysis

Hela nuclear extract was purchased from Cilbiotech (Mons, Belgium). MDC1-GST fragments were affinity purified on Glutathione-Sepharose (GE Healthcare Biosciences) as described previously (Spycher et al, 2008). For peptide pull down analysis, the C-terminally biotinylated phosphopeptide MED[pT]QAIDWDAE[KBtn] (Sigma) was used. Where indicated, 25 nmol of the peptide were pre-incubated with 100 U λ−PPase (New England

BioLabs) at 30°C for 20 min. Peptide pull down analysis was done as described (Stucki et al, 2005).

For in vitro ATM kinase assays, ATM was immunoprecipitated with a rabbit polyclonal ATM antiserum (Hickson et al, 2004) from HeLa nuclear extract (Cilbiotech) in IP buffer (25 mM Hepes pH 7.4, 250 mM KCl, 2 mM $MgCl_2$, 10% glycerol, 0.1% NP-40, 0.5 mM EDTA, 1 mM NaF, 1 mM β-glycerophosphate). The immunocomplex was subsequently bound to Protein A-Sepharose beads (GE Healthcare). The kinase assay was performed by adding 1 µg GST-MDC1 (aa 1-154) to the beads in ATM-kinase buffer (50 mM Hepes pH 7.4, 150 mM NaCl), 4 mM $MnCl_2$, 6 mM $MgCl_2$, 10% glycerol, 1 mM DTT, 1 mM NaF, 1 mM β-glycerophosphate, 0.5 mM ATP and 10 µCi γ-[^{32}P]ATP) and incubating for 30 min at 30°C. Reactions were stopped by boiling in SDS sample buffer and run on an SDS polyacrylamide gel. Gels were analyzed by autoradiography and GelCode Blue Stain Reagent (Pierce) or Coomassie blue staining.

ATM inhibitor KPL0064 and DNA-PK inhibitor NU7026 were a kind gift from Graeme Smith (KuDOS Pharmaceuticals, Cambridge, UK) and were used at 10 µM and 20 µM, respectively.

Expressed protein ligation

Purified Mdc1 1-158 was digested with trypsin (Promega) at a ratio of 1:250 w/w enzyme:substrate to yield a 112 residue fragment (26-138) containing the FHA domain and part of the preceding linker with Cys-26 at its N-terminus. Synthesis of a C-terminally protected pThr-4 peptide (MEDpTQAIDWDVEEEEETEQSSESLR-SBn) and *in vitro* ligation to the Mdc1 26-138 fragment were carried in 200 mM phosphate buffer pH 8.0, 150 mM NaCl, 10mM TCEP, 2% w/v 2-mercaptoethanesulphonic acid (MESNA) overnight at room temperature as described previously (Li et al, 2008).

SEC-MALLS

Samples were applied at a concentration of 80-100 μM to a Superdex 75 10/300 GL column mounted on a Jasco HPLC and equilibrated in 20 mM Tris-HCl pH 8.3, 150 mM NaCl 3 mM DTT at a flow rate of 0.5 ml/min. Scattered light intensities of the column eluate were recorded at sixteen angles using a DAWN-HELEOS laser photometer (Wyatt Technology Corp., Santa Barbara, CA) and protein concentration of the eluted peak fractions were determined from the refractive index change (dn/dc = 0.186) using an OPTILAB-rEX differential refractometer equipped with a temperature-regulated flow cell at 25°C. The weight-averaged molecular weights of proteins and complexes within the elution peaks were determined using the ASTRA software version 5.1 (Wyatt Technology Corp., Santa Barbara, CA).

Isothermal titration calorimetry

ITC was carried out using a VP-ITC calorimeter (MicroCal, USA). Protein and peptides were desalted by dialysis or gel-filtration into a buffer containing 20 mM Tris-HCl pH 8.3, 150 mM NaCl, 0.5 mM TCEP. Typically, 10 μl aliquots of peptide at a syringe concentration of x mM were titrated over 30 injections into Mdc1 FHA domain samples at a concentration in the ITC cell of x μM using an integration time of 5 minutes. Data were corrected for heats of dilution and analysed using the Origin 5.0 software supplied with the instrument. Phosphopeptides were synthesized by Dr. W. Mawby (University of Bristol, UK).

Co-Immunoprecipitation

HEK 293T cells were transiently co-transfected with pcDNA3.1-MDC1(800)-FLAG and pcDNA3.1-MDC1(800)-Myc or the T4A, R58A, T4A/R58A mutants respectively using calcium phosphate. 48 h later, cells were mock- or IR-treated with 10 Gy. After 45 min, cells were lysed in NP-40 buffer (50 mM Hepes-KOH pH 7.9, 100 mM NaCl, 1mM EDTA, 1mM DTT, 0.5 % NP-40, 20% glycerol, PMSF, Leupeptin, Pepstatin A, Bestatin, 10 MM β-glycerophosphate and 1 mM NaF) for 15 min at 4°C and subsequently centrifuged at 14 000 rpm for 30 min at 4°C. Proteins in the supernatant were immunoprecipitated with ANTI-FLAG affinity gel (Sigma) in IP-buffer (see NP-40 buffer, but use of 40 mM Hepes-KOH pH 7.4, 0.05 % NP-40, no glycerol, no DTT) for 4h at 4°C. Immunocomplexes were washed three times in IP-buffer, boiled in SDS sample buffer and loaded on an SDS-polyacrylamide gel. Protein analysis was performed with standard immunoblot methods as described above.

Microirradiation and single-cell analysis

In order to generate DSBs in defined nuclear volumes laser microirradiation was performed with a MMI CELLCUT system containing a 355 nm UVA laser (55 Hz, Molecular Machines & Industries, Switzerland) coupled to an Olympus IX71 microscope station and focused through an LUCPLFLN 40X objective. The MMICELLTOOLS software with MMIUVCUT plug-in assisted the laser operation using an energy output of 55% (unless stated otherwise). Prior to laser irradiation, cells were grown on coverslips in cell culture dishes in the presence of 10 μM BrdU (Bromodeoxyuridine; Sigma) for 24 h. Expression of EYFP-MDC-FHA constructs in U2OS-TetOn cells was induced for 0.5 – 2 h with 1μg/ml Doxocyclin. Coverslips were then transferred into LabTek chamber slides (Nunc) and mounted on the microscope stage for irradiation. After irradiation, cells were placed back in the incubator for 30-60 min before fixation.

In case of live cell imaging, EYFP-MDC1-expressing cells were directly grown on LabTek chamber slides in the presence of 10 µM BrdU for 24 h. Laser irradiation was performed with a 337 nm PALM microlaser workstation (30 Hz, Palm MicroBeam, Carl Zeiss Microimaging Inc.) mounted on an Axiovert 200 microscope (Zeiss) and focused through a LD 40x, NA 0.6 Zeiss Achroplan objective. The microlaser procedure was assisted by the PALMRobo-Software. Images were immediately recorded after laser treatment.

For immunofluorescence analysis, cells grown on coverslips were fixed in 4 % paraformaldehyde for 20 min and permeabilized in 0.25 Triton X-100 in PBS for 15 min. After blocking in 10% FCS/PBS, cells were incubated in 5% FCS/PBS with the indicated primary antibodies for 1 h and secondary antibodies Alexa Fluor 568 (Molecular Probes) or Texas Red (Jackson Immuno Research) for 30 min. Finally, the coverslips were mounted with DAPI-containing Vectashield (Vector Laboratories). Confocal image acquisition was performed on a Leica SP2 microscope with a 40 x (NA 1.25) oil immersion objective or on an LSM-510 (Carl Zeiss Imaging) microscope with a 40 x Plan-Apochromat (NA 1.3) oil immersion objective.

Acknowledgements

We thank Graeme Smith, Junjie Chen and Steve Jackson for providing valuable reagents, Ian Taylor for assistance with MALLS and Philip Walker for help with X-ray data collection. MS acknowledges grants from the Swiss National Foundation (Grant Nr. 3100A0-111818), the UBS AG (Im Auftrag eines Kunden) and the Kanton of Zürich. SJS would like to thank the MRC, UK for continuing support.

Conflict of interest

The authors state that they have no conflicts of interest

Accession numbers

Coordinates and structure factors for the free and complexed Mdc1 FHA domains structures have been deposited with the Protein Data Bank under accession codes 1XYZ and 2XYZ respectively.

References

Ahn J, Prives C (2002) Checkpoint kinase 2 (Chk2) monomers or dimers phosphorylate Cdc25C after DNA damage regardless of threonine 68 phosphorylation. *J Biol Chem* **277**(50)**:** 48418-48426

Bassing CH, Alt FW (2004) H2AX may function as an anchor to hold broken chromosomal DNA ends in close proximity. *Cell Cycle* **3**(2)**:** 149-153

Dimitrova N, de Lange T (2006) MDC1 accelerates nonhomologous end-joining of dysfunctional telomeres. *Genes Dev* **20**(23)**:** 3238-3243

Durocher D, Jackson SP (2002) The FHA domain. *FEBS Lett* **513**(1)**:** 58-66

Durocher D, Taylor IA, Sarbassova D, Haire LF, Westcott SL, Jackson SP, Smerdon SJ, Yaffe MB (2000) The molecular basis of FHA domain:phosphopeptide binding specificity and implications for phospho-dependent signaling mechanisms. *Mol Cell* **6**(5)**:** 1169-1182

Emsley P, Cowtan K (2004) Coot: model-building tools for molecular graphics. *Acta Crystallogr D Biol Crystallogr* **60**(Pt 12 Pt 1)**:** 2126-2132

Goldberg M, Stucki M, Falck J, D'Amours D, Rahman D, Pappin D, Bartek J, Jackson SP (2003) MDC1 is required for the intra-S-phase DNA damage checkpoint. *Nature* **421**(6926)**:** 952-956

Hickson I, Zhao Y, Richardson CJ, Green SJ, Martin NM, Orr AI, Reaper PM, Jackson SP, Curtin NJ, Smith GC (2004) Identification and characterization of a novel and specific inhibitor of the ataxia-telangiectasia mutated kinase ATM. *Cancer Res* **64**(24)**:** 9152-9159

Hofmann K, Bucher P (1995) The FHA domain: a putative nuclear signalling domain found in protein kinases and transcription factors. *Trends Biochem Sci* **20**(9)**:** 347-349

Huen MS, Grant R, Manke I, Minn K, Yu X, Yaffe MB, Chen J (2007) RNF8 transduces the DNA-damage signal via histone ubiquitylation and checkpoint protein assembly. *Cell* **131**(5)**:** 901-914

Kilkenny ML, Doré AS, Roe SM, Nestoras K, Ho JC, Watts FZ, Pearl LH (2008) Structural and functional analysis of the Crb2-BRCT2 domain reveals distinct roles in checkpoint signaling and DNA damage repair. *Genes & Development* **22**(15)**:** 2034-2047

Kolas NK, Chapman JR, Nakada S, Ylanko J, Chahwan R, Sweeney FD, Panier S, Mendez M, Wildenhain J, Thomson TM, Pelletier L, Jackson SP, Durocher D (2007) Orchestration of the DNA-damage response by the RNF8 ubiquitin ligase. *Science* **318**(5856)**:** 1637-1640

Lee GI, Ding Z, Walker JC, Van Doren SR (2003) NMR structure of the forkhead-associated domain from the Arabidopsis receptor kinase-associated protein phosphatase. *Proc Natl Acad Sci U S A* **100**(20)**:** 11261-11266

Li J, Taylor IA, Lloyd J, Clapperton JA, Howell S, MacMillan D, Smerdon SJ (2008) Chk2 oligomerization studied by phosphopeptide ligation: implications for regulation and phosphodependent interactions. *J Biol Chem* **283**(51)**:** 36019-36030

Li J, Williams BL, Haire LF, Goldberg M, Wilker E, Durocher D, Yaffe MB, Jackson SP, Smerdon SJ (2002) Structural and functional versatility of the FHA domain in DNA-damage signaling by the tumor suppressor kinase Chk2. *Mol Cell* **9**(5)**:** 1045-1054

Lou Z, Chini CCS, Minter-Dykhouse K, Chen J (2003a) Mediator of DNA damage checkpoint protein 1 regulates BRCA1 localization and phosphorylation in DNA damage checkpoint control. *Journal of Biological Chemistry* **278**(16)**:** 13599-13602

Lou Z, Minter-Dykhouse K, Franco S, Gostissa M, Rivera MA, Celeste A, Manis JP, van Deursen J, Nussenzweig A, Paull TT, Alt FW, Chen J (2006) MDC1 Maintains Genomic Stability by Participating in the Amplification of ATM-Dependent DNA Damage Signals. *Mol Cell* **21**(2)**:** 187-200

Lou Z, Minter-Dykhouse K, Wu X, Chen J (2003b) MDC1 is coupled to activated CHK2 in mammalian DNA damage response pathways. *Nature* **421**(6926)**:** 957-961

Lukas C, Falck J, Bartkova J, Bartek J, Lukas J (2003) Distinct spatiotemporal dynamics of mammalian checkpoint regulators induced by DNA damage. *Nature Cell Biology* **5**(3)**:** 255-260

Lukas C, Melander F, Stucki M, Falck J, Bekker-Jensen S, Goldberg M, Lerenthal Y, Jackson SP, Bartek J, Lukas J (2004) Mdc1 couples DNA double-strand break recognition by Nbs1 with its H2AX-dependent chromatin retention. *Embo J* **23**(13)**:** 2674-2683

Mahajan A, Yuan C, Lee H, Chen ES, Wu PY, Tsai MD (2008) Structure and function of the phosphothreonine-specific FHA domain. *Sci Signal* **1**(51)**:** re12

Mailand N, Bekker-Jensen S, Faustrup H, Melander F, Bartek J, Lukas C, Lukas J (2007) RNF8 ubiquitylates histones at DNA double-strand breaks and promotes assembly of repair proteins. *Cell* **131**(5)**:** 887-900

McCoy AJ, Grosse-Kunstleve RW, Adams PD, Winn MD, Storoni LC, Read RJ (2007) Phaser crystallographic software. *J Appl Crystallogr* **40**(Pt 4)**:** 658-674

Mohammad DH, Yaffe MB (2009) 14-3-3 proteins, FHA domains and BRCT domains in the DNA damage response. *DNA Repair (Amst)*

Murshudov GN, Vagin AA, Dodson EJ (1997) Refinement of macromolecular structures by the maximum-likelihood method. *Acta Crystallogr D Biol Crystallogr* **53**(Pt 3)**:** 240-255

Nott TJ, Kelly G, Stach L, Li J, Westcott S, Patel D, Hunt DM, Howell S, Buxton RS, O'Hare HM, Smerdon SJ (2009) An intramolecular switch regulates phosphoindependent FHA domain interactions in Mycobacterium tuberculosis. *Sci Signal* **2**(63)**:** ra12

Soulier J, Lowndes NF (1999) The BRCT domain of the S. cerevisiae checkpoint protein Rad9 mediates a Rad9-Rad9 interaction after DNA damage. *Curr Biol* **9**(10)**:** 551-554

Spycher C, Miller ES, Townsend K, Pavic L, Morrice NA, Janscak P, Stewart GS, Stucki M (2008) Constitutive phosphorylation of MDC1 physically links the MRE11-RAD50-NBS1 complex to damaged chromatin. *J Cell Biol* **181**(2)**:** 227-240

Stewart GS, Wang B, Bignell CR, Taylor AMR, Elledge SJ (2003) MDC1 is a mediator of the mammalian DNA damage checkpoint. *Nature* **421**(6926)**:** 961-966

Stucki M, Clapperton JA, Mohammad D, Yaffe MB, Smerdon SJ, Jackson SP (2005) MDC1 Directly Binds Phosphorylated Histone H2AX to Regulate Cellular Responses to DNA Double-Strand Breaks. *Cell* **123**(7)**:** 1213-1226

Terwilliger TC, Berendzen J (1999) Automated MAD and MIR structure solution. *Acta Crystallogr D Biol Crystallogr* **55 (Pt 4):** 849-861

Usui T, Foster SS, Petrini JH (2009) Maintenance of the DNA-damage checkpoint requires DNA-damage-induced mediator protein oligomerization. *Mol Cell* **33**(2)**:** 147-159

van Attikum H, Gasser SM (2009) Crosstalk between histone modifications during the DNA damage response. *Trends Cell Biol* **19**(5)**:** 207-217

Williams RS, Moncalian G, Williams JS, Yamada Y, Limbo O, Shin DS, Groocock LM, Cahill D, Hitomi C, Guenther G, Moiani D, Carney JP, Russell P, Tainer JA (2008) Mre11 dimers coordinate DNA end bridging and nuclease processing in double-strand-break repair. *Cell* **135**(1)**:** 97-109

Xie A, Hartlerode A, Stucki M, Odate S, Puget N, Kwok A, Nagaraju G, Yan C, Alt FW, Chen J, Jackson SP, Scully R (2007) Distinct roles of chromatin-associated proteins MDC1 and 53BP1 in mammalian double-strand break repair. *Mol Cell* **28**(6)**:** 1045-1057

Xu X, Stern DF (2003) NFBD1/MDC1 regulates ionizing radiation-induced focus formation by DNA checkpoint signaling and repair factors. *Faseb J* **17**(13)**:** 1842-1848

Zgheib O, Pataky K, Brugger J, Halazonetis T (2008) An oligomerized 53BP1 tudor domain suffices for recognition of DNA double-strand breaks. *Mol Cell Biol***:** 34

Zhang J, Ma Z, Treszezamsky A, Powell SN (2005) MDC1 interacts with Rad51 and facilitates homologous recombination. *Nat Struct Mol Biol* **12**(10)**:** 902-909

Figure legends

Figure 1 - ATM targets Mdc1 on a conserved threonine residue at its N-terminus.

A - *In vitro* ATM kinase assay of recombinant Mdc1 fragments. Top: Schematic representation of Mdc1's domain architecture and of the GST-fusion fragments derived from its cDNA. Bottom: Upper panel: Coomassie blue stained polyacrylamide gel of the purified GST-fusion fragments. Bottom panel: Autoradiography of *in vitro* phosphorylated Mdc1 fragments

B - A conserved motif at the very N-terminus of Mdc1 is phosphorylated by ATM in vitro. Top: Sequence alignment of the Mdc1 N-terminus. The highly conserved Thr residue at position 4 (T4) is highlighted by an arrowhead. Bottom: ATM-phosphorylation of fragment M-1 and the mutant T4A. AR: Autoradiograph; CB: Coomassie blue; IB: immunoblot; PS: Ponceau red

C - Left panel: Dose titration using the pT4 phosphospecific antibody (α-pT4). Right panel: Kinetics experiment using the pT4 phosphospecific antibody. The band corresponding to Mdc1 is highlighted by an arrowhead.

D - $Mdc1^{+/+}$, $Mdc1^{-/-}$ MEFs were irradiated with various doses of IR. Extracts were probed with the pT4 antibody.

E - Mdc1 Thr-4 phosphorylation in response to IR is ATM-dependent. U2OS cells were pre-treated with ATM inhibitor, DNA-PKcs inhibitor or a combination of both inhibitors. Cell extracts were probed with the phosphospecific pT4 antibody.

Figure 2 - The phosphorylated Mdc1 N-terminus constitutes a recognition motif for the Mdc1 FHA domain.

A - The N-terminal Mdc1 pThr-4 sequence closely resembles the optimal binding motif derived previously {Durocher, 2000 p00534} by oriented peptide library selection. Circled residues highlight exact matches.

B - Immunoblot analysis indicates that endogenous Mdc1 is efficiently pulled down by the T4 phosphopeptide.

C - Coomassie blue-stained PAGE of a Thr-4 phosphopeptide pull-down experiment using purified M-1 GST-fragment (containing the FHA domain) and purified M-8 GST-fragment (containing the BRCT domains).

D - ITC binding isotherm for interaction of a synthetic pThr-4 peptide with recombinant Mdc1 FHA domain. Data were analysed assuming one or two site binding which consistently favoured the latter model, showing tight, stoichiometric (1:1) binding to similar but non-identical sites.

Figure 3 - Mdc1 FHA domain dimerisation

A - Ribbons reporesentation of the dimeric arrangement observed in the peptide-free Mdc1 FHA crystal structure. The position of the local 2-fold symmetry axis is indicated. All structural representations were generated using PyMOL (http://pymol.sourceforge.net/).

B - FHA-FHA interactions are predominantly medited by a conserved cluster of hydrophobic residues (top) that are highly conserved in all available sequences of Mdc1 orthologues (bottom). The location of β-strands observed in the structure are indicated in the lower panel, along with the positions of the four residues most highly conserved in the FHA domain family (circles).

C - SEC-MALLS analysis of the wild-type Mdc1 FHA (27-138) and a mutant form in which two residues that form the core of the observed dimer interface have been substituted with glutamate. The observed weight-avereaged molecular weight of the mutant is substantially less than the wild-type protein. The shorter retention time for the mutant may reflect a more extended shape for monomeric forms, or differential electrostatic effects on interaction with the column matrix.

Figure 4 - Head-to-tail dimerisation is stabilised by pThr-4

A - Structure of the Mdc1/pThr-4 peptide complex is shown as a Ca plot/surface representation with the peptide shown as sticks, viewed along the local 2-fold symmetry axis.

B - The phosphopeptide interacts with conserved FHA domain residues mainly through pThr-4 and main-chain atoms from pT+1 and +3 residues. The Trp-9 indole nestles in a cleft formed at the interface between the two FHA domains in the dimer.

C - SEC-MALLS analysis shows that a substantial stabilization of the Mdc1 FHA dimer by the pThr-4 peptide is greatly reduced by substitution of Trp-9 with alanine (W9A).

D - The sequence C-terminal to the pThr-4 motif (yellow) contains a highly conserved stretch of acidic residues highlighted in blue (top panel). These would be predicted to interact with arginine and lysine residues that are also conserved and form a basic patch adjacent to the binding site for the peptide C-terminus of the bound peptide (bottom).

E - Cartoon showing the three most likely effects of Thr-4 phosphorylation

F - Ligation of an extended pThr-4 peptide to trypsin-cleaved Mdc1 FHA (left) produces a stoichiometrically and specifically phosphorylated protein encompassing the entire N-terminal region that forms a tight dimer by SEC-MALLS analysis (right). M_o- observed molecular weight, M_c - calculated molecular weight.

Figure 5 - Dimerization of the Mdc1 N-terminal region *in vivo*

A - The interaction between differentially tagged Mdc1 N-terminal fragments is dependent upon the intact FHA domain and Thr4 phosphorylation. 293T cells were transiently transfected with Flag-tagged Mdc1(1-800aa) and Myc-tagged Mdc1(1-800aa) wildtype and the indicated mutants, respectively. Protein complexes were immunoprecipitated with monoclonal anti-Flag agarose and immunoblotted with polyclonal anti-Myc and polyclonal anti-Flag antibodies.

B - The Mdc1 FHA domain is recruited to damaged chromatin regions. U2OS expressing a tetracycline-inducible EYFP-FHA(WT)^{TetOn} fusion protein were treated with doxocyclin for 2 hours and subjected to laser irradiation. Cells were fixed 30 min after irradiation and immunostained for γH2AX.

C - Kinetics of Mdc1 FHA domain recruitment. U2OS FHA(WT)-EYFP^{TetOn} cells were incubated with doxocyclin for 1h and subjected to laser irradiation. Time lapse live cell microscopy was performed and images were taken at the indicated times. Note that for technical reasons, 0 min time point was taken about 20 sec after micro-irradiation.

D - Recruitment of Mdc1 FHA domain is dependent on endogenous Mdc1. U2OS FHA(WT)EYFP^{TetOn} cells were either treated with control siRNA or siRNA against endogenous Mdc1. Cells were induced with doxocyclin for 1h, subjected to laser irradiation and images were taken 30 min thereafter. Cells were subsequently fixed and immunostained for γH2AX.

E - Recruitment of Mdc1 FHA domain is dependent on phospho-specific interaction between Thr4 and the FHA domain as well as on an intact hydrophobic interface between FHA monomers. Doxocyclin induced U2OS FHA-EYFP^{TetOn} cells expressing the wild type and indicated mutants were induced with doxocyclin for 1h, subjected to laser irradiation and

images were taken 30 min thereafter. Cells were subsequently fixed and immunostained for γH2AX.

Figure 6 - Regulation of interactions through phospho-dependent and phospho-independent surfaces through ATM-dependent Mdc1 dimerisation.

A - Binding of Thr-phosphorylated partners such as Chk2 (gold) can occur through the canonical phospho-dependent surface on the Mdc1 FHA (green patch) that is subsequently occluded following Thr-4 phosphorylation and tight head-to-tail dimerisation.

B - Interaction of phospho-independent binding partners (red) with some or all of the Mdc1 dimerisation interface residues (yellow) competes with weak FHA-FHA interactions in un-phosphorylated Mdc1, but is occluded in the pThr-4 dimer.

C -Tight Mdc1 dimerisation might create a contiguous phospho-independent binding surface (cyan) spanning the two FHA domains.

Figure 1

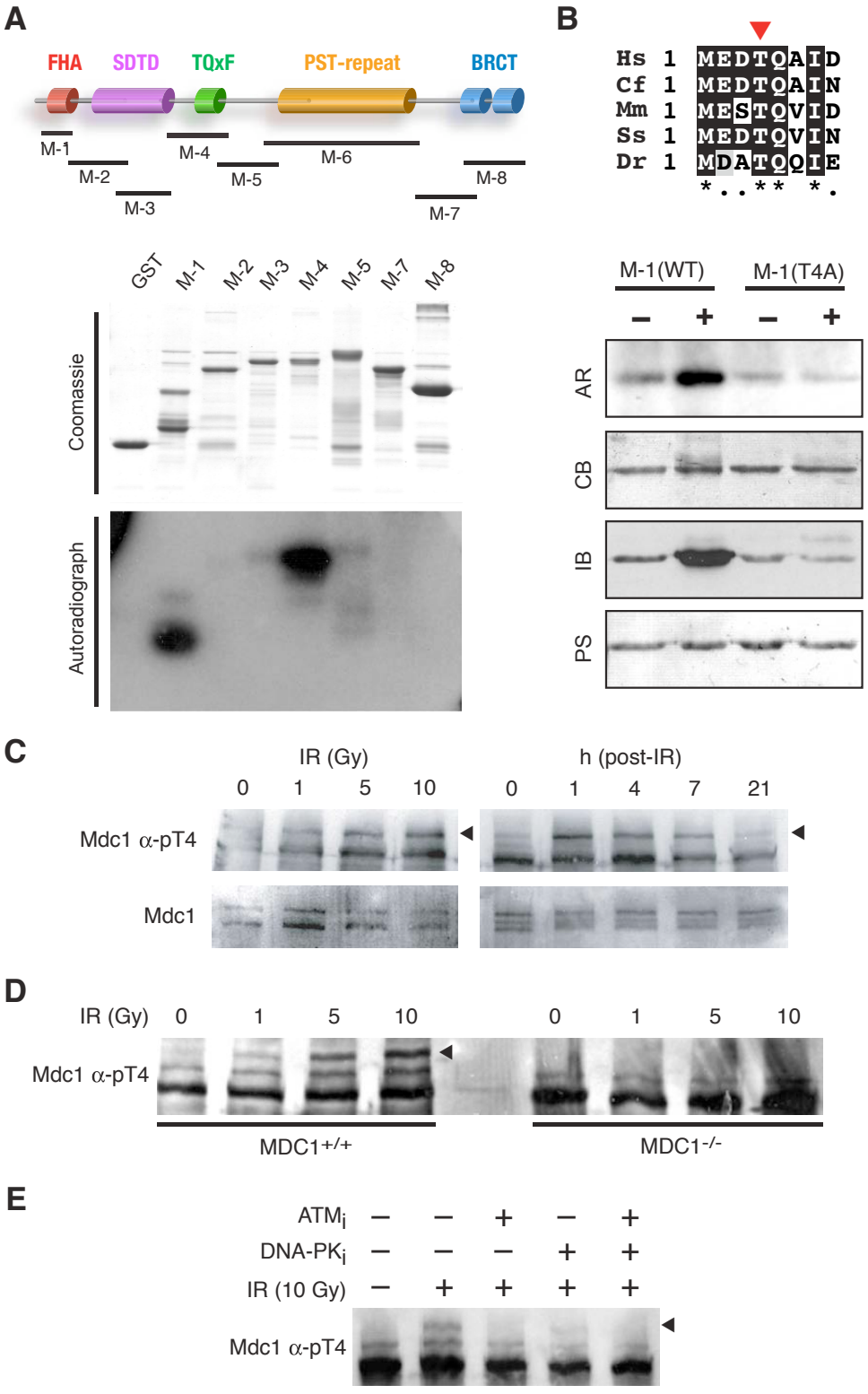
A
FHA
SDTD
TQxF
PST-repeat
BRCT
M-1
M-2
M-3
M-4
M-5
M-6
M-7
M-8
B
Hs 1 MEDTQAID
Cf 1 MEDTQAIN
Mm 1 MESTQVID
Ss 1 MEDTQVIN
Dr 1 MDATQQIE
GST
M-1
M-2
M-3
M-4
M-5
M-7
M-8
Coomassie
Autoradiograph
M-1(WT)
M-1(T4A)
AR
CB
IB
PS
C
IR (Gy)
0 1 5 10
h (post-IR)
0 1 4 7 21
Mdc1 α-pT4
Mdc1
D
IR (Gy) 0 1 5 10 0 1 5 10
Mdc1 α-pT4
MDC1+/+
MDC1-/-
E
ATMi
DNA-PKi
IR (10 Gy)
Mdc1 α-pT4

Figure 2

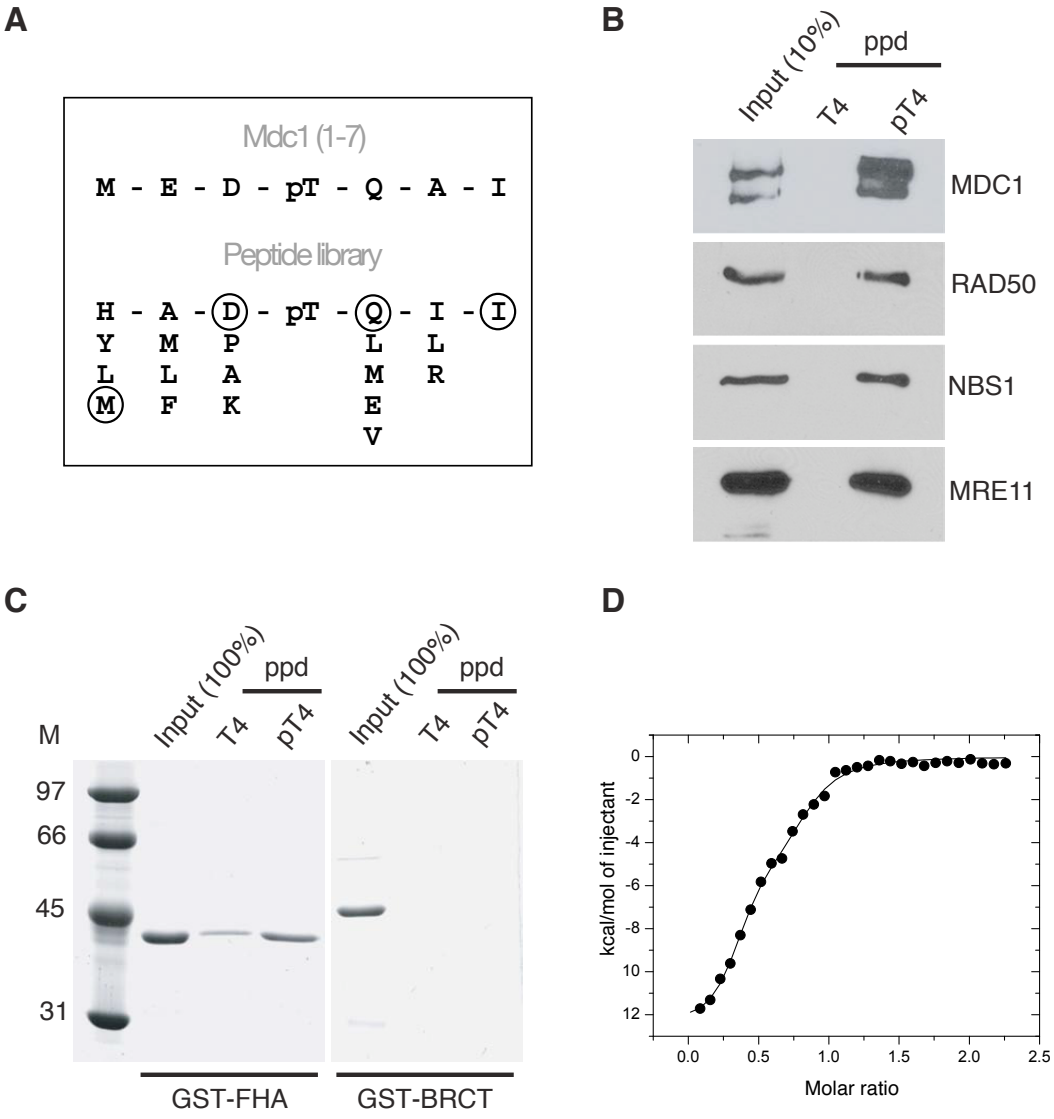
A
Mdc1 (1-7)
M - E - D - pT - Q - A - I
Peptide library
H - A - D - pT - Q - I - I
Y M P L M L
L L A M L R
M F K E
V
B
Input (10%)
ppd
T4
pT4
MDC1
RAD50
NBS1
MRE11
C
M
Input (100%)
ppd
T4
pT4
Input (100%)
ppd
T4
pT4
97
66
45
31
GST-FHA
GST-BRCT
D
kcal/mol of injectant
0
-2
-4
-6
-8
10
12
0.0
0.5
1.0
1.5
2.0
2.5
Molar ratio

Figure 3

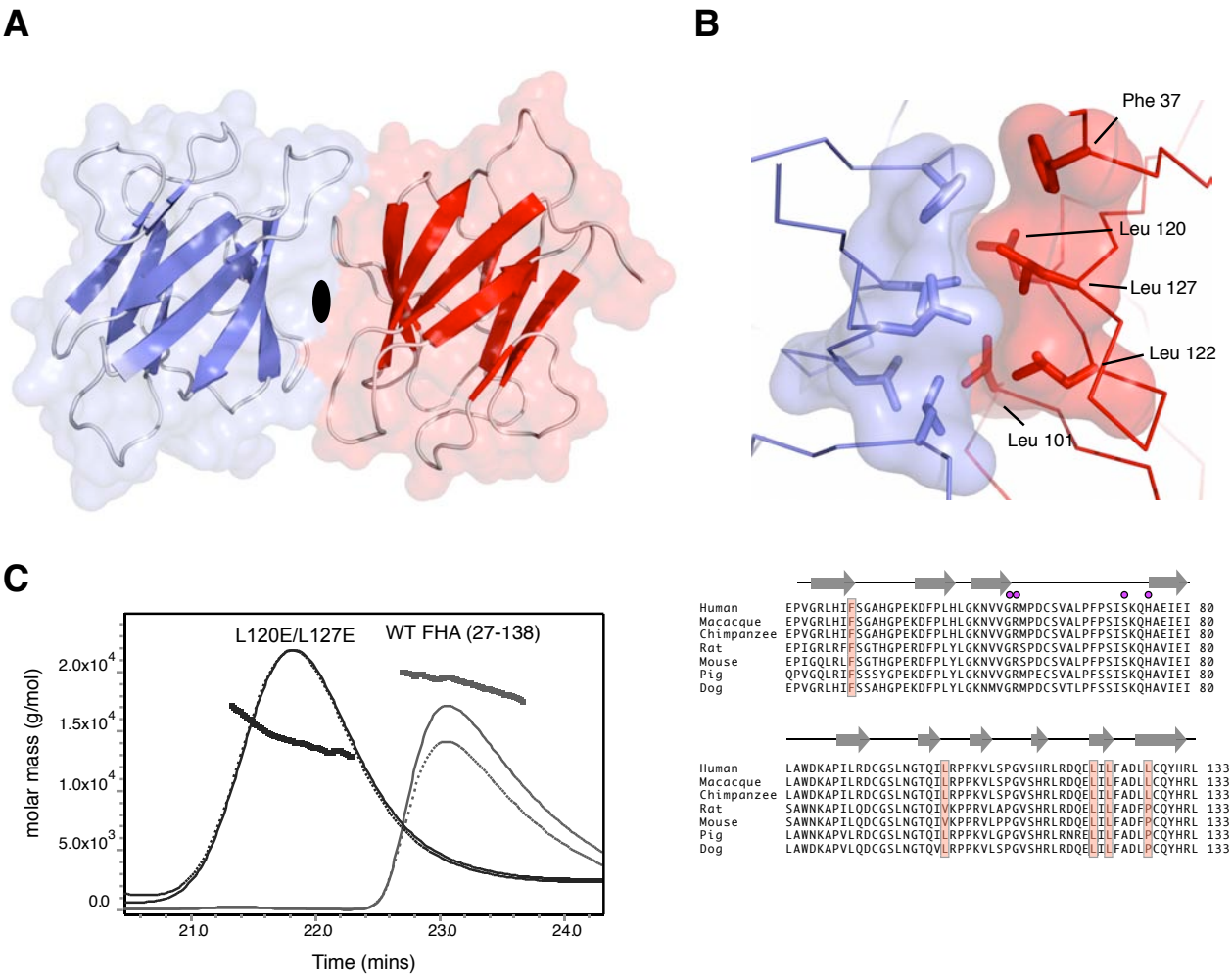
A
B
Phe 37
Leu 120
Leu 127
Leu 122
Leu 101
C
L120E/L127E
WT FHA (27-138)
molar mass (g/mol)
2.0x10^4
1.5x10^4
1.0x10^4
5.0x10^3
0.0
21.0
22.0
23.0
24.0
Time (mins)
Human EPVGRLHIFSGAHGPEKDFPLHLGKNVVGRMPDCSVALPFPSISKQHAEIEI 80
Macacque EPVGRLHIFSGAHGPEKDFPLHLGKNVVGRMPDCSVALPFPSISKQHAEIEI 80
Chimpanzee EPVGRLHIFSGAHGPEKDFPLHLGKNVVGRMPDCSVALPFPSISKQHAEIEI 80
Rat EPIGRLRFFSGTHGPERDFPLYLGKNVVGRSPDCSVALPFPSISKQHAVIEI 80
Mouse EPIGQLRLFSGTHGPERDFPLYLGKNVVGRSPDCSVALPFPSISKQHAVIEI 80
Pig QPVGQLRIFSSSYGPEKDFPLYLGKNVVGRMPECSVALPFSSISKQHAVIEI 80
Dog EPVGRLHIFSSAHGPEKDFPLYLGKNMVGRMPDCSVTLPFSSISKQHAVIEI 80
Human LAWDKAPILRDCGSLNGTQILRPPKVLSPGVSHRLRDQELILFADLLCQYHRL 133
Macacque LAWDKAPILRDCGSLNGTQILRPPKVLSPGVSHRLRDQELILFADLLCQYHRL 133
Chimpanzee LAWDKAPILRDCGSLNGTQILRPPKVLSPGVSHRLRDQELILFADLLCQYHRL 133
Rat SAWNKAPILQDCGSLNGTQIVKPPRVLAPGVSHRLRDQELILFADFPCQYHRL 133
Mouse SAWNKAPILQDCGSLNGTQIVKPPRVLPPGVSHRLRDQELILFADFPCQYHRL 133
Pig LAWNKAPVLRDCGSLNGTQILRPPKVLGPGVSHRLRNRELILFADLPCQYHRL 133
Dog LAWDKAPVLQDCGSLNGTQVLRPPKVLSPGVSHRLRDQELILFADLPCQYHRL 133

Figure 4

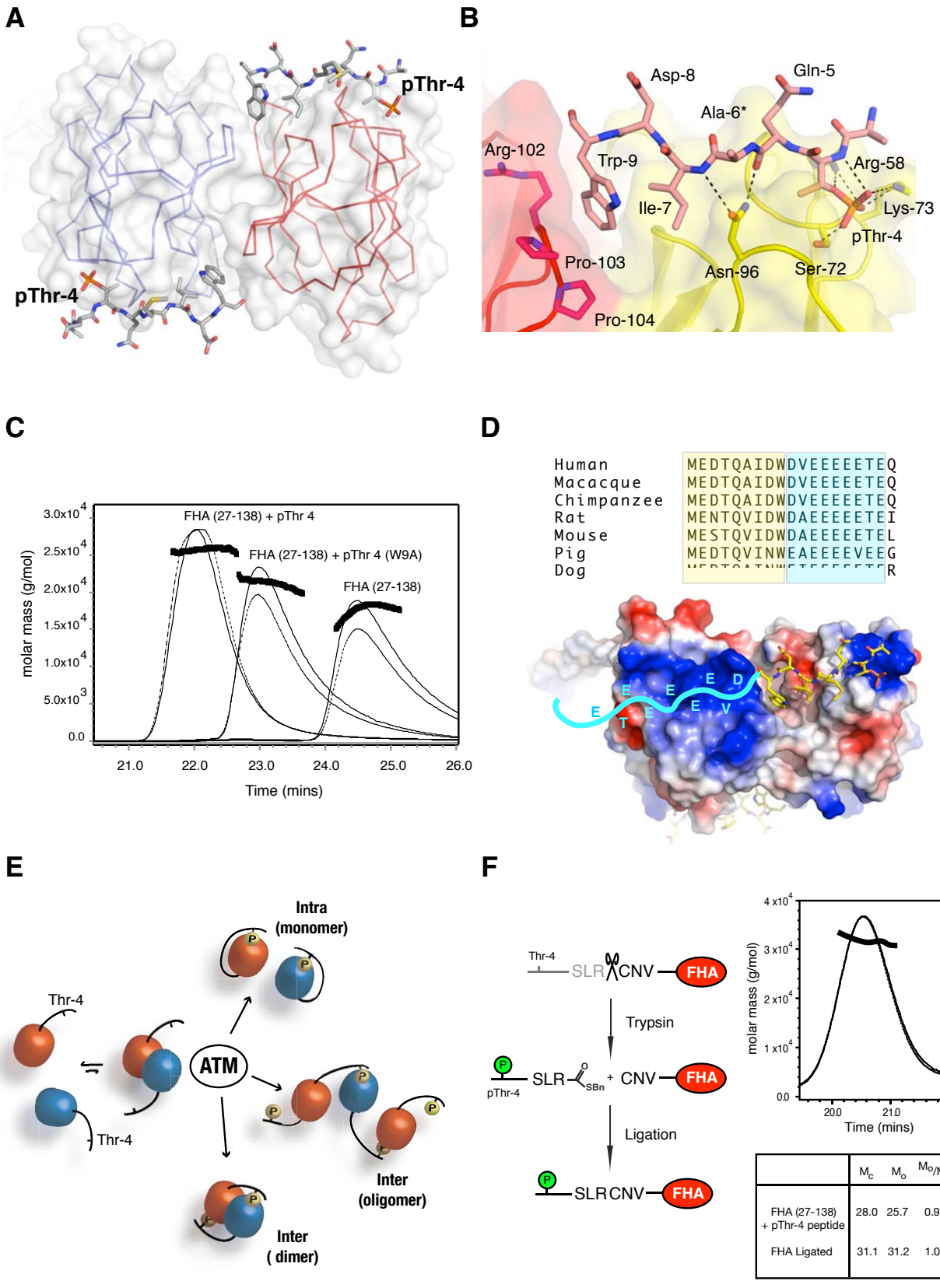

	M_c	M_o	M_o/M_c
FHA (27-138) + pThr-4 peptide	28.0	25.7	0.92
FHA Ligated	31.1	31.2	1.00

Figure 5

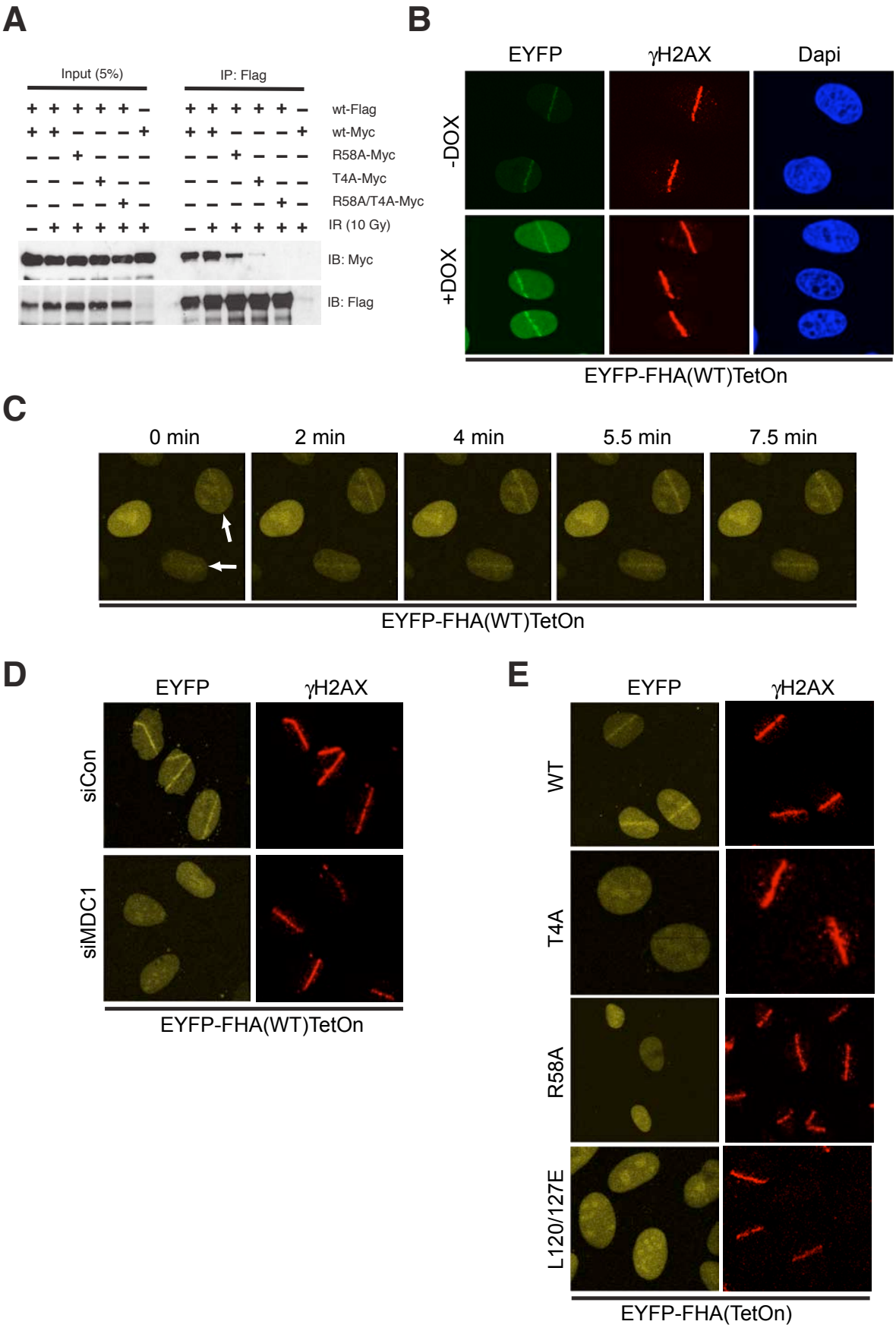
A
Input (5%)
IP: Flag
wt-Flag
wt-Myc
R58A-Myc
T4A-Myc
R58A/T4A-Myc
IR (10 Gy)
IB: Myc
IB: Flag
B
EYFP
γH2AX
Dapi
-DOX
+DOX
EYFP-FHA(WT)TetOn
C
0 min
2 min
4 min
5.5 min
7.5 min
EYFP-FHA(WT)TetOn
D
EYFP
γH2AX
siCon
siMDC1
EYFP-FHA(WT)TetOn
E
EYFP
γH2AX
WT
T4A
R58A
L120/127E
EYFP-FHA(TetOn)

Figure 6

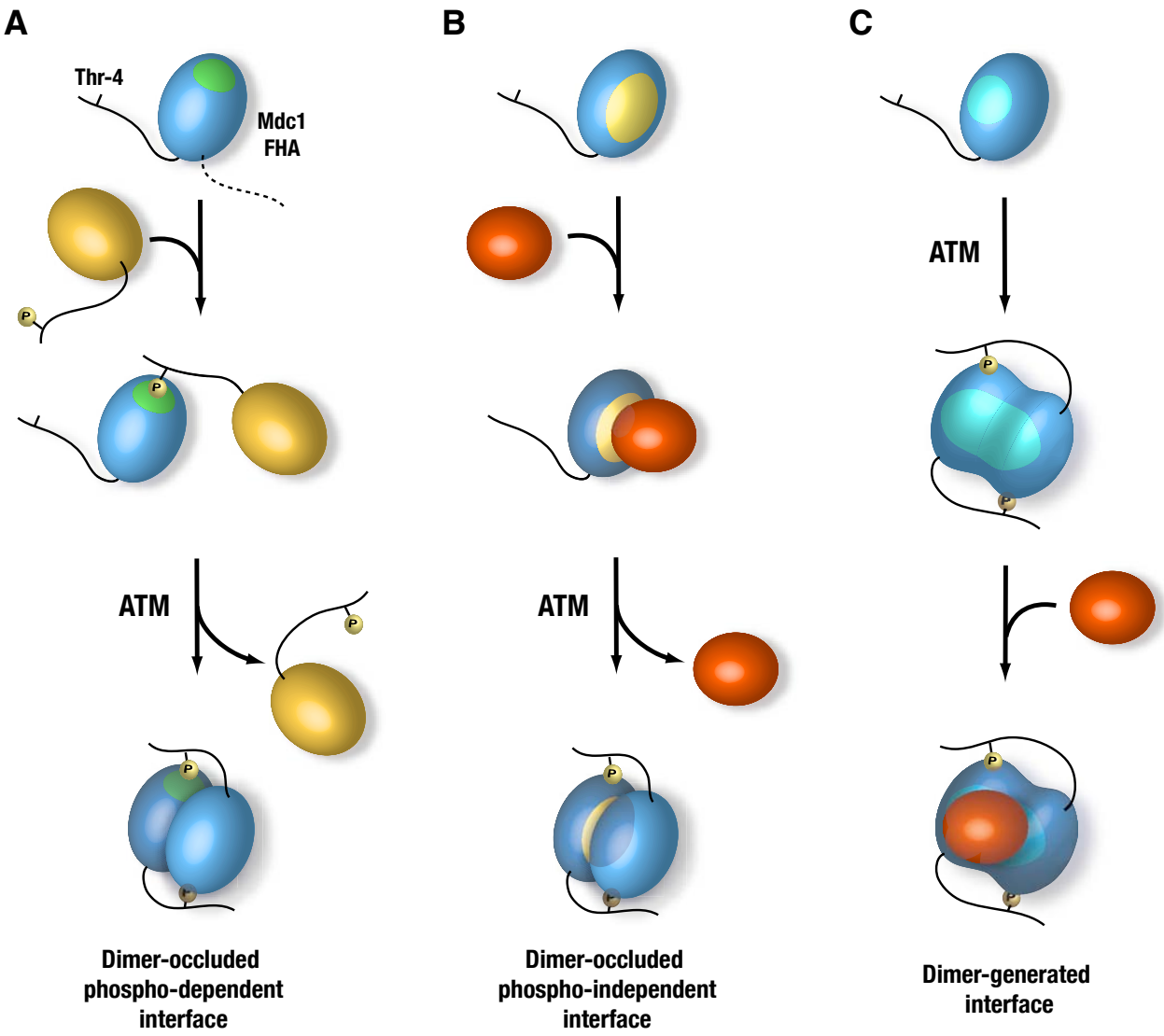
A
Thr-4
Mdc1
FHA
P
ATM
P
Dimer-occluded
phospho-dependent
interface
B
ATM
P
Dimer-occluded
phospho-independent
interface
C
ATM
P
Dimer-generated
interface

Supplementary information

Molecular basis of ATM and FHA-dependent Mdc1 dimerisation in response to DNA-damage

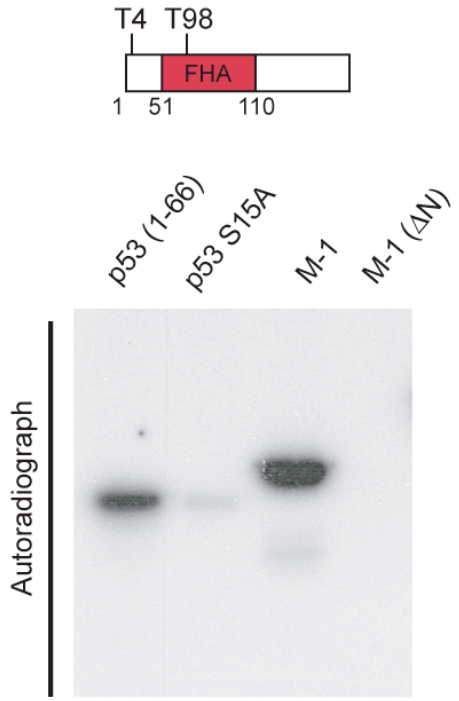

Figure S1 – Autoradiography of in viro-phosphorylated N-terminal MDC1 fragment comprising the FHA domain. In this fragment, two ATM/ATR consensus sites (TQ) are present (T4 and T98). However, only T4 is phosphorylated by ATM in vitro since M1 (ΔN) lacking the N-terminal T4 is not phosphorylated.

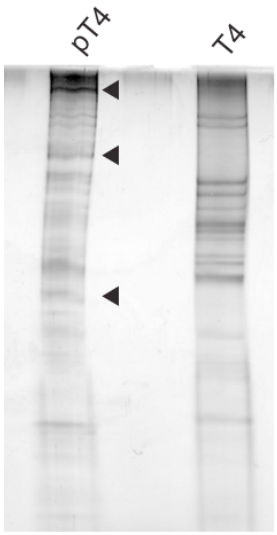

Figure S2 - Silver-stained SDS PAGE gel of proteins pulled down by the Thr-4 phosphopeptide and its unphosphorylated derivative. The major bands present only in the phosphopeptide pull-down are highlighted by arrowheads.

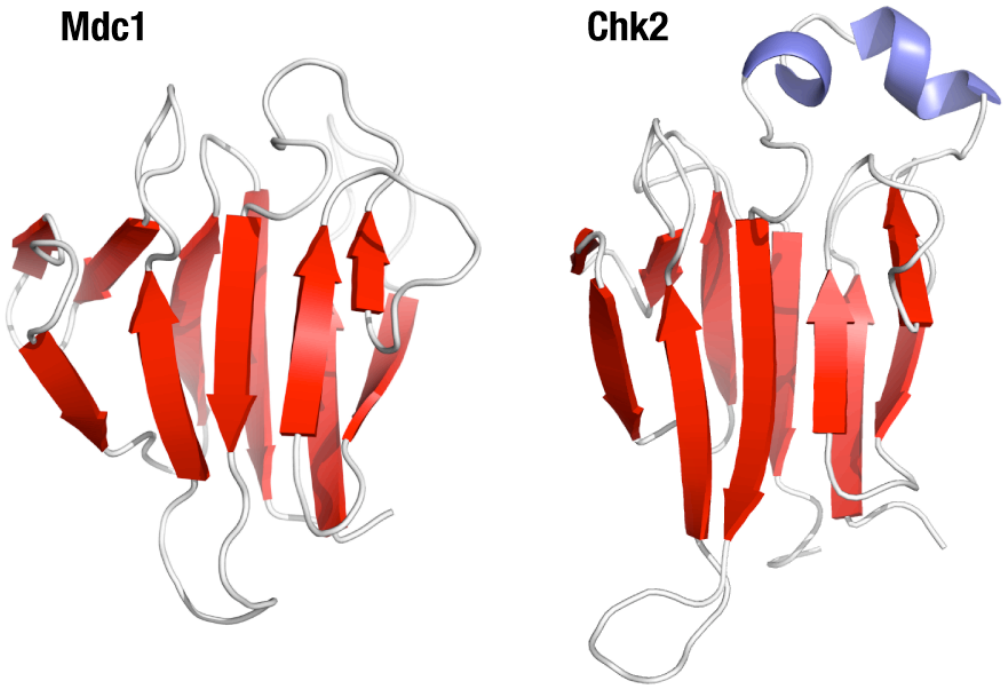

Figure S3 - Comparison of the Mdc1 FHA structure with that of human Chk2 (PDB ID: 1GXC) reveals a similar, characteristic core FHA domain β-sandwich architecture.

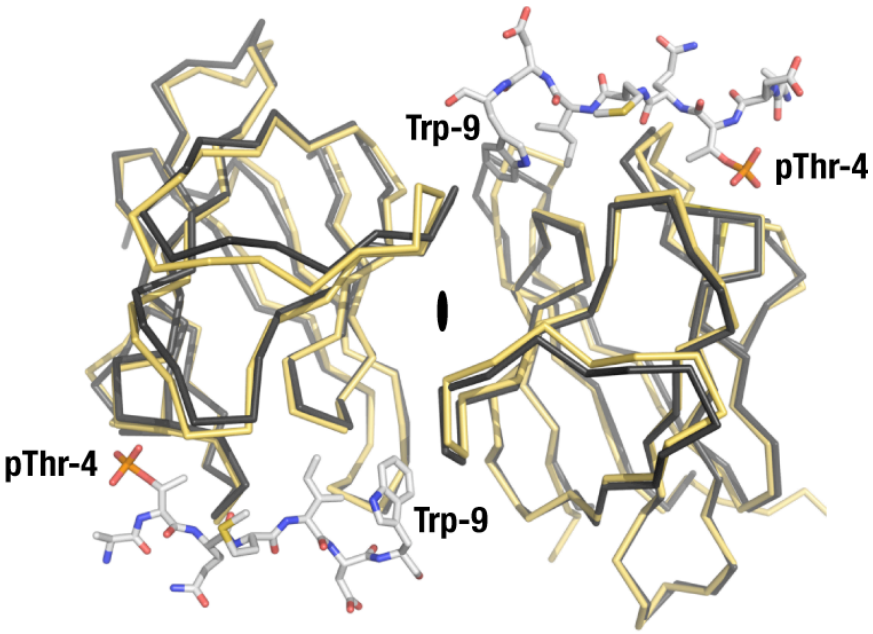

Figure S4 - Least-squares superposition of the Mdc1 FHA domain dimer in the peptide-free (black) and pThr-4 peptide-bound (gold) structures, shown as Cα plots. The bound phosphopeptide is shown in stick representation.

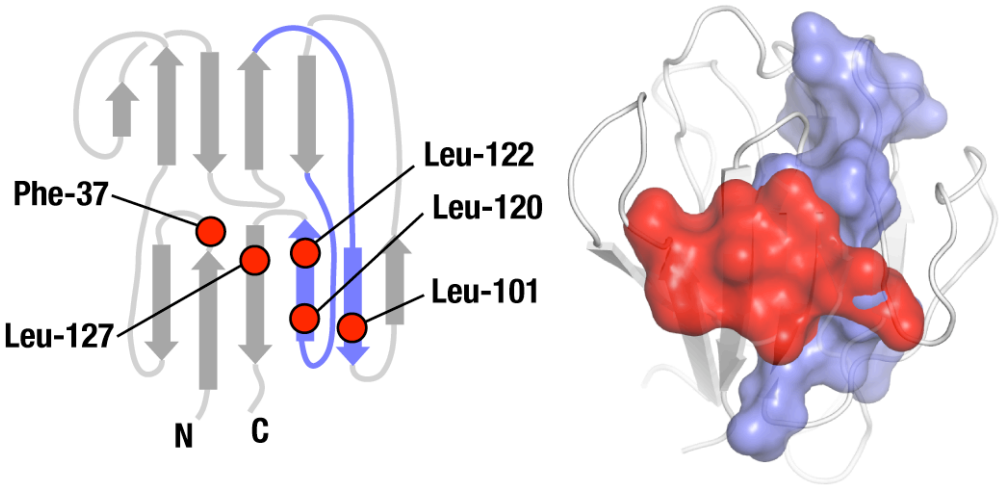

Figure S5 - Topology diagram (left panel) and surface representation (right panel) show that hydrophobic residues that form the conserved Mdc1 FHA-FHA interface (red circles) overlap with a putative self-interacting surface (blue) previously identified by sequence analysis.

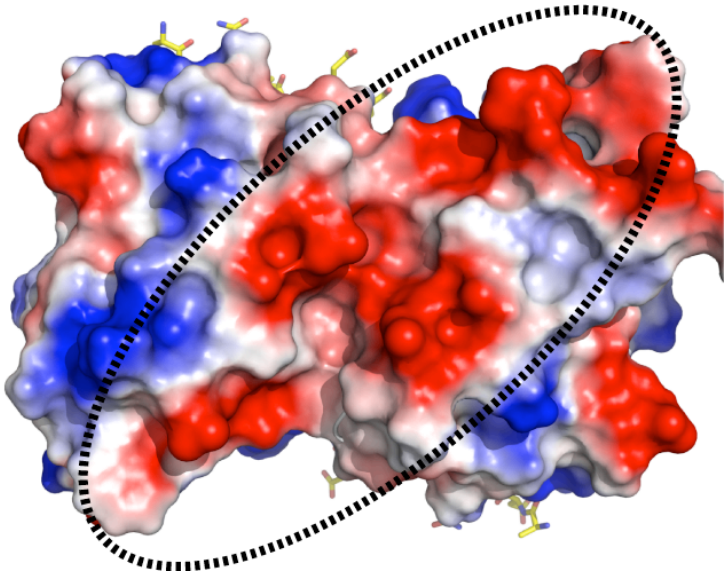

Figure S6 - Electrostatic surface representation of the Mdc1 FHA dimer viewed along the non-crystallographic 2-fold axis. Regions of positive potential are shown in blue and acidic regions in red. Association of the two FHA domains produces a continuous region of negative charge that extends across the dimer.

Table S1 - Crystallographic Statistics

	Mdc1-pT4 (SeMet)	Mdc1
Space group	$P2_12_12_1$	$P2_1$
Unit cell (Å)	a = 58.5, b = 59.9, c = 72.1	a = 55.2, b = 64.9, c = 106.4, β = 96.1°
Number of molecules/au	2	2
Wavelength (Å)	0.9790	0.9757
Resolution (Å)	15.0 – 1.8 (1.86-1.80)	20.0 – 2.3 (2.40-2.30)
Completeness (%)	93.4 (55.3)	94.5 (66.5)
Total observations	134542	113597
Unique observations	42419	30800
Redundancy	3.2 (2.1)	3.7 (3.0)
R_{merge}[a] (%)	3.7 (31.5)	7.0 (40.4)
< I/σ (I) >	27.5 (2.1)	14.9 (2.7)
Structure Solution		
Phasing method	SAD	Molecular replacement
Selenium sites / molecule	2	
Refinement		
Resolution (Å)	15 – 1.8	15.0 - 2.3
R (%)[b]	21.3	
R_{free} (%)	24.0	
r.m.s.d. bond lengths (Å^2)	0.008	
r.m.s.d. bond angles (°)	1.2	
Ramachandran plot		
Preferred regions (%)	97.0	
Allowed regions (%)	3.0	
Outliers (%)	0.0	

[a] $R_{merge} = \Sigma_h\Sigma_i|I_{h,i} - \langle I_h\rangle| / \Sigma_h\Sigma_i I_{h,i}$, where $I_{h,i}$ is the intensity of the individual reflections and $\langle I_h\rangle$ is the mean intensity over symmetrically equivalent reflections

[b] $R = \Sigma_h||F_{o,h}| - |F_{c,h}||/\Sigma_h|F_{o,h}|$, where $|F_{o,h}|$ and $|F_{c,h}|$ are observed and calculated structure factor amplitudes, respectively; R_{free} was calculated with 5% of the data.

6 Discussion

6.1 The interaction between MDC1 and the MRN complex

6.1.1 Summary of own findings

We identified a region in MDC1 that is essential for efficient recruitment and accumulation of the MRN complex in chromatin compartments flanking sites of DSBs. This region contained a repeated acidic sequence motif (the SDT motif) that was constitutively phosphorylated by the acidophilic kinase CK2 on highly conserved Ser and Thr residues. We presented evidence that the doubly phosphorylated SDT motifs regulate accumulation and retention of the MRN complex in DSB-flanking chromatin regions. This retention of MRN involves direct interaction of the NBS1 N-terminal FHA and BRCT domains with the SDT motifs of MDC1. In addition, CK2 was essential for NBS1 accumulation in damaged chromatin and depletion of CK2 disrupted the MDC1-MRN complex *in vivo*. The analysis of different mutants of NBS1 in complemented NBS cell lines showed that the FHA as well as the BRCT domain of NBS1 are important for efficient retention of the protein to DSB-flanking chromatin regions. Finally, we observed a defect in G2/M-checkpoint activation at low doses of irradiation in a NBS cell line complemented with a FHA mutant of NBS1 protein that was defective in MDC1 binding but not with a BRCT mutant that was also defective for MDC1 binding.

6.1.2 The MDC1-MRN complex in the DNA damage response

One of the most important roles of the MRN complex in the DNA damage response is its implication in sensing of DSBs and thereby initiating the DNA damage signaling cascade by recruiting ATM to sites of DSBs and participating in its activation. Our recent findings of the MDC1-MRN complex formation imply that the MRN complex has an additional function

in the amplification of the DNA damage signal and the establishment of the IRIF compartment surrounding the break. Interestingly, it was previously reported that MDC1 and the MRN complex interacted already in unstressed cells (Goldberg et al., 2003; Stewart et al., 2003). We and others confirmed these findings and showed in addition, that complex formation is mediated by the constitutively active casein kinase 2 (This thesis chapter 5.1 and (Melander et al., 2008; Wu et al., 2008)). There are at least two possible reasons for this 'pre-formation' of the complex. First, the recruitment of the MRN complex to the DSB flanking chromatin may be faster if it is not dependent on events that happen after the break occurs. Second, the MDC1-MRN complex may have a physiological role beyond the DDR. MDC1 is known to be chromatin bound even in the absence of DNA damage. Therefore, MDC1 along with the MRN complex may play a role in chromatin organization also in the absence of DNA damage, e.g. during normal DNA replication or in mitosis. It should be mentioned at this point that the interaction between MDC1 and the MRN complex is very dynamic in living cells and no stable holocomplex seems to exist. Evidence for this came from measurements of NBS1 and MDC1 mobility in living cells, that showed that the residence time of MDC1 at DSBs is almost one order of magnitude longer compared to NBS1 (Lukas et al., 2003; Lukas et al., 2004).

The current working model for the sensing and amplification of the DNA damage signal after DSBs included an amplification step mediated by MDC1, which recognizes initial γH2AX formation, recruits more MRN complex and thereby also more ATM (Stucki and Jackson, 2006). This mechanism culminates in the nuclear foci formation of many proteins involved in the DNA damage response. Surprisingly, we did not observe an obvious reduction of γH2AX foci formation in cells with disrupted MDC1-MRN complex formation. This indicates that the recruitment of ATM to DSB flanking chromatin regions is not solely mediated by the NBS1 C-terminus. One possible alternative would be the proposed direct

recruitment of ATM via the FHA domain of MDC1 (Lou et al., 2006). Recent evidence suggested that MDC1 cooperates with ATM to generate high densities of γH2AX near the break. However, the spreading of the γH2AX signal along broken DNA strands was independent of MDC1 (Savic et al., 2009). Therefore, the refined model indicates that MDC1 is important in the establishment of a chromatin region around the DNA break where the equilibrium between phosphorylation and dephosphorylation is shifted towards the kinase activity by protecting γH2AX from phosphatase or chromatin remodeling activities. How the restriction to the damaged chromosome is achieved remains elusive. Moreover, accumulation and retention of the MRN complex by MDC1 does not seem to be required for G2/M checkpoint activation, not even in the presence of low numbers of breaks (chapter 5.2 of this thesis). This indicates an additional role for MDC1-mediated accumulation of the MRN complex. Since the NBS1 FHA domain mutant showed a defect in G2/M checkpoint activation, one possibility could be that the FHA domain has additional binding partners that are essential for checkpoint activation. Another possibility could be the regulation of the intra-S phase checkpoint. It was shown that MDC1 knockout MEFs reconstituted with a deletion mutant of MDC1 that lacks the SDT motifs responsible for MRN binding failed to rescue ionizing radiation-induced intra-S phase checkpoint (Wu et al., 2008). However, these results were in contradiction to a previous publication showing that accumulation of MDC1 on chromatin was not required for activation of intra-S phase checkpoint (Stucki et al., 2005). But it could still be that the direct interaction between MDC1 and the MRN complex is required for the activation of the intra-S phase checkpoint. The mechanism is not known until now. But it is most likely not related to NBS1 phosphorylation (which is essential for the intra-S phase checkpoint), because it was shown that NBS1 phosphorylation is not compromised in MDC1-depleted cells (Goldberg et al., 2003; Stewart et al., 2003). In addition, another possible function of MDC1-mediated accumulation of

MRN may be related to DSB repair. Besides the described role in sensing and signaling of DSBs, the MRN complex seems to have another role in chromatin remodeling during DNA repair. The fact that deficiencies in various chromatin remodeling factors resulted in hypersensitivity to genotoxic agents highlighted the importance of this process during DNA repair via NHEJ and HR (Kouzarides, 2007). In yeast, it was shown that the MRX complex interacts with the chromatin remodeling complex RSC, and this interaction was necessary to recruit RSC to DSBs (Shim et al., 2005). Although there are no detailed mechanisms known how the MRN complex in mammalian cells acts during chromatin remodeling, it is possible that the regulation is similar to the one in yeast. Another aspect of MRN-mediated chromatin remodeling is the regulation of TRRAP (transactivation transformation domain associated protein), a component of the Tip60 HAT complex. Depletion of TRRAP reduced histone acetylation, DNA repair via HR, and foci formation of DNA repair proteins such as RAD51, 53BP1, and BRCA1 (Murr et al., 2006). The MRN complex interacts with TRRAP in the absence of Tip60 and the resulting complex has no HAT activity. After dissociation of TRRAP from MRN, Tip60 could be recruited, which may lead to chromatin structure relaxation through its HAT activity. Therefore, the complex formation between MDC1 and MRN and the MDC1-mediated accumulation of MRN at DSB flanking chromatin may be implicated in DNA damage-induced chromatin structure modulation.

6.2 Dimerization of MDC1

6.2.1 Summary of own findings

We identified a highly conserved Thr residue at the very N-terminus of MDC1 (T4) that is efficiently phosphorylated by purified ATM *in vitro*. By raising a phospho-specific antibody against the N-terminal region of MDC1 we were able to show that the T4 residue is a *bona*

fide ATM target site. Using phospho-peptide pull-down experiments, we showed that the phosphorylated MDC1 N-terminus specifically interacted with full-length MDC1 as well as with the MRN complex. Moreover, we could show a specific interaction of the phosphorylated MDC1 N-terminus with the FHA domain of MDC1. This interaction was confirmed by isothermal titration calorimetry (ITC) and X-ray crystallography, revealing that the FHA domains of two MDC1 molecules associate in a head-to-tail orientation through a conserved hydrophobic patch. Since this interaction is strongly increased after phosphorylation of the T4 residue, DNA damage induces MDC1 dimerization through a specific interaction between its phosphorylated N-terminus and the FHA domain of a second MDC1 molecule. Using biochemical analysis and a life cell imaging approach, we could also show that DNA damage-induced MDC1 dimerization takes place *in vivo*.

6.2.2 Dimerization/multimerization of mediator proteins – a common theme?

Several other mediator/adaptor type proteins involved in the DNA damage response were found to form either homo- or heterodimers and multimers. This is true for 53BP1 in mammals, Crb2 in *S.pombe*, and RAD9p in *S.cerevisiae*. All three proteins contain a tandem Tudor domain, which in the case of 53BP1 and CRB2 has been shown to interact with methylated lysine residues in H3 or H4 (Huyen et al., 2004; Sanders et al., 2004), and is required for the recruitment of the protein to sites of DSBs. The C-terminus of all three proteins consists of a tandem BRCT domain. In RAD9p and Crb2, these BRCT domains were found to be important for dimerization of the protein (Du et al., 2004; Soulier and Lowndes, 1999). Moreover, the tandem BRCT domain of RAD9p and Crb2 interact with the phosphorylated H2A C-terminus (the yeast counterpart of the mammalian H2AX C-terminus) (Hammet et al., 2007; Kilkenny et al., 2008). The crystal structure of the CRB2

BRCT tandem domain was solved, and the biological role of this domain was analyzed *in vivo* by creating mutations that either disrupted dimerization or binding to phosphorylated H2A.1. Cells expressing a dimerization-defective CRB2 protein were shown to be defective for CRB2 recruitment to IRIFs and checkpoint activation, but had little effect on DNA repair. In contrast, a phospho-binding mutant of CRB2 showed normal recruitment to damaged DNA and an intact checkpoint response, but had defects in the DNA repair (Kilkenny et al., 2008). For RAD9, the dimerization via the tandem BRCT domain was shown biochemically using GST pull-down assays as well as in a yeast-two-hybrid approach. In addition, it was shown that the interaction is DNA damage dependent, and that mutations in the BRCT domain that abolished the protein homodimerization led to increased sensitivity of the cells to UV light and defects in checkpoint activation after DNA damage (Soulier and Lowndes, 1999). Another study confirmed the DNA damage dependent RAD9 oligomerization proposing a molecular mechanism where the tandem BRCT domain interacts with the phosphorylated SCD domain. The RAD9 activation was unaffected by mutations that impair oligomerization, but it was required to sustain checkpoint signaling. In addition, RAD53-mediated phosphorylation of RAD9 within its BRCT domain attenuated the BRCT-SCD interaction providing a mechanism how the DNA damage response could be regulated (Usui et al., 2009). For 53BP1, the mammalian ortholog of the described checkpoint proteins in yeast, the requirements for efficient recruitment of the protein were recently resolved (Zgheib et al., 2009). These include the tandem tudor domain as described previously (Huyen et al., 2004; Sanders et al., 2004), as well as an independently folding oligomerization domain and a 15 amino acid C-terminal extension of the tudor domain. In addition, recruitment of 53BP1 to DSBs is dependent on MDC1 phosphorylation and subsequent recruitment of the ubiquitin ligases RNF8 and RNF168, which leads to polyubiquitinylation of histones H2A and H2AX (Doil et al., 2009; Huen et al., 2007; Kolas et

al., 2007; Mailand et al., 2007; Wang and Elledge, 2007). The oligomerization domain of 53BP1 was essential for its efficient recruitment to sites of DSBs, since a protein lacking this region failed to accumulate in chromatin after IR (Zgheib et al., 2009).

In MDC1, the BRCT tandem domain and the FHA domain mediate binding to chromatin after DNA damage and protein dimerization, respectively. We could show that, in contrast to the yeast CRB2 and RAD9 proteins, the recruitment of MDC1 to damaged chromatin via its BRCT tandem domain was not affected by disrupting protein dimerization. Interestingly though, over-expression of the FHA domain exhibits a dominant negative effect on MDC1 foci formation after IR (Goldberg et al., 2003). In addition, MDC1-FHA domain over expression interferes with DSB repair and checkpoint activation (Dimitrova and de Lange, 2006; Goldberg et al., 2003). The mechanism responsible for this dominant-negative effect remains elusive.

In line of the DNA repair defect observed in the dimerization defective forms of CRB2 and RAD9, it was shown that the FHA domain of MDC1 is essential for efficient DSB repair by HR (Xie et al., 2007; Zhang et al., 2005). A possible explanation for this function is the proposed recruitment of ATM through the MDC1-FHA domain (Lou et al., 2006). So far, we were not able to assess the functional relevance of the MDC1 dimerization due to the lack of an efficient complementation system. By analyzing MDC1 mutants that have a defect in dimerization but an otherwise intact FHA domain, it should be possible to dissect the functions of the MDC1 N-terminal region. It is likely that the dimerization of MDC1 plays an important role in some aspect of the mammalian DDR.

There are additional DDR proteins that homo- or hetero-dimerize. Another example is the hetero-dimerization of the tumor suppressor BRCA1 (breast cancer tumor suppressor 1) and its binding partner BARD1 (BRCA1 associated RING domain 1). It was shown that a

complex between these two proteins forms an active E3 ubiquitin ligase (reviewed in (Starita and Parvin, 2006)). Therefore, dimerization in this case leads to a change in enzymatic activity. Since MDC1 has no known enzymatic activity, it is unlikely that MDC1 dimerization has a comparable function to BRCA1/BARD1 dimerization.

TopBP1 is a protein required for the regulation of E2F1-mediated apoptosis. It was shown that Akt phosphorylates TopBP1 *in vitro* and *in vivo*. This phosphorylation mediates the oligomerization of the protein through its seventh and eighth BRCT domains, which in turn allows the interaction of TopBP1 with E2F1 and thereby represses its transcriptional activity (Liu et al., 2006). Similar to TopBP1, the oligomerization of microcephalin (MCPH1) also involves its BRCT domains. In addition, it was shown that the interaction of MCPH1 with the transcription factor E2F1 is also dependent on protein oligomerization of microcephalin. In this case, the interaction regulated the expression of CHK1 and BRCA1, thereby regulating checkpoint activation, DNA repair, and apoptosis (Yang et al., 2008). These examples highlight a possible theme of mediator protein di- or oligomerization in the DDR.

Besides binding to its own phosphorylated N-terminus, the MDC1 FHA domain has been reported to bind to some additional DDR proteins, namely CHK2, ATM and RAD51. So far it is not known if MDC1 dimerization is required for these interactions. Similar to MDC1, the oligomerization of CHK2 is mediated by phosphodependent interaction between a conserved Thr residue (Thr68) and its own FHA domain. This dimerization has been reported to be important for CHK2 activation, signal amplification, and transduction in DNA damage checkpoint pathways (Xu et al., 2002). Moreover, this dimerization may modulate phosphodependent interactions with effector proteins and substrates. In addition, a possible mechanism for the dissociation of the CHK2 dimer is the autophosphorylation of the CHK2 FHA domain at Ser140 (Li et al., 2008). It is still formally possible, that DNA damage-

induced MDC1 dimerization interferes with the binding of the MDC1 FHA domain to another protein, e.g. CHK2. This interaction may be essential for the homo-oligomerization and activation of CHK2. However, MDC1 is not essential for CHK2-mediated events in the DDR. Moreover, CHK2 is not recruited to DSB-flanking chromatin. Clearly, more work needs to be done to decipher the physiological role of MDC1 dimerization in the mammalian DDR.

7 References

Ahn, J.Y., Li, X., Davis, H.L., and Canman, C.E. (2002). Phosphorylation of threonine 68 promotes oligomerization and autophosphorylation of the Chk2 protein kinase via the forkhead-associated domain. J Biol Chem *277*, 19389-19395.

Ahn, J.Y., Schwarz, J.K., Piwnica-Worms, H., and Canman, C.E. (2000). Threonine 68 phosphorylation by ataxia telangiectasia mutated is required for efficient activation of Chk2 in response to ionizing radiation. Cancer Res *60*, 5934-5936.

Alcasabas, A.A., Osborn, A.J., Bachant, J., Hu, F., Werler, P.J., Bousset, K., Furuya, K., Diffley, J.F., Carr, A.M., and Elledge, S.J. (2001). Mrc1 transduces signals of DNA replication stress to activate Rad53. Nat Cell Biol *3*, 958-965.

Bartek, J., Falck, J., and Lukas, J. (2001). CHK2 kinase – a busy messenger. Nat Rev Mol Cell Biol *2*, 877-886.

Bartkova, J., Horejsi, Z., Koed, K., Kramer, A., Tort, F., Zieger, K., Guldberg, P., Sehested, M., Nesland, J.M., Lukas, C.*, et al.* (2005). DNA damage response as a candidate anti-cancer barrier in early human tumorigenesis. Nature *434*, 864-870.

Bassing, C.H., and Alt, F.W. (2004). The cellular response to general and programmed DNA double strand breaks. DNA Repair (Amst) *3*, 781-796.

Bekker-Jensen, S., Lukas, C., Kitagawa, R., Melander, F., Kastan, M.B., Bartek, J., and Lukas, J. (2006). Spatial organization of the mammalian genome surveillance machinery in response to DNA strand breaks. J Cell Biol *173*, 195-206.

Bekker-Jensen, S., Lukas, C., Melander, F., Bartek, J., and Lukas, J. (2005). Dynamic assembly and sustained retention of 53BP1 at the sites of DNA damage are controlled by Mdc1/NFBD1. J Cell Biol *170*, 201-211.

Bernstein, N.K., Williams, R.S., Rakovszky, M.L., Cui, D., Green, R., Karimi-Busheri, F., Mani, R.S., Galicia, S., Koch, C.A., Cass, C.E.*, et al.* (2005). The molecular architecture of the mammalian DNA repair enzyme, polynucleotide kinase. Mol Cell *17*, 657-670.

Bhaskara, V., Dupre, A., Lengsfeld, B., Hopkins, B.B., Chan, A., Lee, J.H., Zhang, X., Gautier, J., Zakian, V., and Paull, T.T. (2007). Rad50 adenylate kinase activity regulates DNA tethering by Mre11/Rad50 complexes. Mol Cell *25*, 647-661.

Burma, S., Chen, B.P., Murphy, M., Kurimasa, A., and Chen, D.J. (2001). ATM phosphorylates histone H2AX in response to DNA double-strand breaks. J Biol Chem *276*, 42462-42467.

Byeon, I.J., Li, H., Song, H., Gronenborn, A.M., and Tsai, M.D. (2005). Sequential phosphorylation and multisite interactions characterize specific target recognition by the FHA domain of Ki67. Nat Struct Mol Biol *12*, 987-993.

Celeste, A., Difilippantonio, S., Difilippantonio, M.J., Fernandez-Capetillo, O., Pilch, D.R., Sedelnikova, O.A., Eckhaus, M., Ried, T., Bonner, W.M., and Nussenzweig, A. (2003a). H2AX haploinsufficiency modifies genomic stability and tumor susceptibility. Cell *114*, 371-383.

Celeste, A., Fernandez-Capetillo, O., Kruhlak, M.J., Pilch, D.R., Staudt, D.W., Lee, A., Bonner, R.F., Bonner, W.M., and Nussenzweig, A. (2003b). Histone H2AX phosphorylation is dispensable for the initial recognition of DNA breaks. Nat Cell Biol *5*, 675-679.

Celeste, A., Petersen, S., Romanienko, P.J., Fernandez-Capetillo, O., Chen, H.T., Sedelnikova, O.A., Reina-San-Martin, B., Coppola, V., Meffre, E., Difilippantonio, M.J*., et al.* (2002). Genomic instability in mice lacking histone H2AX. Science *296*, 922-927.

Cerosaletti, K., and Concannon, P. (2004). Independent roles for nibrin and Mre11-Rad50 in the activation and function of Atm. J Biol Chem *279*, 38813-38819.

Cerosaletti, K., Wright, J., and Concannon, P. (2006). Active role for nibrin in the kinetics of atm activation. Mol Cell Biol *26*, 1691-1699.

Cerosaletti, K.M., and Concannon, P. (2003). Nibrin forkhead-associated domain and breast cancer C-terminal domain are both required for nuclear focus formation and phosphorylation. J Biol Chem *278*, 21944-21951.

Clapperton, J.A., Manke, I.A., Lowery, D.M., Ho, T., Haire, L.F., Yaffe, M.B., and Smerdon, S.J. (2004). Structure and mechanism of BRCA1 BRCT domain recognition of phosphorylated BACH1 with implications for cancer. Nat Struct Mol Biol *11*, 512-518.

Costanzo, V., Paull, T., Gottesman, M., and Gautier, J. (2004). Mre11 assembles linear DNA fragments into DNA damage signaling complexes. PLoS Biol *2*, E110.

D'Amours, D., and Jackson, S.P. (2002). The Mre11 complex: at the crossroads of dna repair and checkpoint signalling. Nat Rev Mol Cell Biol *3*, 317-327.

de Jager, M., van Noort, J., van Gent, D.C., Dekker, C., Kanaar, R., and Wyman, C. (2001). Human Rad50/Mre11 is a flexible complex that can tether DNA ends. Mol Cell *8*, 1129-1135.

Difilippantonio, S., Celeste, A., Fernandez-Capetillo, O., Chen, H.T., Reina San Martin, B., Van Laethem, F., Yang, Y.P., Petukhova, G.V., Eckhaus, M., Feigenbaum, L*., et al.* (2005). Role of Nbs1 in the activation of the Atm kinase revealed in humanized mouse models. Nat Cell Biol *7*, 675-685.

Difilippantonio, S., Celeste, A., Kruhlak, M.J., Lee, Y., Difilippantonio, M.J., Feigenbaum, L., Jackson, S.P., McKinnon, P.J., and Nussenzweig, A. (2007). Distinct domains in Nbs1 regulate irradiation-induced checkpoints and apoptosis. J Exp Med *204*, 1003-1011.

Dimitrova, N., and de Lange, T. (2006). MDC1 accelerates nonhomologous end-joining of dysfunctional telomeres. Genes Dev *20*, 3238-3243.

Ding, Z., Wang, H., Liang, X., Morris, E.R., Gallazzi, F., Pandit, S., Skolnick, J., Walker, J.C., and Van Doren, S.R. (2007). Phosphoprotein and phosphopeptide interactions with the FHA domain from Arabidopsis kinase-associated protein phosphatase. Biochemistry *46*, 2684-2696.

DiTullio, R.A., Jr., Mochan, T.A., Venere, M., Bartkova, J., Sehested, M., Bartek, J., and Halazonetis, T.D. (2002). 53BP1 functions in an ATM-dependent checkpoint pathway that is constitutively activated in human cancer. Nat Cell Biol *4*, 998-1002.

Doil, C., Mailand, N., Bekker-Jensen, S., Menard, P., Larsen, D.H., Pepperkok, R., Ellenberg, J., Panier, S., Durocher, D., Bartek, J.*, et al.* (2009). RNF168 binds and amplifies ubiquitin conjugates on damaged chromosomes to allow accumulation of repair proteins. Cell *136*, 435-446.

Du, L.L., Moser, B.A., and Russell, P. (2004). Homo-oligomerization is the essential function of the tandem BRCT domains in the checkpoint protein Crb2. J Biol Chem *279*, 38409-38414.

Durocher, D., Smerdon, S.J., Yaffe, M.B., and Jackson, S.P. (2000a). The FHA domain in DNA repair and checkpoint signaling. Cold Spring Harb Symp Quant Biol *65*, 423-431.

Durocher, D., Taylor, I.A., Sarbassova, D., Haire, L.F., Westcott, S.L., Jackson, S.P., Smerdon, S.J., and Yaffe, M.B. (2000b). The molecular basis of FHA domain:phosphopeptide binding specificity and implications for phospho-dependent signaling mechanisms. Mol Cell *6*, 1169-1182.

Falck, J., Coates, J., and Jackson, S.P. (2005). Conserved modes of recruitment of ATM, ATR and DNA-PKcs to sites of DNA damage. Nature *434*, 605-611.

Fernandez-Capetillo, O., Celeste, A., and Nussenzweig, A. (2003). Focusing on foci: H2AX and the recruitment of DNA-damage response factors. Cell Cycle *2*, 426-427.

Fernandez-Capetillo, O., Chen, H.T., Celeste, A., Ward, I., Romanienko, P.J., Morales, J.C., Naka, K., Xia, Z., Camerini-Otero, R.D., Motoyama, N.*, et al.* (2002). DNA damage-induced G2-M checkpoint activation by histone H2AX and 53BP1. Nat Cell Biol *4*, 993-997.

Goldberg, M., Stucki, M., Falck, J., D'Amours, D., Rahman, D., Pappin, D., Bartek, J., and Jackson, S.P. (2003). MDC1 is required for the intra-S-phase DNA damage checkpoint. Nature *421*, 952-956.

Gorgoulis, V.G., Vassiliou, L.V., Karakaidos, P., Zacharatos, P., Kotsinas, A., Liloglou, T., Venere, M., Ditullio, R.A., Jr., Kastrinakis, N.G., Levy, B.*, et al.* (2005). Activation of the DNA damage checkpoint and genomic instability in human precancerous lesions. Nature *434*, 907-913.

Halazonetis, T.D., Gorgoulis, V.G., and Bartek, J. (2008). An oncogene-induced DNA damage model for cancer development. Science *319*, 1352-1355.

Hammet, A., Magill, C., Heierhorst, J., and Jackson, S.P. (2007). Rad9 BRCT domain interaction with phosphorylated H2AX regulates the G1 checkpoint in budding yeast. EMBO Rep *8*, 851-857.

Harper, J.W., and Elledge, S.J. (2007). The DNA damage response: ten years after. Mol Cell *28*, 739-745.

Hofmann, K., and Bucher, P. (1995). The FHA domain: a putative nuclear signalling domain found in protein kinases and transcription factors. Trends Biochem Sci *20*, 347-349.

Horejsi, Z., Falck, J., Bakkenist, C.J., Kastan, M.B., Lukas, J., and Bartek, J. (2004). Distinct functional domains of Nbs1 modulate the timing and magnitude of ATM activation after low doses of ionizing radiation. Oncogene *23*, 3122-3127.

Huen, M.S., Grant, R., Manke, I., Minn, K., Yu, X., Yaffe, M.B., and Chen, J. (2007). RNF8 transduces the DNA-damage signal via histone ubiquitylation and checkpoint protein assembly. Cell *131*, 901-914.

Huyen, Y., Zgheib, O., Ditullio, R.A., Jr., Gorgoulis, V.G., Zacharatos, P., Petty, T.J., Sheston, E.A., Mellert, H.S., Stavridi, E.S., and Halazonetis, T.D. (2004). Methylated lysine 79 of histone H3 targets 53BP1 to DNA double-strand breaks. Nature *432*, 406-411.

Jazayeri, A., Falck, J., Lukas, C., Bartek, J., Smith, G.C., Lukas, J., and Jackson, S.P. (2006). ATM- and cell cycle-dependent regulation of ATR in response to DNA double-strand breaks. Nat Cell Biol *8*, 37-45.

Khanna, K.K., and Jackson, S.P. (2001). DNA double-strand breaks: signaling, repair and the cancer connection. Nat Genet *27*, 247-254.

Kilkenny, M.L., Dore, A.S., Roe, S.M., Nestoras, K., Ho, J.C., Watts, F.Z., and Pearl, L.H. (2008). Structural and functional analysis of the Crb2-BRCT2 domain reveals distinct roles in checkpoint signaling and DNA damage repair. Genes Dev *22*, 2034-2047.

Kobayashi, J., Tauchi, H., Sakamoto, S., Nakamura, A., Morishima, K., Matsuura, S., Kobayashi, T., Tamai, K., Tanimoto, K., and Komatsu, K. (2002). NBS1 localizes to gamma-H2AX foci through interaction with the FHA/BRCT domain. Curr Biol *12*, 1846-1851.

Kolas, N.K., Chapman, J.R., Nakada, S., Ylanko, J., Chahwan, R., Sweeney, F.D., Panier, S., Mendez, M., Wildenhain, J., Thomson, T.M.*, et al.* (2007). Orchestration of the DNA-damage response by the RNF8 ubiquitin ligase. Science *318*, 1637-1640.

Kouzarides, T. (2007). Chromatin modifications and their function. Cell *128*, 693-705.

Lee, J.H., Xu, B., Lee, C.H., Ahn, J.Y., Song, M.S., Lee, H., Canman, C.E., Lee, J.S., Kastan, M.B., and Lim, D.S. (2003a). Distinct functions of Nijmegen breakage syndrome in ataxia telangiectasia mutated-dependent responses to DNA damage. Mol Cancer Res *1*, 674-681.

Lee, S.J., Schwartz, M.F., Duong, J.K., and Stern, D.F. (2003b). Rad53 phosphorylation site clusters are important for Rad53 regulation and signaling. Mol Cell Biol *23*, 6300-6314.

Li, H., Byeon, I.J., Ju, Y., and Tsai, M.D. (2004). Structure of human Ki67 FHA domain and its binding to a phosphoprotein fragment from hNIFK reveal unique recognition sites and new views to the structural basis of FHA domain functions. J Mol Biol *335*, 371-381.

Li, J., Lee, G.I., Van Doren, S.R., and Walker, J.C. (2000). The FHA domain mediates phosphoprotein interactions. J Cell Sci *113 Pt 23*, 4143-4149.

Li, J., Taylor, I.A., Lloyd, J., Clapperton, J.A., Howell, S., MacMillan, D., and Smerdon, S.J. (2008). Chk2 oligomerization studied by phosphopeptide ligation: implications for regulation and phosphodependent interactions. J Biol Chem *283*, 36019-36030.

Liao, H., Yuan, C., Su, M.I., Yongkiettrakul, S., Qin, D., Li, H., Byeon, I.J., Pei, D., and Tsai, M.D. (2000). Structure of the FHA1 domain of yeast Rad53 and identification of binding sites for both FHA1 and its target protein Rad9. J Mol Biol *304*, 941-951.

Liu, K., Paik, J.C., Wang, B., Lin, F.T., and Lin, W.C. (2006). Regulation of TopBP1 oligomerization by Akt/PKB for cell survival. EMBO J *25*, 4795-4807.

Lou, Z., Minter-Dykhouse, K., Franco, S., Gostissa, M., Rivera, M.A., Celeste, A., Manis, J.P., van Deursen, J., Nussenzweig, A., Paull, T.T*., et al.* (2006). MDC1 maintains genomic stability by participating in the amplification of ATM-dependent DNA damage signals. Mol Cell *21*, 187-200.

Lou, Z., Minter-Dykhouse, K., Wu, X., and Chen, J. (2003). MDC1 is coupled to activated CHK2 in mammalian DNA damage response pathways. Nature *421*, 957-961.

Lukas, C., Falck, J., Bartkova, J., Bartek, J., and Lukas, J. (2003). Distinct spatiotemporal dynamics of mammalian checkpoint regulators induced by DNA damage. Nat Cell Biol *5*, 255-260.

Lukas, C., Melander, F., Stucki, M., Falck, J., Bekker-Jensen, S., Goldberg, M., Lerenthal, Y., Jackson, S.P., Bartek, J., and Lukas, J. (2004). Mdc1 couples DNA double-strand break recognition by Nbs1 with its H2AX-dependent chromatin retention. EMBO J *23*, 2674-2683.

Luo, G., Yao, M.S., Bender, C.F., Mills, M., Bladl, A.R., Bradley, A., and Petrini, J.H. (1999). Disruption of mRad50 causes embryonic stem cell lethality, abnormal embryonic development, and sensitivity to ionizing radiation. Proc Natl Acad Sci U S A *96*, 7376-7381.

Ma, J.L., Lee, S.J., Duong, J.K., and Stern, D.F. (2006). Activation of the checkpoint kinase Rad53 by the phosphatidyl inositol kinase-like kinase Mec1. J Biol Chem *281*, 3954-3963.

Mahajan, A., Yuan, C., Lee, H., Chen, E.S., Wu, P.Y., and Tsai, M.D. (2008). Structure and function of the phosphothreonine-specific FHA domain. Sci Signal *1*, re12.

Mahajan, A., Yuan, C., Pike, B.L., Heierhorst, J., Chang, C.F., and Tsai, M.D. (2005). FHA domain-ligand interactions: importance of integrating chemical and biological approaches. J Am Chem Soc *127*, 14572-14573.

Mailand, N., Bekker-Jensen, S., Faustrup, H., Melander, F., Bartek, J., Lukas, C., and Lukas, J. (2007). RNF8 ubiquitylates histones at DNA double-strand breaks and promotes assembly of repair proteins. Cell *131*, 887-900.

Manke, I.A., Lowery, D.M., Nguyen, A., and Yaffe, M.B. (2003). BRCT repeats as phosphopeptide-binding modules involved in protein targeting. Science *302*, 636-639.

Melander, F., Bekker-Jensen, S., Falck, J., Bartek, J., Mailand, N., and Lukas, J. (2008). Phosphorylation of SDT repeats in the MDC1 N terminus triggers retention of NBS1 at the DNA damage-modified chromatin. J Cell Biol *181*, 213-226.

Murr, R., Loizou, J.I., Yang, Y.G., Cuenin, C., Li, H., Wang, Z.Q., and Herceg, Z. (2006). Histone acetylation by Trrap-Tip60 modulates loading of repair proteins and repair of DNA double-strand breaks. Nat Cell Biol *8*, 91-99.

O'Driscoll, M., Gennery, A.R., Seidel, J., Concannon, P., and Jeggo, P.A. (2004). An overview of three new disorders associated with genetic instability: LIG4 syndrome, RS-SCID and ATR-Seckel syndrome. DNA Repair (Amst) *3*, 1227-1235.

Osborn, A.J., and Elledge, S.J. (2003). Mrc1 is a replication fork component whose phosphorylation in response to DNA replication stress activates Rad53. Genes Dev *17*, 1755-1767.

Paulsen, R.D., and Cimprich, K.A. (2007). The ATR pathway: fine-tuning the fork. DNA Repair (Amst) *6*, 953-966.

Pike, B.L., Yongkiettrakul, S., Tsai, M.D., and Heierhorst, J. (2003). Diverse but overlapping functions of the two forkhead-associated (FHA) domains in Rad53 checkpoint kinase activation. J Biol Chem *278*, 30421-30424.

Rodriguez, M., Yu, X., Chen, J., and Songyang, Z. (2003). Phosphopeptide binding specificities of BRCA1 COOH-terminal (BRCT) domains. J Biol Chem *278*, 52914-52918.

Rogakou, E.P., Pilch, D.R., Orr, A.H., Ivanova, V.S., and Bonner, W.M. (1998). DNA double-stranded breaks induce histone H2AX phosphorylation on serine 139. J Biol Chem *273*, 5858-5868.

Rouse, J., and Jackson, S.P. (2002). Interfaces between the detection, signaling, and repair of DNA damage. Science *297*, 547-551.

Sanders, S.L., Portoso, M., Mata, J., Bahler, J., Allshire, R.C., and Kouzarides, T. (2004). Methylation of histone H4 lysine 20 controls recruitment of Crb2 to sites of DNA damage. Cell *119*, 603-614.

Savic, V., Yin, B., Maas, N.L., Bredemeyer, A.L., Carpenter, A.C., Helmink, B.A., Yang-Iott, K.S., Sleckman, B.P., and Bassing, C.H. (2009). Formation of dynamic gamma-H2AX domains along broken DNA strands is distinctly regulated by ATM and MDC1 and dependent upon H2AX densities in chromatin. Mol Cell *34*, 298-310.

Schwartz, M.F., Lee, S.J., Duong, J.K., Eminaga, S., and Stern, D.F. (2003). FHA domain-mediated DNA checkpoint regulation of Rad53. Cell Cycle *2*, 384-396.

Shim, E.Y., Ma, J.L., Oum, J.H., Yanez, Y., and Lee, S.E. (2005). The yeast chromatin remodeler RSC complex facilitates end joining repair of DNA double-strand breaks. Mol Cell Biol *25*, 3934-3944.

Songyang, Z., Shoelson, S.E., Chaudhuri, M., Gish, G., Pawson, T., Haser, W.G., King, F., Roberts, T., Ratnofsky, S., Lechleider, R.J.*, et al.* (1993). SH2 domains recognize specific phosphopeptide sequences. Cell *72*, 767-778.

Soulier, J., and Lowndes, N.F. (1999). The BRCT domain of the S. cerevisiae checkpoint protein Rad9 mediates a Rad9-Rad9 interaction after DNA damage. Curr Biol *9*, 551-554.

Starita, L.M., and Parvin, J.D. (2006). Substrates of the BRCA1-dependent ubiquitin ligase. Cancer Biol Ther *5*, 137-141.

Stewart, G.S., Wang, B., Bignell, C.R., Taylor, A.M., and Elledge, S.J. (2003). MDC1 is a mediator of the mammalian DNA damage checkpoint. Nature *421*, 961-966.

Stracker, T.H., Morales, M., Couto, S.S., Hussein, H., and Petrini, J.H. (2007). The carboxy terminus of NBS1 is required for induction of apoptosis by the MRE11 complex. Nature *447*, 218-221.

Stracker, T.H., Theunissen, J.W., Morales, M., and Petrini, J.H. (2004). The Mre11 complex and the metabolism of chromosome breaks: the importance of communicating and holding things together. DNA Repair (Amst) *3*, 845-854.

Stucki, M., Clapperton, J.A., Mohammad, D., Yaffe, M.B., Smerdon, S.J., and Jackson, S.P. (2005). MDC1 directly binds phosphorylated histone H2AX to regulate cellular responses to DNA double-strand breaks. Cell *123*, 1213-1226.

Stucki, M., and Jackson, S.P. (2006). gammaH2AX and MDC1: anchoring the DNA-damage-response machinery to broken chromosomes. DNA Repair (Amst) *5*, 534-543.

Sun, Z., Hsiao, J., Fay, D.S., and Stern, D.F. (1998). Rad53 FHA domain associated with phosphorylated Rad9 in the DNA damage checkpoint. Science *281*, 272-274.

Sweeney, F.D., Yang, F., Chi, A., Shabanowitz, J., Hunt, D.F., and Durocher, D. (2005). Saccharomyces cerevisiae Rad9 acts as a Mec1 adaptor to allow Rad53 activation. Curr Biol *15*, 1364-1375.

Tanaka, K., Boddy, M.N., Chen, X.B., McGowan, C.H., and Russell, P. (2001). Threonine-11, phosphorylated by Rad3 and atm in vitro, is required for activation of fission yeast checkpoint kinase Cds1. Mol Cell Biol *21*, 3398-3404.

Tanaka, K., and Russell, P. (2004). Cds1 phosphorylation by Rad3-Rad26 kinase is mediated by forkhead-associated domain interaction with Mrc1. J Biol Chem *279*, 32079-32086.

Tauchi, H., Kobayashi, J., Morishima, K., Matsuura, S., Nakamura, A., Shiraishi, T., Ito, E., Masnada, D., Delia, D., and Komatsu, K. (2001). The forkhead-associated domain of NBS1 is essential for nuclear foci formation after irradiation but not essential for hRAD50-hMRE11-NBS1 complex DNA repair activity. J Biol Chem *276*, 12-15.

Usui, T., Foster, S.S., and Petrini, J.H. (2009). Maintenance of the DNA-damage checkpoint requires DNA-damage-induced mediator protein oligomerization. Mol Cell *33*, 147-159.

Wang, B., and Elledge, S.J. (2007). Ubc13/Rnf8 ubiquitin ligases control foci formation of the Rap80/Abraxas/Brca1/Brcc36 complex in response to DNA damage. Proc Natl Acad Sci U S A *104*, 20759-20763.

Wang, P., Byeon, I.J., Liao, H., Beebe, K.D., Yongkiettrakul, S., Pei, D., and Tsai, M.D. (2000). II. Structure and specificity of the interaction between the FHA2 domain of Rad53 and phosphotyrosyl peptides. J Mol Biol *302*, 927-940.

Ward, I.M., and Chen, J. (2001). Histone H2AX is phosphorylated in an ATR-dependent manner in response to replicational stress. J Biol Chem *276*, 47759-47762.

Ward, I.M., Minn, K., and Chen, J. (2004). UV-induced ataxia-telangiectasia-mutated and Rad3-related (ATR) activation requires replication stress. J Biol Chem *279*, 9677-9680.

Ward, I.M., Minn, K., Jorda, K.G., and Chen, J. (2003). Accumulation of checkpoint protein 53BP1 at DNA breaks involves its binding to phosphorylated histone H2AX. J Biol Chem *278*, 19579-19582.

Williams, R.S., Lee, M.S., Hau, D.D., and Glover, J.N. (2004). Structural basis of phosphopeptide recognition by the BRCT domain of BRCA1. Nat Struct Mol Biol *11*, 519-525.

Wu, L., Luo, K., Lou, Z., and Chen, J. (2008). MDC1 regulates intra-S-phase checkpoint by targeting NBS1 to DNA double-strand breaks. Proc Natl Acad Sci U S A *105*, 11200-11205.

Xiao, Y., and Weaver, D.T. (1997). Conditional gene targeted deletion by Cre recombinase demonstrates the requirement for the double-strand break repair Mre11 protein in murine embryonic stem cells. Nucleic Acids Res *25*, 2985-2991.

Xie, A., Hartlerode, A., Stucki, M., Odate, S., Puget, N., Kwok, A., Nagaraju, G., Yan, C., Alt, F.W., Chen, J.*, et al.* (2007). Distinct roles of chromatin-associated proteins MDC1 and 53BP1 in mammalian double-strand break repair. Mol Cell *28*, 1045-1057.

Xu, X., Tsvetkov, L.M., and Stern, D.F. (2002). Chk2 activation and phosphorylation-dependent oligomerization. Mol Cell Biol *22*, 4419-4432.

Xu, Y.J., Davenport, M., and Kelly, T.J. (2006). Two-stage mechanism for activation of the DNA replication checkpoint kinase Cds1 in fission yeast. Genes Dev *20*, 990-1003.

Yaffe, M.B., and Smerdon, S.J. (2004). The use of in vitro peptide-library screens in the analysis of phosphoserine/threonine-binding domain structure and function. Annu Rev Biophys Biomol Struct *33*, 225-244.

Yang, S.Z., Lin, F.T., and Lin, W.C. (2008). MCPH1/BRIT1 cooperates with E2F1 in the activation of checkpoint, DNA repair and apoptosis. EMBO Rep *9*, 907-915.

Yu, X., Chini, C.C., He, M., Mer, G., and Chen, J. (2003). The BRCT domain is a phospho-protein binding domain. Science *302*, 639-642.

Zgheib, O., Pataky, K., Brugger, J., and Halazonetis, T.D. (2009). An oligomerized 53BP1 tudor domain suffices for recognition of DNA double-strand breaks. Mol Cell Biol *29*, 1050-1058.

Zhang, J., Ma, Z., Treszezamsky, A., and Powell, S.N. (2005). MDC1 interacts with Rad51 and facilitates homologous recombination. Nat Struct Mol Biol *12*, 902-909.

Zhao, S., Renthal, W., and Lee, E.Y. (2002). Functional analysis of FHA and BRCT domains of NBS1 in chromatin association and DNA damage responses. Nucleic Acids Res *30*, 4815-4822.

Zhou, B.B., and Elledge, S.J. (2000). The DNA damage response: putting checkpoints in perspective. Nature *408*, 433-439.

Zhu, J., Petersen, S., Tessarollo, L., and Nussenzweig, A. (2001). Targeted disruption of the Nijmegen breakage syndrome gene NBS1 leads to early embryonic lethality in mice. Curr Biol *11*, 105-109.

8 Curriculum Vitae

Personal information

Name	SPYCHER
First name	Christoph
Date of birth	October 11th, 1977
Place of birth	Frauenfeld (TG)
Place of origin	Zurich (ZH), Koeniz (BE)

Education

2005-present	**Ph.D. student in Molecular Biology**, Institute of Veterinary Biochemistry and Molecular Biology, University of Zurich, Switzerland; Topic: “Identification and Functional Characterization of Novel Phosphorylation Sites in MDC1”
1998-2004	**Masters degree in Biochemistry and Molecular Biology**, with minors in Biotechnology, Genetics, and Immunology, ETH Zurich, Switzerland
2004	Diploma thesis at the Institute of Biotechnology, ETH Zurich, Switzerland; Prof. Dr. A. Schmid; Topic: “Impact of feed composition on styrene epoxidation activity in *E. coli* JM101 (pSPZ10)”
1992-1997	**Matura Type C**, Kantonsschule Frauenfeld (TG)

9 Acknowledgments

I would like to thank Dr. Manuel Stucki for giving me the opportunity to work in his lab and for his constant support in planning and performing the experiments. I could profit and learn a lot from his experience and knowledge. It was an honor for me to be the first Ph.D. student in his group.

Furthermore, I would like to thank all members of the lab, Lucijana Pavic, Stephanie Jungmichel, Flurina Hari, and Mario Bonalli, for all the scientific and non-scientific discussions. In addition, I thank all members of our institute for creating a good working atmosphere.

This work would not have been possible without fruitful collaborations: I thank Dr. Pavel Janscak, the group of Dr. Grant Stewart, the group of Prof. Dr. Stephen J. Smerdon, and the group of Prof. Dr. Jiri Lukas.

I thank my thesis committee Prof. Dr. Michael O. Hengartner, Prof. Dr. Dr. Michael O. Hottiger, and Prof. Dr. Thanos D. Halazonetis for their helpful inputs and comments during the annual meetings and for evaluating my thesis.

Special thanks go to my wife Franziska for her love and care she gave me during the past six years. This work would not have been possible without her support, encouragement, and interest in my work. I also thank my family and friends for all their support.

This work was supported by grants from the Swiss National Foundation (grant 3100A0-111818), the UBS AG (Im Auftrag eines Kunden), and the Kanton of Zürich.